uOttawa

L'Université canadienne
Canada's university

FACULTÉ DES ÉTUDES SUPÉRIEURES ET POSTOCTORALES

uOttawa

L'Université canadienne
Canada's university

FACULTY OF GRADUATE AND POSDOCTORAL STUDIES

Joanne McBane
AUTEUR DE LA THÈSE / AUTHOR OF THESIS

Ph.D. (Biochemistry)
GRADE / DEGREE

Department of Biochemistry, Microbiology and Immunology
FACULTÉ, ÉCOLE, DÉPARTEMENT / FACULTY, SCHOOL, DEPARTMENT

Protein Kinase C and the Respiratory Burst in the Macrophage-mediated Biodegradation of Polyurethanes: Dependence on Material Surface Chemistry

TITRE DE LA THÈSE / TITLE OF THESIS

Rosalind Labow
DIRECTEUR (DIRECTRICE) DE LA THÈSE / THESIS SUPERVISOR

CO-DIRECTEUR (CO-DIRECTRICE) DE LA THÈSE / THESIS CO-SUPERVISOR

EXAMINATEURS (EXAMINATRICES) DE LA THÈSE / THESIS EXAMINERS

Brian Amsden

Robert Screaton

Patrick Burgon

Natalie Goto

Gary W. Slater
Le Doyen de la Faculté des études supérieures et postdoctorales / Dean of the Faculty of Graduate and Postdoctoral Studies

PROTEIN KINASE C AND THE RESPIRATORY BURST IN THE MACROPHAGE-MEDIATED BIODEGRADATION OF POLYURETHANES: DEPENDENCE ON MATERIAL SURFACE CHEMISTRY

by

JOANNE MCBANE

A thesis submitted to the Faculty of Graduate and Postdoctoral Studies in partial fulfillment of the requirement for the degree of

DOCTOR OF PHILOSOPHY

Department of Biochemistry, Microbiology and Immunology

University of Ottawa

Ottawa, Ontario, Canada

Your file Votre référence
ISBN: 978-0-494-41636-5
Our file Notre référence
ISBN: 978-0-494-41636-5

ACKNOWLEDGEMENTS

To begin I would like to thank my supervisor Dr. Rosalind Labow who has been a wonderful mentor to me over my honours project and graduate student years. Upon entering her lab she quickly became my second mother and I her baby PhD. In addition to being a dedicated scientist she is also a fabulous storyteller. After her retirement from science she has promised to pen several novels that are destined to be best sellers. I also need to thank Dr. Stanley Labow and my golf pro Paul Sherratt who conspired together to give me a summer job in Dr. Rosalind Labow's lab without her permission. As much as he insists, I still do not believe Stanley hates me, even if I can beat him at golf. I would also like to thank my two lab sisters Dr. Loren Matheson and Dr. Donna Dinnes. Both are tremendous role models, teachers, friends and travel-mates. Loren, a fellow redhead from Manotick, took the hard road by being our fearless oldest sister. Donna is the adventurous middle child who took off to Australia in search of love and science.

Furthermore, I would like to thank my biological family for all their support and DNA. From my grandmothers I inherited my red hair and height. From my father I inherited my determination, work ethic and golf swing. I wish they were still here to see me put them to good use. From my mother I inherited a quirky sense of humour and my constant compulsion to feed people. Thanks mom for letting me live with you all these years, allowing me to stay in school for so long. Also, I would like to thank the rest of my family: my siblings Jennifer, Patrick and Julie; my in-laws Bud and Tahlia; and my nephews and nieces Jacob, Taylor, Amelia and Owen. They have been with me through the celebrations and tragedies and will no doubt be there with me through many more.

Next, I would like to thank my surrogate lab family consisting of Dr. Paul Santerre and the Santerre group. First of all, I need to thank Dr. Meilin Yang for the polyurethane synthesis and Robert Chernecky for the fabulous microscopy pictures. I would also like to thank Paul for inviting me to his lab and letting me become part of his family, an experience that confirmed my decision to do a post-doc in the Santerre lab. In addition I would like to thank Soroor Sharifpoor for teaching me about polyurethane synthesis and becoming a great friend. I look forward to working together, to a wonderful conference trip to Amsterdam, and officially becoming a part of the Santerre group.

There are many other past and present members of the Heart Institute that have been instrumental in keeping me motivated during this time. Among them are my adopted lab sisters Margaret Neuspiel and Katey Rayner. Without their support and encouragement I would not have gone to as many seminars or had nearly as much fun. Also thanks to the entire 4th floor and the lab next door including Suzanne, Mireille, Thet, Chris, Jon, Serena, Angela, Liz Y, Shawn, Drew and Jessica among many others. All of who made me feel a part of a group even when my own lab was really only two. Thanks to the many honours and summer students who have added interest to each year, especially: Janet, Tiffany, Allison, Mike, Sarah, Alex, Liz G, Lorenne, Kate, Ruth and Laura.

Finally, thanks to my boyfriend Dan Mustard for his care, concern and encouragement. Thanks for listening to my little science problems even when they made absolutely no sense to you whatsoever. I have enjoyed every minute we have spent together at home and away. For all of this I owe you another sugar pie and some Lego®.

ABSTRACT

Polyurethanes are versatile materials used in the manufacture of diverse medical devices. Monocytes attach to the material surface and differentiate to monocyte-derived macrophages (MDM)s during the foreign body response. MDMs degrade polyurethanes by releasing reactive oxygen species (ROS) and hydrolytic enzymes (cholesterol esterase and monocyte-specific esterase (MSE)) by an unknown mechanism. To study this mechanism, model polycarbonate-based polyurethanes (PCNU)s have been made with hexane (HDI) or methylene bisphenyl diisocyanate (MDI) with poly (1,6-hexyl carbonate) diol (PCN) and 1,4-butanediol (BD) in a 4:3:1 ratio of HDI:PCN:BD (HDI431) or a 3:2:1 ratio of HDI:PCN:BD or MDI:PCN:BD (HDI321 or MDI321 respectively). HDI431 is the most degradable by MDM- and esterase-mediated degradation followed by HDI321 and MDI321. Manuscript#1 investigated the effects of phorbol myristate acetate (PMA) on MDM-mediated degradation of model PCNUs. In this study PMA inhibited the degradation of HDI PCNUs correlating with decreased esterase activity and MSE, but had no effect on the degradation of MDI321. Manuscript#2 suggested that H_2O_2 treatment degraded PCNUs and affected subsequent MDM-mediated degradation, esterase and acid phosphatase activity in a material surface specific manner. In addition, this study found that material surface stimulated ROS production in MDM. PMA affected ROS production in MDM differently based on material surface. Manuscript#3 investigated the role of protein kinase C (PKC) activation and the respiratory burst in MDM-mediated PCNU degradation. This study showed that the PMA inhibition of MDM-mediated degradation of HDI PCNUs, esterase activity and MSE protein were dependent on PKC activation. The activation marker high

molecular weight group box 1 protein secretion was highest on HDI431 and was prevented by PMA, matching the decreased degradation. A degradative pathway in MDM on MDI321 was triggered with PKC inactive PMA, ROS scavengers or PMA with a PKC inhibitor. This thesis proposes that material degradation by hydrolytic and oxidative pathways are channeled by MDM in varying amounts depending on material chemistry, supporting the theory that MDM respond to material chemistry first and then to environmental factors. Therefore these studies suggest that each polyurethane be tested under physiologically appropriate conditions in order to determine if it is suitable for the desired application and implant location.

TABLE OF CONTENTS **PAGE**

LIST OF ABBREVIATIONS

4αPMA	phorbol myristate acetate with the hydroxy at the 4-carbon in the alpha position
ANOVA	analysis of variance
ATP	adenosine triphosphate
BD	1,4-butanediol
BIM	Bisindolylmaleimide I
CAT+SOD	catalase and superoxide dismutase, used as reactive oxygen species scavengers
CE	cholesterol esterase
CIHR	Canadian Institutes of Health Research
CPM	counts per minute
CXE	carboxyl esterase
DAG	diacylglycerol
DMAC	dimethylacetamide
DNA	deoxyribonucleic acid
EC	endothelial cell
EDTA	ethylenediaminetetraacetic acid
ESC	environmental stress cracking
FBGC	foreign body giant cell
FBS	fetal bovine serum
GAPDH	glyceraldehyde-3-phosphate dehydrogenase
GM-CSF	granulocyte/macrophage-colony stimulating factor
GTP	guanosine triphosphate

H_2O_2	hydrogen peroxide
H7	H7 dihydrochloride, protein kinase C inhibitor
HDI	1,6-hexane diisocyanate
HDI321	HDI:PCN:BD – 3:2:1
HDI431	HDI:PCN:BD – 4:3:1
HOCl	hypochlorous acid
IFN-γ	interferon-gamma
IgG	immunoglobulin G
IL	interleukin
kDa	kiloDalton
LDI	lysine diisocyanate
LSCM	laser scanning confocal microscopy
MDA	methylene dianiline
MDI	4,4'-methylene bis-phenyl diisocyanate
MDI321	MDI:PCN:BD – 3:2:1
MDM	monocyte-derived macrophage
MIO	metal ion oxidation
MSE	monocyte-specific esterase
MW	molecular weight
NA	not available
NADPH	nicotinamide adenine dinucleotide phosphate
NaF	sodium fluoride
NaN_3	sodium azide

NaT	sodium taurocholate
NSERC	Natural Sciences and Engineering Research Council
PAGE	polyacrylamide gel electrophoresis
PBS	phosphate buffered saline
PCN	polycarbonate / poly (1,6-hexyl carbonate) diol
PCNU	polycarbonate-based polyurethane / polycarbonate-urethane
PESU	polyester-based polyurethane
PEU	polyether-based polyurethane
PKC	protein kinase C
PLA_2	phospholipase A_2
PMA	phorbol 12-myristate 13-acetate
PNB	*p*-nitrophenylbutyrate
RAGE	receptor for advanced glycation end-products
RLR	radiolabel release
ROS	reactive oxygen species
RPMI	Roswell Park Memorial Institute
SDS	sodium dodecyl sulfate
SEM	scanning electron microscopy
TBST	Tris-buffered saline with Tween-20
TDA	2,4-toluene diamine
TDI	toluene diisocyanate
TNFα	tumour necrosis factor-alpha
VPU	vinyl-lysine diisocyanate polycarbonate-based polyurethane

VSMC vascular smooth muscle cell

LIST OF FIGURES

Introduction

Manuscript 1

McBane JE, Santerre JP, Labow RS. The role of protein kinase C in the monocyte-derived macrophage-mediated biodegradation of polycarbonate-based polyurethanes. Journal of Biomedical Materials Research. 2005; 74A: 1-11.

Manuscript 2

McBane JE, Santerre JP, Labow RS. The interaction between hydrolytic and oxidative pathways in macrophage-mediated polyurethane degradation. Journal of Biomedical Materials Research. 2007; 82(4): 984-994.

Manuscript 3

McBane JE, Matheson LA, Santerre, JP, and Labow RS. The effects of phorbol ester activation, inhibition, and reactive oxygen species scavengers on the macrophage-mediated foreign body reaction to polyurethanes. Submitted to Biochemistry and Cell Biology, December 2007.

LIST OF TABLES

Introduction

Manuscript 1

McBane JE, Santerre JP, and Labow RS. The role of protein kinase C in the monocyte-derived macrophage-mediated biodegradation of polycarbonate-based polyurethanes. Journal of Biomedical Materials Research. 2005; 74A: 1-11.

Manuscript 2

McBane JE, Santerre JP, and Labow RS. The interaction between hydrolytic and oxidative pathways in macrophage-mediated polyurethane degradation. Journal of Biomedical Materials Research. 2007; 82(4): 984-994.

Manuscript 3

McBane JE, Matheson LA, Santerre, JP, and Labow RS. The effects of phorbol ester activation, inhibition, and reactive oxygen species scavengers on the macrophage-mediated foreign body reaction to polyurethanes. Submitted to Biochemistry and Cell Biology, December 2007.

1.0 INTRODUCTION

The human body is an amazing machine, but like any other machine it is subject to wear and tear. When parts of the human body are damaged beyond repair, biomaterials are used to repair or replace the ailing body part. Over the past fifty years of modern biomaterials research there have been tremendous advances in terms of both material design and methods of material evaluation (1-5). Among those advances was the development of polyurethane biomaterials. It is impossible for any one material to have the right properties for each application; however, polyurethanes as a group can satisfy the demands for many medical devices since polyurethane chemistry can be easily manipulated to change its physical properties. Polyurethanes have been used in the generation of several stable implanted medical devices including: dental implants (6-8), artificial heart bladders (9), artificial heart valves (10, 11), vascular grafts (12-14), pacemaker leads (15), intervertebral discs (16), and bio-artificial liver support systems (17). Biodegradable polyurethanes have become popular for use in drug delivery systems and in tissue regeneration applications such as: drug-eluting stents (18-20); cartilage (21), meniscus (22), and bone regeneration (21, 23, 24); skin regeneration (25); and other tissue engineering applications (26-30). Therefore, it is necessary to address the human body's response to both degradable and more stable polyurethanes. In this thesis three model polycarbonate-based polyurethanes (PCNU)s that vary in susceptibility to degradation (31) will be assessed for the types of responses they will provoke *in vivo* by testing them *in vitro* with human monocyte-derived macrophages (MDMs).

When the human body is faced with an assault, numerous immune system cells are called upon to defend the body from attack. The immune system can be broken into two functions: the adaptive immune response and the innate immune response. Adaptive immune responses occur when the body produces antibodies against a specific antigen. Innate immune responses are more general in that an unrecognized foreign body triggers the inflammatory response. This is great for clearing pathogens, but not appropriate when trying to integrate implants, such as a life-saving medical device, within the body. Biomaterials, specifically polyurethanes, initiate the innate immune response following implantation and this leads to a host of reactions that ultimately influence the biocompatibility of the device.

Neutrophils, monocytes and MDMs are the most important cells involved in the innate immune response to a polyurethane biomaterial. MDMs can be activated by the polyurethane surface to fuse and form foreign body giant cells (FBGC)s (32-34) which are thought to be responsible for the failure of implanted polyurethane medical devices (35, 36). MDM and FBGC can cause material degradation through oxidative and hydrolytic means. Oxidative degradation of polyurethanes is caused by reactive oxygen species (ROS) and hydrolytic degradation occurs by the release of candidate esterases, cholesterol esterase (CE) and monocyte-specific esterase (MSE) (37). Mechanisms of esterase and ROS release from MDM are not fully understood. The initiating enzyme in the respiratory burst, nicotinamide adenine dinucleotide phosphate (NADPH) oxidase, requires phosphorylation by protein kinase C (PKC) for activation (38, 39) and ROS production, and therefore the PKC pathway is of interest. This thesis will investigate

the role of PKC in the oxidative and hydrolytic pathways that determine the mode of degradation of polyurethanes by MDM.

1.1 HYPOTHESIS

The material surface chemistry of PCNUs directs the activation of oxidative and hydrolytic pathways in MDM that determine the mechanism(s) of subsequent material degradation.

1.2 GLOBAL OBJECTIVE

The overall objective is to define how PCNU chemistry directs PKC activation of the respiratory burst in human MDM and to provide evidence linking this pathway to the biodegradation that occurs via hydrolytic or oxidative pathways.

1.2.1 SPECIFIC OBJECTIVES

1) Use phorbol myristate acetate (PMA) to activate PKC in MDM on different PCNU surfaces that varied in hard segment molar content and chemistry (aromatic versus linear hydrocarbon chain) in order to investigate the effects on MDM-mediated material degradation, esterase activity and intracellular MSE protein.

2) Determine if the PMA effects on MDM-mediated PCNU degradation and esterase activity are dependent on PKC activation and/or ROS production.

3a) Determine if PKC activation is required for ROS production in MDM cultured on PCNUs since most *in vitro* assays of ROS production require exogenous activation of PKC.

3b) Investigate the effects of oxidation of PCNUs on subsequent MDM-mediated degradation since neutrophils, monocytes and MDM will release ROS altering the surface chemistry and its susceptibility to further MDM-mediated degradation.

1.3 BACKGROUND

This background provides a general overview of polyurethanes, their use as medical implanted materials, and a detailed review of MDM, including their function and activation pathways related to enzymes and ROS within the cells. Section 1.3.1 will include a discussion on polyurethane use and synthesis, followed by a detailed analysis of the chemistry of the model PCNUs used in this thesis (subsection 1.3.1.1). This section will describe, in more detail than the manuscripts, the material characteristics of different polyurethanes and what makes a PCNU a better biomaterial than other polyurethanes. In section 1.3.2 there will be an overview of the foreign body response and then more specifically the foreign body response to a biomaterial. The foreign body response is a more general inflammatory response triggered by any foreign invader (i.e. phagocytosis of bacteria or a particle). However, the foreign body response to a biomaterial is the set of reactions initiated when an MDM responds to an implanted material too large to engulf. Section 1.3.3 will focus on MDM, the most important cells in the foreign body response. MDM are the cells used in all the experiments described in this thesis and have

been found to be the primary cells responsible for polyurethane biodegradation. This section will include enzymes expressed and/or secreted by MDM including acid phosphatase (AP, subsection 1.3.3.1), high molecular weight group box 1 protein (HMGB1, subsection 1.3.3.2), and esterases (subsection 1.3.3.3). AP, HMGB1 and esterases are possible markers of MDM activation, however esterases have also been found to be candidate enzymes responsible for the degradation of polyurethanes by MDM. The literature on the MDM-mediated biodegradation of polyurethanes will be reviewed in section 1.3.4 as will the *in vitro* esterase-mediated degradation of polyurethanes in subsection 1.3.4.1. Section 1.3.5 will discuss the inflammatory signaling pathways with potential implications in the foreign body response to materials. Literature describing the importance of phospholipase A_2 (PLA_2) signaling will be briefly introduced along with a more thorough background of the cell signaling pathways that can be initiated by PKC activation by PMA. Subsection 1.3.5.1 will review the PKC family of serine/threonine kinases, and their substrates. Next, subsection 1.3.5.2 will focus on how PKC initiates the respiratory burst in phagocytic cells and discuss the impact of ROS production by monocytes, neutrophils and MDMs on both cell function and material surface chemistry.

1.3.1 POLYURETHANE BIOMATERIALS

Polyurethane elastomers are segmented polymers that have a long history in the field of biomaterials. There are three basic chemical components of polyurethanes (as previously reviewed (1, 40)): the diisocyanate; the macrodiol, which can be either a high molecular

weight polyether, polyester or polycarbonate diol; and the chain extender, which can be a low molecular weight diol or a diamine.

Polyurethanes can be synthesized by one-step, two-step or semi-continuous processes depending on the reactivity of the monomers (41). The two-step process as described in Figure 1.1 allows for a greater control of polymer structure and can be carried out in bulk or in solution (i.e. solvents such as dimethylacetamide) (41). Step one involves reacting the diisocyanate and polydiol to form the prepolymer. Step two requires the reaction of the prepolymer with the chain extender in predetermined molar ratios to create polyurethanes of desired polymer length. Diisocyanate and chain extender components combine together to make the hard segment and the macrodiol is considered the soft segment (See Figure 1.2). Phase separation of the polyurethane refers to the amount that the hard and soft segments interact (41).

The earliest polyurethane materials used in medical devices were synthesized with toluene diisocyanate (TDI) and methylene bisphenyl diisocyanate (MDI). Subsequently, 2,4-toluene diamine (TDA), a putative carcinogen, has been proposed as a byproduct of TDI polyurethane foam degradation (42); whereas, other studies have shown TDA derivatives to be degradation products of TDI polyurethanes but not TDA (43, 44). Studies with methylene dianiline (MDA), the precursor of MDI, have shown that ingestion or inhalation can cause serious complications such as retinopathy (45), acute liver damage (46), or cancer (47). MDA has been shown to be a product of the CE-mediated hydrolysis of an MDI-based polyurethane *in vitro* (48).

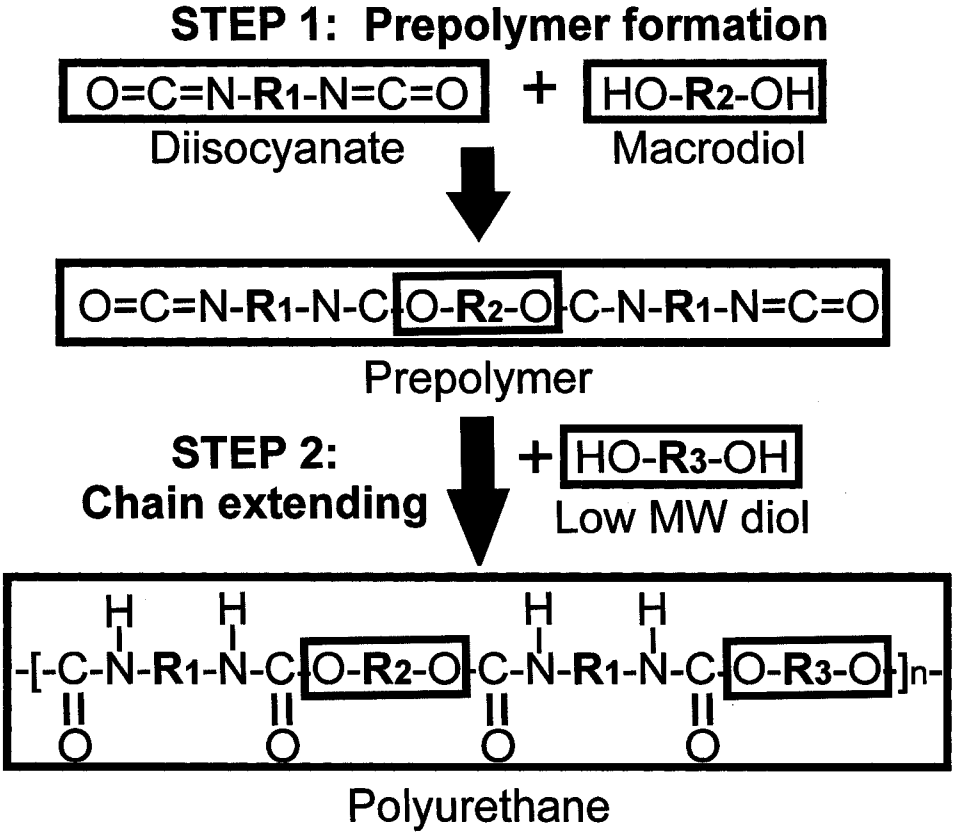

Figure 1.1: Two-step polyurethane synthesis. In step 1 the diisocyanate (R_1=aliphatic or aromatic) is reacted with a macrodiol (R_2= a polyester, polyether or polycarbonate) to make a macrodiol end-capped with diisocyanate (prepolymer). This step may require the use of a solvent (i.e. dimethylacetamide) and a catalyst (i.e. dibutyltin dilaurate). Step 2 is the chain extension step where the prepolymers are reacted with a low molecular weight (MW) diol (R_3=short aliphatic chain such as butane). This step may also require a catalyst, which needs to be washed out following polymerization. If the chain extender is a low MW diamine (H_2N-R-NH_2) the resulting polymer is a polyurethane-urea. (41, 63)

Because of the controversy surrounding the toxicity of the hydrolysis products of TDI and MDI-based polyurethanes used for long term implants, the search was on for alternative diisocyanates to make biodegradable hard segments that could be used in drug-eluting stents or tissue engineering applications where degradation is desired. 1,6-Hexane diisocyanate (HDI) (49), 1,4-diisocyanatobutane (26), lysine diisocyanate (LDI) (25, 28, 30, 50-53), and 2,2,4-trimethyl-hexamethylene diisocyanate (50) are some of the candidate diisocyanates for use in biodegradable polyurethanes. LDI-based polyurethanes have gained in favour since the amino acid lysine is one of its degradation products (25, 28, 53, 54).

Subtle changes in soft segment chemistry can also impart differences in the polyurethane's susceptibility to degradation. Polyurethanes with polyester soft segments (PESU)s have been shown to be susceptible to hydrolytic degradation (40, 55) and so have ceased to be used in implantable devices requiring long-term stability of physical properties. Polyether soft segment polyurethanes (PEU)s are susceptible to degradation by oxidation (56), but have been proven to be relatively resistant to hydrolytic degradation (57). However, previously it was found that the processing method affected the CE-mediated degradation of a PEU scaffold (58). One of the more promising polyurethane families in terms of versatility and biocompatibility is the PCNU (1, 40, 59-61). Biocompatibility does not mean non-degradable, but that the material chemistry can be tailored for a desired application so that the material can perform the necessary *in vivo* function and will not invoke an undesired response from the body.

1.3.1.1 POLYCARBONATE-BASED POLYURETHANES

The chemistry of the model PCNUs used in this thesis were previously described in detail (62, 63). Either HDI or MDI diisocyanates were used while the soft segment (1,6-hexyl carbonate diol) and chain extender (1,4-butanediol) remained constant (see Figure 1.2). Table 1.1 reviews the literature available to date characterizing these three model PCNUs.

Tang *et al* have previously shown that the stoichiometric ratio of hard segment to soft segment significantly affects the material's susceptibility to degradation by CE (63). In one study, four polyurethanes were made with varying hard segment percentages (HDI and 1,4-butanediol hard segment, a poly (1,6-hexyl 1,2-ethyl carbonate) diol soft segment). It was found that the higher hard segment content polyurethanes had fewer non-hydrogen bonded carbonate-linkages, more hydrogen bonding and consequently were less degradable by CE (63). Hydrogen bonding is a strong dipole-dipole interaction between hydrogen and oxygen or hydrogen and nitrogen when electron densities shift to make hydrogen atoms positive and oxygen (nitrogen) negative. These forces are not covalent bonds but they are strong enough to influence polymer organization, crystallinity and resistance to degradation. This result suggested that the non-hydrogen bonded carbonate linkages were the most susceptible to CE-mediated degradation (63).

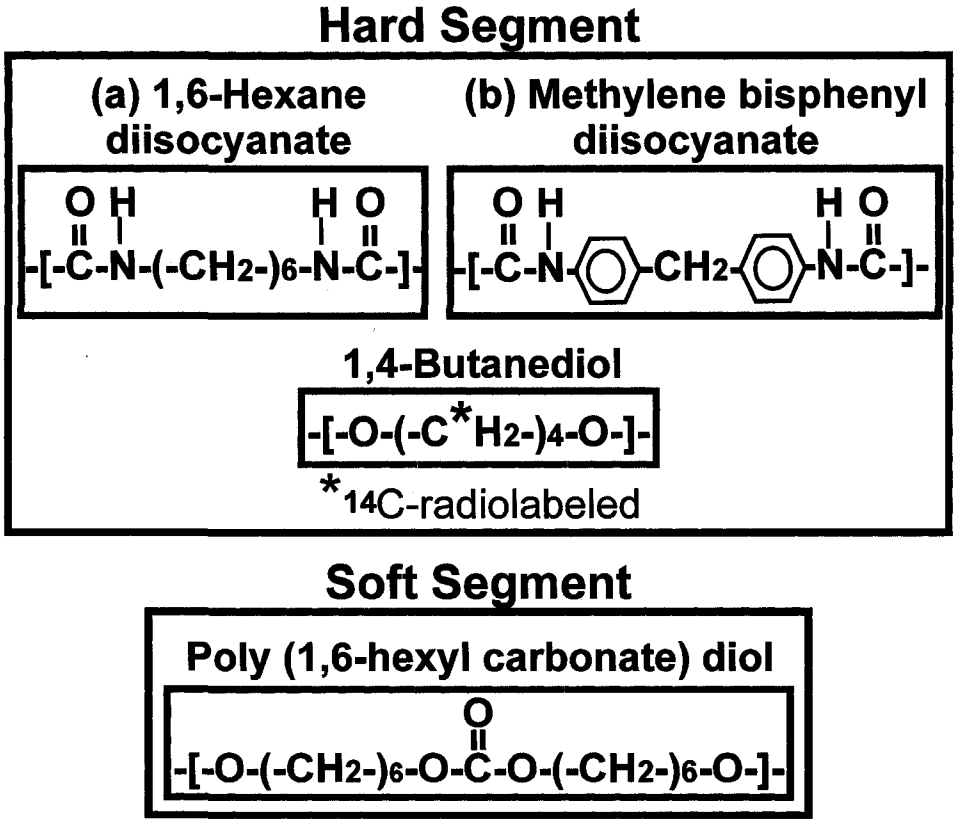

Figure 1.2: Model polycarbonate-based polyurethane chemistry. The three model PCNUs used in this study were synthesized with either (a) 1,6-hexane (HDI) or (b) methylene bisphenyl diisocyanate (MDI). All were synthesized with the same chain extender (1,4-butanediol, BD) and macrodiol (poly (1,6-hexyl carbonate) diol, PCN). The four carbons in BD were ^{14}C-radiolabeled for biodegradation studies. PCNU are named according to their diisocyanate and the ratio of diisocyanate:PCN:BD. There are two HDI based PCNUs with differing stoichiometric ratios 4:3:1 and 3:2:1 (HDI431 and HDI321 respectively). There is one MDI based PCNU with a 3:2:1 ratio of diisocyanate:PCN:BD (MDI321) (62, 63).

TABLE 1.1:
Review of the literature associated with the MDM response on the three model PCNUs used in this thesis

Parameter	HDI431	HDI321	MDI321
MDM-mediated degradation (31, 64)	+++	++	+
CE-mediated degradation (62, 63)	+++	++	+
CXE-mediated degradation (37, 65)	+++	+=	+=
CE protein synthesis (66)	+++	**NA**	++
MSE protein synthesis (66)	+++	**NA**	++
Esterase activity- intracellular (31)	+++	+=	+=
Esterase activity- released (31)	+++	+=	+=
Response to MDA(67)	**-20% RLR**	**No effect RLR**	**-60% RLR**
Acid phosphatase activity intracellular (31)	+=	+=	+=
Acid phosphatase activity-released (31)	+=	+=	+=
DNA/cell attachment (31)	+=	+=	+=
Arachidonic acid release from MDM (68)	+=	+=	+=

RLR-radiolabel release
+++ Greatest stimulation
++ Second greatest stimulation
+ Least stimulated
+= Stimulation equal to stimulation on at least one other material surface
NA Data not available/unpublished

Another study of PCNU stability by Tang *et al* showed that varying hard segment content changed the hydrogen bonding of the carbonate and urethane groups (62). HDI, MDI and 4,4'-methylene biscyclohexyl diisocyanate (HMDI)-based PCNUs were compared in terms of hydrogen bonding, phase separation and susceptibility to CE-mediated degradation. The HDI based PCNU was found to be more phase separated than the MDI or HMDI based PCNUs (62). There were significantly more hydrogen-bonded carbonate linkages in the bulk MDI PCNU than the HDI PCNUs, however there were fewer hydrogen-bonded urethane linkages (62). Subsurface analysis by attenuated total reflectance Fourier transform infrared spectroscopy showed that MDI PCNUs had more hydrogen-bonded amine and carbonate linkages at the subsurface than the HDI PCNUs and a higher ratio of hydrogen bonded urethane linkages than the bulk polymer (62). These results fit with the degradation data that showed MDI321 was the least susceptible to CE-mediated degradation (62).

1.3.2 FOREIGN BODY RESPONSE TO A BIOMATERIAL

The ability of the human body to react to a foreign invader is critical. Many pathogens can be destroyed due to this response. During the process of phagocytosis, neutrophils, monocytes and MDMs engulf foreign pathogens into a vacuole and release degradative activities from the lysosome into the vacuole to kill the invader. When a foreign body such as a biomaterial is too large to engulf, a different mechanism of inflammation is invoked called the foreign body reaction to a biomaterial, which previously has been called frustrated phagocytosis (69-71). Although this has been extensively studied (1, 28,

34-37, 44, 60, 64, 67, 72-75), there are still knowledge gaps in the mechanism of the release of these activities.

The known steps in the inflammatory response to a biomaterial were delineated thanks in part to the cage implant studies performed by Marchant and Anderson (33, 76, 77). Implantation causes an injury or wound allowing blood to contact the material surface. Extracellular matrix and blood proteins such as immunoglobulin G (IgG), fibronectin, high molecular weight kininogen, factor VIII, Hageman factor, collagen, albumin, and fibrinogen attach to the surface of the biomaterial (78, 79). Protein adsorption is an important step affected by: protein concentration, affinity for the surface, protein conformation (denaturation), and the Vroman Effect (78-82). The Vroman Effect has established that high abundance low affinity proteins bind first (such as fibrinogen) and are gradually replaced at the surface by lower concentration, high affinity proteins (high molecular weight kininogen) (83); however, material chemistry can be the deciding factor for protein binding to the surface. Previously, it has been shown that fibrinogen could displace vitronectin for binding to polyethylene, silicone rubber, Teflon, and a poly(tetramethylene oxide) urethane, but not to the hydrophilic poly(ethylene oxide) urethane (84). Grafting of polyethylene oxide onto polyurethanes has been found to decrease total protein adsorption (85).

The complement cascade, coagulation cascade, kinin system and fibrinolysis can be activated during the foreign body response to a biomaterial. The classic role of the complement system is to opsonize pathogens and induce an inflammatory response so

that antibody responses mediated by the adaptive immune system are improved. Phagocytes have complement receptors so that they may recognize these pathogens/foreign bodies and initiate phagocytosis or the foreign body response. On some biomaterial surfaces C3 complement fragment C3b adsorbs onto the surface initiating the alternative complement pathway, thereby recruiting leukocytes to the material surface (86). The coagulation cascade, kinin system and fibrinolysis are involved in the formation, propagation, and control of blood clots. Injury associated with the implantation of a medical device releases tissue factor from endothelial cells. Once tissue factor comes into contact with blood, there is initiation of the coagulation cascade, which can be propagated by the adsorbed proteins leading to platelet adhesion, aggregation and blood clot formation. Platelet adhesion has been modestly correlated to fibrinogen adhesion to the polyurethane surface (87) however platelet activation has been related to fibrinogen adsorbing to the material surface in a specific conformation that exposes the appropriate epitopes (88). Leukocytes such as neutrophils and monocytes may aid in platelet recruitment, leading to thrombus formation in varying degrees depending on the material surface (89).

The first phagocytic cell recruited to the site of the foreign body is the neutrophil. Neutrophils are activated by the surface to express integrin receptor Mac-1 (89) and release ROS (hypochlorous acid, HOCl), granulocyte elastase (89), lysosomal hydrolases (72) and chemokines to help recruit monocytes to the surface. Previously, it was shown that neutrophil binding to complement C5a can delay apoptosis (90) and be chemoattractant to other neutrophils. Biodegradation by neutrophils is limited by both

their short lifespan at the material surface and the type of degradative activities released (serine proteases rather than esterases, (72, 74)). *In vitro* experiments incubating neutrophils on polyurethanes showed that degradation continued for only up to 18 hours, since past this time cell viability was greatly decreased (91). A previous study showed that neutrophils and monocytes migrate into inflammatory sites simultaneously but monocytes are the predominant cell type after 12 hours because of continued migration (92). Monocytes can then differentiate to become MDMs. Activated MDM can fuse to form FBGCs, large multinucleated cells with an increased capacity to secrete degradative enzymes (32). FBGCs have been previously shown to remain adherent to the material surface for the lifetime of the implanted device (93) and have an increased resistance to apoptosis (94). *In vitro* formation of FBGCs can be stimulated by the material surface (66) or through the use of cytokines such as interleukin-4 (IL-4) (95, 96) and IL-13 (97), which would be lymphocyte-derived *in vivo*. The monocyte differentiation to MDM and fusion to form FBGC requires rearrangements in cytoskeletal structures including the formation of the adhesive structures called podosomes (82). Podosomes have been found in dendritic cells (98), eosinophils (99), osteoclasts (100), MDMs and FBGCs (82, 97). These adhesive structures are thought to be important for cell motility and invasiveness (97, 98, 100) and can be induced in MDM and FBGC on different biomaterials (82, 97).

Similar to the normal wound healing response, a fibrous capsule of varying thickness surrounds the MDMs and FBGCs during the foreign body reaction. The fibrous tissue generation is caused by fibroblasts being stimulated by MDM to deposit collagen. Initially type III collagen forms the capsule and in later stages if the capsule reaches a

steady state it can be replaced by type I collagen representing a transition from inflammation to repair (101, 102). As this transition occurs, there is a decrease in the pro-inflammatory cytokine tumor necrosis factor-α (TNF-α) and an increase in IL-10 production (102). Previously it has been found that material surface (102-107) and implant location (108) affect capsule formation. Capsule formation can be problematic for many implants, especially breast augmentation implants. In breast implants there has been much investigation into using materials such as silicone or polyurethanes to try to prevent capsule contraction, which can distort or destroy the implant (103, 104, 106). Although the formation of the capsule cannot be stopped, the use of more biocompatible surface coatings such as certain polyurethanes or silicone can lead to a thinner capsule forming around the implant (104). The MDMs and FBGCs remain in the layer between the material and the fibrous capsule. One study found that the degree of FBGC multi-nucleation varied depending on the material surface, with PEU surface Estane® causing greater multi-nucleation and fibrous encapsulation than the silicone derived Silastic® (108). Therefore in the foreign body response MDM and FBGC activation leads to material degradation and fibrous capsule formation.

1.3.3 MONOCYTE-DERIVED MACROPHAGES

The differentiation of a monocyte to an inflammatory MDM can take two pathways: classical (inflammatory) or alternative (wound healing) (109). A classical activation state is stimulated by opsonized particles, hypoxia, bacterial lipoproteins, bacterial deoxyribonucleic acid (DNA), abnormal extracellular matrix or interferon-γ (pro-inflammatory cytokines) (109). Previously it has been found that the proteins adsorbed to

the material surface affect subsequent cytokine release. Bonfield and Anderson found that materials preadsorbed with fibronectin or fibrinogen had more IL-1β (proinflammatory cytokine (110)) activity than those preadsorbed with IgG or no protein at all, however quantitative secretion levels of IL-1β showed the opposite trend (111). IL-1, TNF-α, and IL-6 have also been found to be stimulated in MDM in response to polyethylene particulates such as wear debris from an orthopedic implant (112). Modulating PKC in cells has been shown to affect monocyte-to-MDM cellular differentiation (113-115); however, material surface has also been shown to affect monocyte differentiation (67, 116). The alternative activation state leads to a more wound healing phenotype for the MDM. Alternative activation of MDM can be stimulated by IL-4, IL-10, IL-13, glucocorticoids, and transforming growth factor-beta (TGF-β) (109). Alternatively stimulated MDM can generate anti-inflammatory cytokines (such as IL-10) and have suppressed synthesis of pro-inflammatory cytokines (such as IL-1β and TNFα), making them resistant to classical activation (109).

1.3.3.1 ACID PHOSPHATASE (AP)

AP is a lysosome-localized protein found in oestoclasts, dendritic cells, MDM and other cells of the monohistiocytic lineage (117). Previously, a mouse study found that AP was necessary for proper immune functioning *in vivo* (118). MDM-derived multi-nucleated giant cells have more AP activity per cell than MDM (119), which also suggests a role for AP in the foreign body response. Several studies on MDM-biomaterial or polyurethane interactions have used AP activity as an indicator of MDM activation (31, 33, 120-123). Investigation into the role of AP in the foreign body reaction has led to

some interesting results. Previously it was found that uniaxial and biaxial mechanical strain could stimulate intracellular and released AP activity in differing amounts based on the extracellular matrix coating of siloxane (124). Recently, it was found that the release of AP (activity and protein) was stimulated more from MDM on polydimethylsiloxane compared to MDM on polystyrene or PCNUs (31).

1.3.3.2 HIGH MOLECULAR WEIGHT GROUP BOX 1 PROTEIN (HMGB1)

Another proposed marker of material surface activation of the MDM has been HMGB1 (see section 4.0). HMGB1 is a non-histone nuclear-localized DNA binding protein found in most eukaryotic cells. When located intracellularly, HMGB1 has a role in transcriptional regulation. Recently, it has been shown to be an inflammatory protein since when it is released from MDM it acts as a pro-inflammatory cytokine causing the secretion of other pro-inflammatory cytokines (IL-1β and TNFα), which further stimulate MDM. Many diseases linked to inflammation have shown the release of HMGB1 and its interaction with the receptor for acetylated glycolation end-products (RAGE) (125). HMGB1 can bind to other receptors such as Toll-like receptor 2 (TLR-2), however a recent study found that when HMGB1 binds RAGE in mouse macrophages there was an increase in pro-inflammatory cytokines TNFα, IL-1β, and IL-6 that was not seen when HMGB1 was bound to TLR-2 (126). Previously, HMGB1 has been found in atherosclerotic lesions (127) suggesting a role in cardiovascular diseases (128). In addition, HMGB1 has been suggested to have a role in arthritis (129), cancers (130, 131), and diabetes (125). HMGB1 release from monocytes and MDM can be stimulated by pro-inflammatory cytokines (127), lipopolysaccharide (132), or hydrogen peroxide

(H_2O_2) (133). It has been suggested that HMGB1 as a late inflammatory mediator can suppress anti-inflammatory cytokines such as IL-10 and TGF-β1 (132). Inhibiting PKC inhibits cytokine-induced HMGB1 secretion in MDM (134). Few studies have looked into the stimulation of HMGB1 in MDM by material surfaces. However, one recent study has identified HMGB1 as a tyrosine-phosphorylated protein in monocytes that has altered levels of phosphorylation based on the peptide adsorbed to the polystyrene surface (135).

1.3.3.3 ESTERASES

When studying biodegradation, esterolytic activity has been shown to be the most destructive (see subsection 1.3.4.1). Esterases such as CE and MSE have been proposed to be markers of MDM activation since their release can be triggered in varying amounts based on the material surface or stimulus (31, 66, 121, 124). CE is an important enzyme for cholesterol metabolism, however it is not known how it is secreted from MDM or its role when it is secreted (136). There is a lysosomal acid CE and a neutral CE (neutral cholesteryl ester hydrolase), which was previously found in the cytoplasm of various tissue macrophages (137). Wolman disease and cholesteryl ester storage disease (CESD) are two diseases of varying phenotype and severity where there is a loss or decrease in lysosomal acid CE activity (138). Patients with Wolman disease have a more severe phenotype, with diarrhea and problems with lipid absorption that may lead to death in infancy; however CESD patients are normally asymptomatic (138).

There has been research into MSE as a marker protein in monocytes for inflammation and disease however it has no known physiological function. In the non-activated MDM cellular localization of MSE has not been confirmed. However, MSE has been proposed to be a soluble intracellular protein that may be found in the endoplasmic reticulum (ER) since it has a C-terminal ER localization domain (139, 140). Variations in MSE expression have been used to classify monocyte maturation in leukemias (141, 142). MSE deficiency is an inheritable genetic abnormality that can be increased in patients with lymphoproliferative or gastrointestinal malignant neoplastic diseases (143). One hypothesis for its regulated release is by being enveloped into a vacuole and released by the fusion of the vacuole with a lysosome and then the plasma membrane, a process previously described in host-parasite relations as the cytoplasm to vacuole pathway (144-146). Recently CE and MSE have been found to be candidate enzymes in MDM responsible for polyurethane degradation (see subsection 1.3.4.1).

1.3.4 BIODEGRADATION OF POLYURETHANES

Polyurethane degradation can occur by either hydrolytic or oxidative means of degradation or a combination of both in varying amounts. For instance, the ester bond in a polyester-polyurethane is very susceptible to hydrolysis (40). Since the human body is composed of over 70% water, it makes the polyester-polyurethane a poor choice for a stable implanted device. Polyether polyurethanes are resistant to hydrolysis but susceptible to oxidative degradation. During the respiratory burst (see subsection 1.3.5.2), ROS such as hydroxyl radicals, superoxide anion and H_2O_2 produced by neutrophils, monocytes, MDM and FBGC are released onto the surface of the device

where they can initiate auto-oxidation of the polyurethane by hydrogen proton extraction or chain cleavage (40). This reaction is propagated by the degradation of hydroperoxide groups and then terminated by the creation of non-reactive products (40). Metal ion oxidation (MIO) is an important phenomenon associated with polyurethanes in contact with metallic corrosion products such as a polyurethane pacemaker lead (15). H_2O_2 and metal alloys together can accelerate auto-oxidation *in vitro* (147-149). Cobalt species have been proposed to be responsible for the MIO occurring in PEU pacemaker leads (150). Environmental stress cracking (ESC), one of the causes of material failure (40), is the phenomenon that involves deep surface cracking due to various types of material strains. This includes mechanical strain due to device function, material strain due to the manufacturing process, and indirect material strain *in vivo* due to the foreign body response. MIO and ESC are not interchangeable. MIO is not dependent on residual material stress and can occur in locations where there is no foreign body response or fibrotic encapsulation, whereas both are requirements for ESC (40). ESC can be decreased by decreasing the ether soft segment content (40), whereas there have been promising results using PCNUs under ESC and MIO conditions (40, 147, 148, 151).

There have been several model systems developed to evaluate the degradation of polyurethanes and PCNUs *in vivo* and *in vitro*. The cage implant studies have been essential studies in delineating the foreign body response to a biomaterial (33, 76, 77). In the cage implant system, the biomaterial surrounded by a cage is surgically implanted into the animal so that the polymer may be analyzed and removed without sacrificing the animal (76). Cage implant analysis has shown that PCNUs undergo a similar foreign

body response to a PEU with monocytes adhering and differentiating to MDM and FBGCs (60). However, a 10-week cage implant study with different polyurethanes showed that *in vivo* degradation of the PCNU was significantly less than the PEU (34). The minimal PCNU degradation seen after 10 weeks *in vivo* was attributed to hydrolysis of the soft segment polycarbonate bond (34).

Rigorous *in vitro* testing provides invaluable degradation and toxicology data prior to *in vivo* animal testing. Although neutrophils can cause polyurethane degradation (72, 73, 91, 152), most studies focus on the role of the MDM since both *in vitro* and *in vivo* MDM have a longer lifespan and capability to degrade than the neutrophil. As a result, there have been several model systems of the foreign body response developed that use primary monocytes and MDMs. Isolated human peripheral blood monocytes can be induced to differentiate to different cells depending on the exogenous agents applied. For instance, monocytes can differentiate to dendritic cells when treated in culture with IL-4 and granulocyte-macrophage colony stimulating factor (GM-CSF) (153). GM-CSF (153), IL-4, and IL-13 have previously been used to differentiate monocytes to MDM (154). The model system used in previous studies by the Labow and Santerre groups and in this thesis requires freshly isolated monocytes to be seeded onto polystyrene and incubated at 37°C in 10% fetal bovine serum in RPMI (Roswell Park Memorial Institute) medium for 14 days prior to trypsinization and re-seeding onto the desired material surface (91). This model system has been able to distinguish between material surfaces with respect to FBGC formation (66), esterase activity (66), as well as illustrate different degrees of biodegradation of PEU (91) and PCNU material surfaces (37, 64).

Although primary cells and human monocytes are the most physiologically relevant, many *in vitro* models to assess biocompatibility and biodegradation involve the use of human or animal cell lines in order to expedite research. Commonly used cell lines for these purposes are: the U937 human pro-monocytic cell line (155), THP-1 human acute leukemic monocytic cell line (9), and J774 mouse tumour macrophage cell line (50, 156). Cell lines are attractive alternatives to primary cells since they can be grown in continuous culture and then differentiated to MDM-like cells in a relatively short period of time. For instance U937 cells can be differentiated from pro-monocytic cells in suspension into adherent MDM-like cells by seeding cells in 100nM PMA for 72 hours (157, 158). These MDM-like PMA-differentiated U937 cells have been previously validated as a model cell system for the MDM-mediated degradation of polyurethanes (155). Using this U937 cell model system it was found that of the three model PCNUs used in this study HDI431 was the most susceptible to MDM-mediated degradation followed by HDI321, with MDI321 being the most stable (31). However this model system did not show the same effects when studying PMA activation of PKC as primary human MDM (data not shown). Therefore, in this thesis the use of primary cells was necessary in order to elucidate PKC effects on the MDM-mediated biodegradation of polyurethanes.

Cell-free models of material degradation are also popular methods to show the effects of long-term *in vivo* degradation in a shorter time frame. A classic cell-free model to assess the susceptibility of a material to ESC is the human plasma/0.01M cobalt chloride/10% H_2O_2 model system developed by Zhao *et al* (159). This model of oxidation was used to

confirm PCNUs are more stable to oxidative degradation than PEUs (151). Wiggins *et al* used a variation of this model with biaxial strain to show that PEUs were more susceptible to ESC than PCNUs (160). Tanzi *et al* showed the greater *in vitro* stability of PCNUs versus PEUs under acid (HNO_3) and alkaline (NaClO) oxidative conditions and constant strain to mimic ESC (161). Another study treated a PEU with 25% H_2O_2 at 100°C to mimic ESC *in vitro* (162). These methods show an accelerated version of ESC from long-term implantation. However, none take into account hydrolytic degradation by enzymes released by MDM (see subsection 1.3.4.1).

1.3.4.1 ESTERASE-MEDIATED PCNU DEGRADATION

Although ESC has been attributed to oxidative damage, the release of hydrolytic esterases by MDM has also been shown to degrade polyurethanes (37, 66). CE and MSE are the two candidate hydrolytic enzymes previously shown to be synthesized by MDM (136, 142) that have been used in various *in vitro* models of polyurethane/biomaterial degradation. Compelling evidence indicates that they contribute to PCNU surface biodegradation (37). Immunoblotting of MDM after PCNU incubation showed both CE and MSE were present in the cell supernatant and cell lysate (66). The esterase activity (163) as well as the *de novo* esterase synthesis and amount of CE and MSE in MDM were higher on HDI431 than the less degradable MDI321 (66). The incubation of MDM on polyurethanes in the presence of phenylmethylsulfonylfluoride, an esterase inhibitor, significantly decreased MDM-mediated polyurethane and PCNU degradation (37, 64, 65). *In vitro* testing where CE and carboxyl esterase ((CXE) commercially available

esterase with the same specificity as MSE) were incubated on polyurethanes showed that both esterases elicited polyurethane degradation (37).

Recent studies have evaluated the susceptibility of polyurethanes to CE versus MSE/CXE degradation (37, 65, 164). It has been found that the degradation of PCNU by CE has a dose dependent effect, whereby the increase in biodegradation did not increase linearly with increasing CE concentration, but could sharply increase at high CE doses (63). As a result, *in vitro* tests with esterases such as CE and CXE require a dose response curve with the esterase substrate *p*-nitrophenylbutyrate (PNB, hydrolyzed to *p*-nitrophenol) to find the pseudosaturation value for each enzyme/polyurethane combination (37, 65). CE *in vitro* could stimulate more HDI431 radiolabel release and required less units of esterase activity than CXE (37). Maximal degradation of MDI321 by CE required 60 times more PNB units than maximal degradation of HDI321 (65). The number of PNB units for maximal CXE degradation was less for HDI321 and MDI321 (65) than for HDI431 (37). In order to determine the importance of CE and MSE in MDM-mediated degradation, sodium fluoride (NaF, inhibitor of CXE) and sodium taurocholate (NaT, stimulator of CE) were added to cells cultured on the three model PCNUs (37, 65). Results suggested that CXE activity (resembling MSE in MDM) was more involved in the MDM-mediated degradation of HDI-based PCNUs (37, 65) and CE activity was more involved in the MDM-mediated degradation of MDI321 (65). The active site of MSE, CXE and CE contain the catalytic triad histidine-serine-aspartate; however, CE and MSE/CXE have different substrate specificities. Although both CE and MSE/CXE are capable of hydrolyzing PCNUs and PNB, the preferred *in vivo* substrates for CE are long

chain fatty acid esters of cholesterol. The *in vivo* substrates of MSE are unknown. *In vitro* CXE cannot hydrolyze cholesterol esters but cleaves short chain (acetate and butyrate) fatty acid esters of toxic materials such as drugs and organophosphates (165) and are sensitive to organophosphate inhibitors such as diisopropylfluorophosphate (166, 167).

In addition to the substrate specificity of MSE/CXE versus CE, the susceptibility of PCNUs to esterase-mediated degradation can be explained by differences in material surface chemistry. As described in subsection 1.3.1.1, HDI and MDI based PCNUs have different material chemistries and as a result have different bonds that are susceptible to cleavage by esterases. Figure 1.3 shows the bonds that can be cleaved by CE for HDI and MDI PCNUs based on a previous study analyzing the products of CE-mediated PCNU degradation (48). A recent study of CE induced degradation of HDI and MDI polymers suggested that increased hydrogen bonding in MDI polymers due to phase mixing and larger aromatic diisocyanate shielding the susceptible carbonate bonds, decreased biodegradation when compared to the phase separated HDI based polyurethanes (62). The reasoning for this observation is that phase mixing allows for hydrogen bonding which protects the carbonate bond from cleavage by CE, leaving only the stable urethane linkages (75, 168). CE will attack the non-hydrogen bonded carbonate preferentially in HDI PCNUs, causing fewer urethane bonds to be cleaved (48). Another recent study showed that HDI polymers with a higher ratio of diisocyanate to polydiol segment showed less degradation when incubated with CE (168).

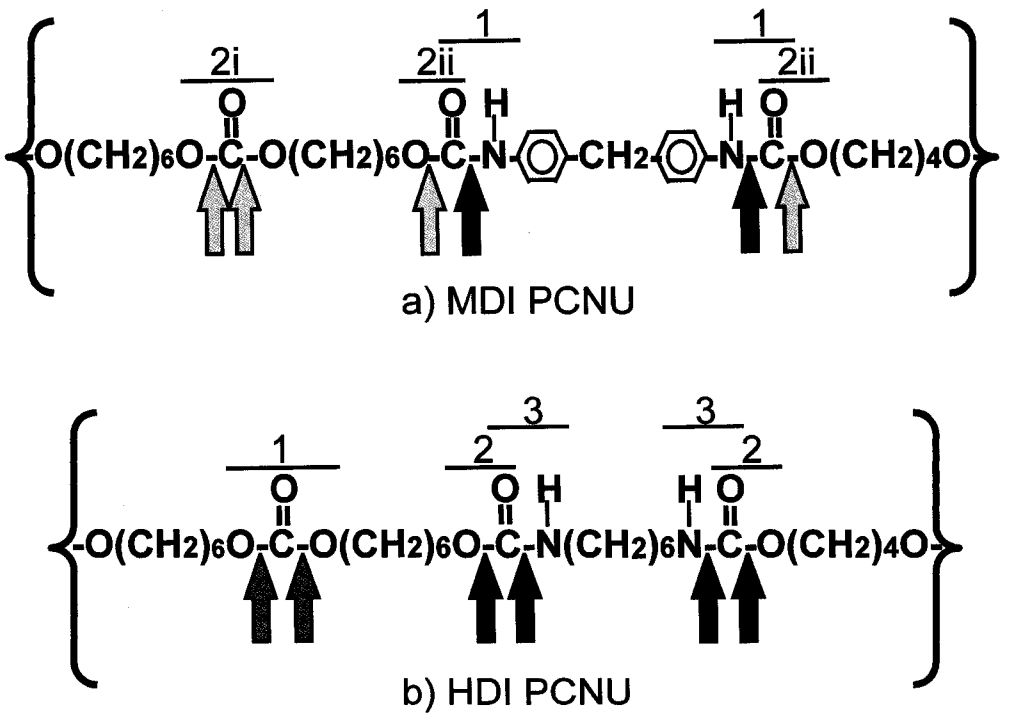

Figure 1.3: PCNU sites susceptible to hydrolytic cleavage by MSE/CXE or CE. Each arrow represents a potential site of cleavage on either (a) an MDI-based PCNU or (b) an HDI-based PCNU. (a) MDI PCNUs are the most susceptible to cleavage of the 1) urethane bond (40%) compared to the 2i) soft segment carbonate or 2ii) the carbonate bond attached to the urethane linkage (both 30%). (b) HDI PCNUs are susceptible to cleavage of the 1) soft segment carbonate bond (44-50%), then 2) the carbonate adjacent to the urethane bond (38.9%) and the least susceptible at 3) the urethane bond (11-16%) (48).

Since increasing hard segment content decreases the number of total carbonate bonds available for cleavage, overall degradation is inhibited.

1.3.5 INFLAMMATORY SIGNALING PATHWAYS

Investigation of key players in cell signaling pathways hopefully will help elucidate the mechanism of MDM-mediated biodegradation of biomaterials and polyurethanes in particular. One of the signaling pathways of interest has been the PLA_2 pathway. PLA_2 enzymes hydrolyze the *sn*-2 ester bond of cell membrane glycerophospholipids to release arachidonic acid (169), a precursor for pro-inflammatory molecules. Asbestos has been shown to induce arachidonic acid release and prostaglandin synthesis in P388D1 macrophage-like cells (170). Recently a role for the PLA_2 pathway in the macrophage-mediated degradation of polyurethanes (68, 73, 155, 171-173) was established. Previously, it has been shown that inhibiting PLA_2 with aristolochic acid or quinacrine could decrease neutrophil (73) and MDM-mediated (155) polyurethane degradation. PKC has previously been found to be involved in the activation of the PLA_2 pathway (174-179). Mouse macrophage studies have found that activating specific PKC isoforms with zymosan or PMA stimulated arachidonic acid production (174, 175, 177). Arachidonic acid release in MDM has been shown to stimulate NADPH oxidase and the respiratory burst through PKC activation (180-184). This along with the fact that PKC activation had been shown to affect neutrophil-mediated polyurethane degradation (73) made PKCs useful targets in the further study of the foreign body response to a biomaterial.

1.3.5.1 PROTEIN KINASE C

The PKC family of serine/threonine kinases mediate various cellular processes associated with cell growth, mRNA stabilization (185), differentiation (157, 186), and cell death via apoptosis (186-189). There are three main types of PKCs: conventional PKCs, novel PKCs, and atypical PKCs (190). Conventional PKC isoforms (PKC-α, -βI, -βII, -γ) are activated by phosphatidylserine, diacylglycerol (DAG), and phorbol esters in a calcium-dependent manner. Novel PKC isoforms (PKC-ε, -η, -δ, and -θ) are activated by phosphatidylserine, DAG and phorbol esters but do not require calcium for activation (deemed calcium-independent). Atypical PKC isoforms (PKC-ι, -μ, and -ζ) are calcium-independent and do not respond to DAG or phorbol ester activation. In conventional and novel PKCs, phorbol esters compete for the DAG binding site.

DAG is a lipid second messenger produced by lipid biosynthesis and lipid turnover. Both DAG and phorbol esters recruit PKC to the membrane where it can associate with phosphatidylserine and become an active kinase (191). Previously it has been shown that PKC isozymes -α, –β, –δ, –ε, –θ, –ι, –ζ, and –λ are present in human MDM but not PKC-γ, –η, or –μ (192). Phorbol esters like PMA with the C-4 hydroxyl in the β position (4-β phorbol esters) are diterpene esters of plant origin that override the DAG second messenger system and activate PKC; however, those phorbol esters with the C-4 hydroxyl in the α-position do not activate PKC (4-α phorbol esters, i.e. 4αPMA) (193). Some studies use 4-α phorbol esters as a negative control for the 4-β phorbol esters to prove that PKC is involved in diverse cellular processes such as actin assembly in neutrophils and monocyte attachment to endothelium (194, 195).

Since there are many isoforms of PKC, there are different inhibitors of PKC that target these PKC isoforms, specific types of PKC isoforms (conventional, novel or atypical PKCs) or protein kinases in general. H-7 is a non-specific PKC inhibitor that can also inhibit protein kinase A. Previously, it was found that H-7 did not fully reverse the effects of PKC activation by PMA (196). Bisindolylmaleimide I (BIM) has been shown to be a specific inhibitor for conventional and novel PKC isoforms that inhibits PKC by competitively binding to the adenosine triphosphate (ATP) binding site (197). BIM was developed by chemically modifying the general kinase inhibitor, staurosporine, in order to make it more selective for PKC (197). Synthetic inhibitors of PKC isoforms are also available. For example, Go6976 is an inhibitor selective for PKCα (174), LY333531 is an inhibitor selective for PKCβ (198) and rottlerin is an inhibitor selective for PKCδ (199). Other signaling studies have used various techniques such as the expression of dominant-negative PKC proteins (189), anti-sense oligonucleotides (38), or over-expression of specific PKC isoforms (189) in order to tease out the importance of specific PKC isoforms. However, these studies are easily done with a cell line as compared to transfection of primary cells such as the human MDM, which is considerably more difficult. In this thesis, the potentially important PKC isoforms that can be activated by PMA and are present in MDM are PKC-α, -βI, -βII, -δ, -ε, and –θ, however there were no experiments performed to specifically identify the different isoforms up-regulated in MDM on the surfaces with or without PMA.

1.3.5.2 THE RESPIRATORY BURST

PMA activates several PKCs and therefore has the possibility of phosphorylating more than one substrate. Another important biological pathway that PKC is involved in is the respiratory burst (see Figure 1.4). PKC phosphorylates the p47-*phox* cytosolic subunit of NADPH oxidase. This helps translocate the subunit to the membrane where it assembles to form the active NADPH oxidase complex consisting of p67-*phox*, $p21^{rac1}$ (Rac-related guanine triphosphate (GTP) binding protein) and the membrane-bound cytochrome *b*-558 (39, 200). NADPH oxidase activity can be down regulated when p40-*phox* competes with p67-*phox* and binds p47-*phox*'s proline-rich C-terminal tail (via Src homology domain-3, SH3) (201). In the neutrophil-mediated biodegradation of polyurethanes, PMA inhibited the radiolabel release from neutrophils seeded on ^{14}C-radiolabeled poly (ester) polyurethanes whereas the PKC inhibitor H7 and myeloperoxidase inhibitor sodium azide (NaN_3) had no effect (73). However, the inhibition of radiolabel release by PMA could be reversed by using PMA in the presence of H7 or NaN_3 (152). The radiolabel release inhibition coincided with an increase in H_2O_2 release and formation of HOCl. This study suggested there was a relationship between oxidation and the release of polymer degradation products, but this relationship was complex since oxidation did not increase but inhibited chain lysis.

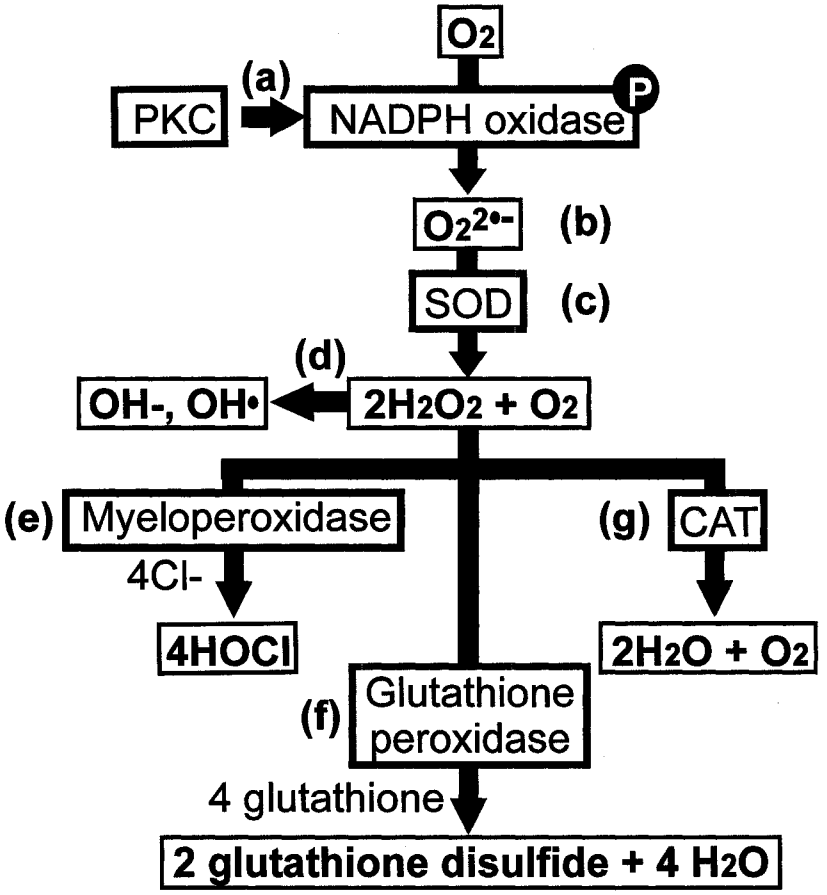

Figure 1.4: The respiratory burst in phagocytic cells. (a) PKC phosphorylates the p47 phox subunit of NADPH oxidase to activate the complex assembly. (b) The activated NADPH oxidase complex catalyzes the conversion of oxygen (O_2) to superoxide anion (O_2^{2-}). (c) Superoxide dismutase catalyzes the conversion of superoxide anion to hydrogen peroxide (H_2O_2). The hydrogen peroxide produced can have different fates. (d) Hydrogen peroxide can be reduced to hydroxyl, hydroxyl radicals or singlet oxygen, all of which can provoke tissue injury or alter material surface chemistry. (e) Hydrogen peroxide in the presence of halides like chloride ions can be converted to hypochlorous acid by myeloperoxidase (in neutrophils and monocytes). Hydrogen peroxide can be reduced to H_2O by: (f) glutathionine peroxidases or (g) catalase.

Phagocytes such as neutrophils, eosinophils, monocytes and MDMs can be stimulated to produce many different types of reactive species, including: radical and non-radical ROS, radical and non-radical reactive nitrogen species, non-radical reactive bromine species, and non-radical reactive chlorine species (202). Some species are more reactive than others. The hydroxyl radical is the most reactive species and is the product of the breakdown of several other reactive species including H_2O_2 and HOCl (202). HOCl has been found to oxidize the surface of the polyurethane affecting its susceptibility to hydrolytic degradation (152), however HOCl is formed in neutrophils and monocytes by myeloperoxidase, an enzyme that is absent in MDM (203).

In order to protect the phagocyte from damage by oxidants different mechanisms of excess oxidant removal have evolved. Human monocytes have been found to induce a glutathione transporter when H_2O_2 is released in the cell so that glutathione peroxidase in the presence of glutathione can reduce H_2O_2 to water and glutathione disulfide (204). Catalase is a known H_2O_2 scavenger that catalyzes the conversion of H_2O_2 to water and oxygen. It has been shown that without activation, MDM *in vitro* have a reduced capacity to secrete superoxide anion and H_2O_2 compared to human monocytes (203) suggesting that differentiation alone cannot induce the respiratory burst.

1.4 SUMMARY

The MDM-mediated biodegradation of PCNUs or biomaterials in general is only partially understood. The studies described in this thesis used the PKC activating phorbol ester PMA to investigate the effect of material chemistry on the MDM-mediated degradation of PCNUs. The goal of this thesis was to understand the link between hydrolytic and oxidative mechanisms of MDM-mediated PCNU degradation through an in-depth study of PKC. It was hypothesized that PKC modulation would affect these pathways in a material surface dependent manner, since PKC activation is an important source of oxidizing compounds. MSE and CE are hydrolytic enzymes that are candidates for degradation, but few studies have investigated the link between hydrolytic enzymes and oxidation by ROS. Since *in vivo* neutrophils, monocytes and MDM all produce ROS when a material comes into contact with tissues and/or blood, it is necessary to determine if these ROS aid or hamper the degradation of PCNUs by hydrolytic enzymes. Combining both of these inflammatory activities into one model provided significant new information helping to elucidate the overall mechanism of MDM-mediated biodegradation of biomaterials, specifically PCNUs.

1.5 REFERENCES

1. Santerre JP, Woodhouse K, Laroche G, Labow RS. Understanding the biodegradation of polyurethanes: from classical implants to tissue engineering materials. Biomaterials 2005;26(35):7457-70.

2. von Recum AF, LaBerge M. Educational goals for biomaterials science and engineering: prospective view. J Appl Biomater 1995;6(2):137-44.

3. Belanger MC, Marois Y. Hemocompatibility, biocompatibility, inflammatory and in vivo studies of primary reference materials low-density polyethylene and polydimethylsiloxane: a review. J Biomed Mater Res 2001;58(5):467-77.

4. Metcalfe AD, Ferguson MW. Tissue engineering of replacement skin: the crossroads of biomaterials, wound healing, embryonic development, stem cells and regeneration. J R Soc Interface 2007;4(14):413-37.

5. Anderson JM, Miller KM. Biomaterial biocompatibility and the macrophage. Biomaterials 1984;5(1):5-10.

6. Finer Y, Jaffer F, Santerre JP. Mutual influence of cholesterol esterase and pseudocholinesterase on the biodegradation of dental composites. Biomaterials 2004;25(10):1787-93.

7. Finer Y, Santerre JP. The influence of resin chemistry on a dental composite's biodegradation. J Biomed Mater Res A 2004;69(2):233-46.

8. Yang L, Hong J, Wang J, Pilliar RM, Santerre JP. Influence of anionic monomer content on the biodegradation and toxicity of polyvinyl-urethane carbonate-ceramic interpenetrating phase composites. Biomaterials 2005;26(30):5951-9.

9. Belanger MC, Marois Y, Roy R, Mehri Y, Wagner E, Zhang Z, et al. Selection of a polyurethane membrane for the manufacture of ventricles for a totally implantable artificial heart: blood compatibility and biocompatibility studies. Artif Organs 2000;24(11):879-88.

10. Wheatley DJ, Raco L, Bernacca GM, Sim I, Belcher PR, Boyd JS. Polyurethane: material for the next generation of heart valve prostheses? Eur J Cardiothorac Surg 2000;17(4):440-8.

11. Bischoff F. Organic polymer biocompatibility and toxicology. Clin Chem 1972;18(9):869-94.

12. Carson RJ, Edwards A, Szycher M. Resistance to biodegradative stress cracking in microporous vascular access grafts. J Biomater Appl 1996;11(2):121-34.

13. Rubens FD, Labow RS, Meek E, Dudani AK, Ganz PR. Tissue factor expression by cells used for sodding of prosthetic vascular grafts. J Surg Res 1997;72(1):22-8.

14. Shin CK, Rodino W, Kirwin JD, Ramirez JA, Wisselink W, Papierman G, et al. Histology and electron microscopy of explanted bifurcated endovascular aortic grafts: evidence of early incorporation and healing. J Endovasc Surg 1999;6(3):246-50.

15. Wiggins MJ, Wilkoff B, Anderson JM, Hiltner A. Biodegradation of polyether polyurethane inner insulation in bipolar pacemaker leads. J Biomed Mater Res 2001;58(3):302-7.

16. Taksali S, Grauer JN, Vaccaro AR. Material considerations for intervertebral disc replacement implants. Spine J 2004;4(6 Suppl):231S-238S.

17. Linti C, Zipfel A, Schenk M, Dauner M, Doser M, Viebahn R, et al. Cultivation of porcine hepatocytes in polyurethane nonwovens as part of a biohybrid liver support system. Int J Artif Organs 2002;25(10):994-1000.

18. Abou-Chebl A, Bashir Q, Yadav JS. Drug-Eluting Stents for the Treatment of Intracranial Atherosclerosis. Initial Experience and Midterm Angiographic Follow-up. Stroke 2005;36:e165-e168.

19. Lee YK, Hyung Park J, Tae Moon H, Yun Lee D, Han Yun J, Byun Y. The short-term effects on restenosis and thrombosis of echinomycin-eluting stents topcoated with a hydrophobic heparin-containing polymer. Biomaterials 2007;28(8):1523-30.

20. Quizhpe AR, Feres F, de Ribamar Costa J, Jr., Abizaid A, Maldonado G, Costa R, et al. Drug-eluting stents vs bare metal stents for the treatment of large coronary vessels. Am Heart J 2007;154(2):373-8.

21. Grad S, Kupcsik L, Gorna K, Gogolewski S, Alini M. The use of biodegradable polyurethane scaffolds for cartilage tissue engineering: potential and limitations. Biomaterials 2003;24(28):5163-71.

22. Buma P, Ramrattan NN, van Tienen TG, Veth RP. Tissue engineering of the meniscus. Biomaterials 2004;25(9):1523-32.

23. Saad B, Casotti M, Huber T, Schmutz P, Welti M, Uhlschmid GK, et al. In vitro evaluation of the biofunctionality of osteoblasts cultured on DegraPol-foam. J Biomater Sci Polym Ed 2000;11(8):787-800.

24. Zhang J, Doll BA, Beckman EJ, Hollinger JO. A biodegradable polyurethane-ascorbic acid scaffold for bone tissue engineering. J Biomed Mater Res A 2003;67(2):389-400.

25. Bruin P, Smedinga J, Pennings AJ, Jonkman MF. Biodegradable lysine diisocyanate-based poly(glycolide-co-epsilon-caprolactone)-urethane network in artificial skin. Biomaterials 1990;11(4):291-5.

26. Guan J, Sacks MS, Beckman EJ, Wagner WR. Synthesis, characterization, and cytocompatibility of elastomeric, biodegradable poly(ester-urethane)ureas based on poly(caprolactone) and putrescine. J Biomed Mater Res 2002;61(3):493-503.

27. Gunatillake PA, Adhikari R. Biodegradable synthetic polymers for tissue engineering. Eur Cell Mater 2003;5:1-16; discussion 16.

28. Zhang JY, Beckman EJ, Hu J, Yang GG, Agarwal S, Hollinger JO. Synthesis, biodegradability, and biocompatibility of lysine diisocyanate-glucose polymers. Tissue Eng 2002;8(5):771-85.

29. Petrini P, Fare S, Piva A, Tanzi MC. Design, synthesis and properties of polyurethane hydrogels for tissue engineering. J Mater Sci Mater Med 2003;14(8):683-6.

30. Zhang JY, Beckman EJ, Piesco NP, Agarwal S. A new peptide-based urethane polymer: synthesis, biodegradation, and potential to support cell growth in vitro. Biomaterials 2000;21(12):1247-58.

31. Matheson LA, McBane JE, Malowany JI, Santerre JP, Labow RS. Is cell culture stressful? Effects of degradable and nondegradable culture surfaces on U937 cell function. Biotechniques 2007;42(6):744, 746-50.

32. Anderson JM. Multinucleated giant cells. Curr Opin Hematol 2000;7(1):40-7.

33. Marchant RE, Miller KM, Anderson JM. In vivo biocompatibility studies. V. In vivo leukocyte interactions with Biomer. J Biomed Mater Res 1984;18(9):1169-90.

34. Mathur AB, Collier TO, Kao WJ, Wiggins M, Schubert MA, Hiltner A, et al. In vivo biocompatibility and biostability of modified polyurethanes. J Biomed Mater Res 1997;36(2):246-57.

35. Anderson JM. Mechanisms of inflammation and infection with implanted devices. Cardiovasc Pathol 1993;2(3):33S-41S.

36. Anderson JM. Inflammatory response to implants. ASAIO Trans 1988;34(2):101-7.

37. Labow RS, Meek E, Matheson LA, Santerre JP. Human macrophage-mediated biodegradation of polyurethanes: assessment of candidate enzyme activities. Biomaterials 2002;23(19):3969-75.

38. Bey EA, Xu B, Bhattacharjee A, Oldfield CM, Zhao X, Li Q, et al. Protein kinase C delta is required for p47phox phosphorylation and translocation in activated human monocytes. J Immunol 2004;173(9):5730-8.

39. Jackson SH, Gallin JI, Holland SM. The p47phox mouse knock-out model of chronic granulomatous disease. J Exp Med 1995;182(3):751-8.

40. Stokes K, McVenes R, Anderson JM. Polyurethane elastomer biostability. J Biomater Appl 1995;9(4):321-54.

41. Gunatillake PA, Martin DJ, Meijs GF, McCarthy SJ, Adhikari R. Designing Biostable Polyurethane Elastomers for Biomedical Implants. Aust J Chem 2003;56:545-557.

42. Shanmugam K, Subrahmanyam S, Tarakad SV, Kodandapani N, Stanly DF. 2,4-Toluene diamines--their carcinogenicity, biodegradation, analytical techniques and an approach towards development of biosensors. Anal Sci 2001;17(12):1369-74.

43. Santerre JP, Labow RS, Duguay DG, Erfle D, Adams GA. Biodegradation evaluation of polyether and polyester-urethanes with oxidative and hydrolytic enzymes. J Biomed Mater Res 1994;28(10):1187-99.

44. Wang GB, Labow RS, Santerre JP. Biodegradation of a poly(ester)urea-urethane by cholesterol esterase: isolation and identification of principal biodegradation products. J Biomed Mater Res 1997;36(3):407-17.

45. Leong BK, Lund JE, Groehn JA, Coombs JK, Sabaitis CP, Weaver RJ, et al. Retinopathy from inhaling 4,4'-methylenedianiline aerosols. Fundam Appl Toxicol 1987;9(4):645-58.

46. Tillmann HL, van Pelt FN, Martz W, Luecke T, Welp H, Dorries F, et al. Accidental intoxication with methylene dianiline p,p'-diaminodiphenylmethane: acute liver damage after presumed ecstasy consumption. J Toxicol Clin Toxicol 1997;35(1):35-40.

47. Weisburger EK, Murthy AS, Lilja HS, Lamb JCt. Neoplastic response of F344 rats and B6C3F1 mice to the polymer and dyestuff intermediates 4,4'-methylenebis(N,N-dimethyl)-benzenamine, 4,4'-oxydianiline, and 4,4'-methylenedianiline. J Natl Cancer Inst 1984;72(6):1457-63.

48. Tang YW, Labow RS, Santerre JP. Isolation of methylene dianiline and aqueous-soluble biodegradation products from polycarbonate-polyurethanes. Biomaterials 2003;24(17):2805-19.

49. Woo GL, Mittelman MW, Santerre JP. Synthesis and characterization of a novel biodegradable antimicrobial polymer. Biomaterials 2000;21(12):1235-46.

50. Saad B, Hirt TD, Welti M, Uhlschmid GK, Neuenschwander P, Suter UW. Development of degradable polyesterurethanes for medical applications: in vitro and in vivo evaluations. J Biomed Mater Res 1997;36(1):65-74.

51. Abraham GA, Marcos-Fernandez A, Roman JS. Bioresorbable poly(ester-ether urethane)s from L-lysine diisocyanate and triblock copolymers with different hydrophilic character. J Biomed Mater Res A 2006;76(4):729-36.

52. Ernsting MJ, Labow RS, Santerre JP. Surface modification of a polycarbonate-urethane using a vitamin-E-derivatized fluoroalkyl surface modifier. J Biomater Sci Polym Ed 2003;14(12):1411-26.

53. Zhang C, Zhang N, Wen X. Synthesis and characterization of biocompatible, degradable, light-curable, polyurethane-based elastic hydrogels. J Biomed Mater Res A 2007;82(3):637-50.

54. Guelcher S, Srinivasan A, Hafeman A, Gallagher K, Doctor J, Khetan S, et al. Synthesis, in vitro degradation, and mechanical properties of two-component poly(ester urethane)urea scaffolds: effects of water and polyol composition. Tissue Eng 2007;13(9):2321-33.

55. Batich C, Williams J, King R. Toxic hydrolysis product from a biodegradable foam implant. J Biomed Mater Res 1989;23(A3 Suppl):311-9.

56. Takahara A, Coury AJ, Hergenrother RW, Cooper SL. Effect of soft segment chemistry on the biostability of segmented polyurethanes. I. In vitro oxidation. J Biomed Mater Res 1991;25(3):341-56.

57. Boretos JW, Pierce WS. Segmented polyurethane: a polyether polymer. An initial evaluation for biomedical applications. J Biomed Mater Res 1968;2(1):121-30.

58. Haugen H, Gerhardt LC, Will J, Wintermantel E. Biostability of polyether-urethane scaffolds: a comparison of two novel processing methods and the effect of higher gamma-irradiation dose. J Biomed Mater Res B Appl Biomater 2005;73(2):229-37.

59. Tanzi MC, Mantovani D, Petrini P, Guidoin R, Laroche G. Chemical stability of polyether urethanes versus polycarbonate urethanes. J Biomed Mater Res 1997;36(4):550-9.

60. Christenson EM, Dadsetan M, Wiggins M, Anderson JM, Hiltner A. Poly(carbonate urethane) and poly(ether urethane) biodegradation: in vivo studies. J Biomed Mater Res A 2004;69(3):407-16.

61. Szelest-Lewandowska A, Masiulanis B, Szymonowicz M, Pielka S, Paluch D. Modified polycarbonate urethane: synthesis, properties and biological investigation in vitro. J Biomed Mater Res A 2007;82(2):509-20.

62. Tang YW, Labow RS, Santerre JP. Enzyme-induced biodegradation of polycarbonate-polyurethanes: dependence on hard-segment chemistry. J Biomed Mater Res 2001;57(4):597-611.

63. Tang YW, Labow RS, Santerre JP. Enzyme-induced biodegradation of polycarbonate polyurethanes: dependence on hard-segment concentration. J Biomed Mater Res 2001;56(4):516-28.

64. Labow RS, Meek E, Santerre JP. Hydrolytic degradation of poly(carbonate)-urethanes by monocyte-derived macrophages. Biomaterials 2001;22(22):3025-33.

65. Labow RS, Sa D, Matheson LA, Santerre JP. Polycarbonate-urethane hard segment type influences esterase substrate specificity for human macrophage mediated biodegradation. J Biomater Sci Polym Ed 2005;16(9):1167-1177.

66. Matheson LA, Santerre JP, Labow RS. Changes in macrophage function and morphology due to biomedical polyurethane surfaces undergoing biodegradation. J Cell Physiol 2004;199(1):8-19.

67. Labow RS, Sa D, Matheson LA, Dinnes DL, Santerre JP. The human macrophage response during differentiation and biodegradation on polycarbonate-based polyurethanes: dependence on hard segment chemistry. Biomaterials 2005;26(35):7357-66.

68. Dinnes DL, Paul Santerre J, Labow RS. Phospholipase A(2) pathway association with macrophage-mediated polycarbonate-urethane biodegradation. Biomaterials 2005;26(18):3881-9.

69. Cannon GJ, Swanson JA. The macrophage capacity for phagocytosis. J Cell Sci 1992;101 (Pt 4):907-13.

70. Heiple JM, Wright SD, Allen NS, Silverstein SC. Macrophages form circular zones of very close apposition to IgG-coated surfaces. Cell Motil Cytoskeleton 1990;15(4):260-70.

71. Kruskal BA, Maxfield FR. Cytosolic free calcium increases before and oscillates during frustrated phagocytosis in macrophages. J Cell Biol 1987;105(6 Pt 1):2685-93.

72. Labow RS, Erfle DJ, Santerre JP. Neutrophil-mediated degradation of segmented polyurethanes. Biomaterials 1995;16(1):51-9.

73. Labow RS, Meek E, Santerre JP. Neutrophil-mediated biodegradation of medical implant materials. J Cell Physiol 2001;186(1):95-103.

74. Labow RS, Meek E, Santerre JP. The biodegradation of poly(urethane)s by the esterolytic activity of serine proteases and oxidative enzyme systems. J Biomater Sci Polym Ed 1999;10(7):699-713.

75. Tang YW, Labow RS, Santerre JP. Enzyme induced biodegradation of polycarbonate-polyurethanes: dose dependence effect of cholesterol esterase. Biomaterials 2003;24(12):2003-11.

76. Marchant R, Hiltner A, Hamlin C, Rabinovitch A, Slobodkin R, Anderson JM. In vivo biocompatibility studies. I. The cage implant system and a biodegradable hydrogel. J Biomed Mater Res 1983;17(2):301-25.

77. Marchant RE, Anderson JM, Dillingham EO. In vivo biocompatibility studies. VII. Inflammatory response to polyethylene and to a cytotoxic polyvinylchloride. J Biomed Mater Res 1986;20(1):37-50.

78. Anderson JM, Bonfield TL, Ziats NP. Protein adsorption and cellular adhesion and activation on biomedical polymers. Int J Artif Organs 1990;13(6):375-82.

79. Bonfield TL, Colton E, Anderson JM. Plasma protein adsorbed biomedical polymers: activation of human monocytes and induction of interleukin 1. J Biomed Mater Res 1989;23(6):535-48.

80. Park JH, Bae YH. Hydrogels based on poly(ethylene oxide) and poly(tetramethylene oxide) or poly(dimethyl siloxane): synthesis, characterization, in vitro protein adsorption and platelet adhesion. Biomaterials 2002;23(8):1797-808.

81. DeFife KM, Yun JK, Azeez A, Stack S, Ishihara K, Nakabayashi N, et al. Adhesion and cytokine production by monocytes on poly(2-methacryloyloxyethyl phosphorylcholine-co-alkyl methacrylate)-coated polymers. J Biomed Mater Res 1995;29(4):431-9.

82. Anderson JM, DeFife KM, McNally AK, Collier TO, Jenney CR. Monocyte, macrophage and foreign body giant cell interactions with molecularly engineered surfaces. Journal of materials science: materials in medicine 1999;10:579-588.

83. Mulzer SR, Brash JL. Identification of plasma proteins adsorbed to hemodialyzers during clinical use. J Biomed Mater Res 1989;23(12):1483-504.

84. Fabrizius-Homan DJ, Cooper SL. Competitive adsorption of vitronectin with albumin, fibrinogen, and fibronectin on polymeric biomaterials. J Biomed Mater Res 1991;25(8):953-71.

85. Archambault JG, Brash JL. Protein resistant polyurethane surfaces by chemical grafting of PEO: amino-terminated PEO as grafting reagent. Colloids Surf B Biointerfaces 2004;39(1-2):9-16.

86. Kao WJ. Evaluation of leukocyte adhesion on polyurethanes: the effects of shear stress and blood proteins. Biomaterials 2000;21(22):2295-303.

87. Wu Y, Simonovsky FI, Ratner BD, Horbett TA. The role of adsorbed fibrinogen in platelet adhesion to polyurethane surfaces: a comparison of surface hydrophobicity, protein adsorption, monoclonal antibody binding, and platelet adhesion. J Biomed Mater Res A 2005;74(4):722-38.

88. Massa TM, Yang ML, Ho JY, Brash JL, Santerre JP. Fibrinogen surface distribution correlates to platelet adhesion pattern on fluorinated surface-modified polyetherurethane. Biomaterials 2005;26(35):7367-76.

89. Sundaram S, Lim F, Cooper SL, Colman RW. Role of leucocytes in coagulation induced by artificial surfaces: investigation of expression of Mac-1, granulocyte elastase release and leucocyte adhesion on modified polyurethanes. Biomaterials 1996;17(10):1041-7.

90. Perianayagam MC, Balakrishnan VS, King AJ, Pereira BJ, Jaber BL. C5a delays apoptosis of human neutrophils by a phosphatidylinositol 3-kinase-signaling pathway. Kidney Int 2002;61(2):456-63.

91. Labow RS, Meek E, Santerre JP. Model systems to assess the destructive potential of human neutrophils and monocyte-derived macrophages during the acute and chronic phases of inflammation. J Biomed Mater Res 2001;54(2):189-97.

92. Issekutz TB, Issekutz AC, Movat HZ. The in vivo quantitation and kinetics of monocyte migration into acute inflammatory tissue. Am J Pathol 1981;103(1):47-55.

93. Brodbeck WG, Shive MS, Colton E, Ziats NP, Anderson JM. Interleukin-4 inhibits tumor necrosis factor-alpha-induced and spontaneous apoptosis of biomaterial-adherent macrophages. J Lab Clin Med 2002;139(2):90-100.

94. Brodbeck WG, Shive MS, Colton E, Nakayama Y, Matsuda T, Anderson JM. Influence of biomaterial surface chemistry on the apoptosis of adherent cells. J Biomed Mater Res 2001;55(4):661-8.

95. Jenney CR, DeFife KM, Colton E, Anderson JM. Human monocyte/macrophage adhesion, macrophage motility, and IL-4-induced foreign body giant cell formation on silane-modified surfaces in vitro. Student Research Award in the Master's Degree Candidate Category, 24th Annual Meeting of the Society for Biomaterials, San Diego, CA, April 22-26, 1998. J Biomed Mater Res 1998;41(2):171-84.

96. Kao WJ, McNally AK, Hiltner A, Anderson JM. Role for interleukin-4 in foreign-body giant cell formation on a poly(etherurethane urea) in vivo. J Biomed Mater Res 1995;29(10):1267-75.

97. DeFife KM, Jenney CR, Colton E, Anderson JM. Cytoskeletal and adhesive structural polarizations accompany IL-13-induced human macrophage fusion. J Histochem Cytochem 1999;47(1):65-74.

98. Linder S, Aepfelbacher M. Podosomes: adhesion hot-spots of invasive cells. Trends Cell Biol 2003;13(7):376-85.

99. Johansson MW, Lye MH, Barthel SR, Duffy AK, Annis DS, Mosher DF. Eosinophils adhere to vascular cell adhesion molecule-1 via podosomes. Am J Respir Cell Mol Biol 2004;31(4):413-22.

100. Buccione R, Orth JD, McNiven MA. Foot and mouth: podosomes, invadopodia and circular dorsal ruffles. Nat Rev Mol Cell Biol 2004;5(8):647-57.

101. Jacob JT, Gebhardt BM, Lewando J. Synthetic scleral reinforcement materials. II. Collagen types in the fibrous capsule. J Biomed Mater Res 1996;32(2):181-6.

102. Gretzer C, Emanuelsson L, Liljensten E, Thomsen P. The inflammatory cell influx and cytokines changes during transition from acute inflammation to fibrous repair around implanted materials. J Biomater Sci Polym Ed 2006;17(6):669-87.

103. Bocchiotti G, Verna G, Fracalvieri M, Fanton E, Datta G, Robotti E. Carbofilm-covered prostheses in plastic surgery: preliminary observations. Plast Reconstr Surg 1993;91(1):80-8; discussion 89-90.

104. Bucky LP, Ehrlich HP, Sohoni S, May JW, Jr. The capsule quality of saline-filled smooth silicone, textured silicone, and polyurethane implants in rabbits: a long-term study. Plast Reconstr Surg 1994;93(6):1123-31; discussion 1132-3.

105. Carvalho TL, Araujo CA, Teofilo JM, Brentegani LG. Histologic and histometric evaluation of rat alveolar wound healing around polyurethane resin implants. Int J Oral Maxillofac Surg 1997;26(2):149-52.

106. Imber G, Schwager RG, Guthrie RH, Jr., Gray GF. Fibrous capsule formation after subcutaneous implanation of synthetic materials in experimental animals. Plast Reconstr Surg 1974;54(2):183-6.

107. Zhang YZ, Bjursten LM, Freij-Larsson C, Kober M, Wesslen B. Tissue response to commercial silicone and polyurethane elastomers after different sterilization procedures. Biomaterials 1996;17(23):2265-72.

108. Bakker D, van Blitterswijk CA, Hesseling SC, Grote JJ. Effect of implantation site on phagocyte/polymer interaction and fibrous capsule formation. Biomaterials 1988;9(1):14-23.

109. Duffield JS. The inflammatory macrophage: a story of Jekyll and Hyde. Clin Sci (Lond) 2003;104(1):27-38.

110. Hou FF, Boyce J, Zhang Y, Owen WF, Jr. Phenotypic and functional characteristics of macrophage-like cells differentiated in pro-inflammatory cytokine-containing cultures. Immunol Cell Biol 2000;78(3):205-13.

111. Bonfield TL, Anderson JM. Functional versus quantitative comparison of IL-1 beta from monocytes/macrophages on biomedical polymers. J Biomed Mater Res 1993;27(9):1195-9.

112. Boynton EL, Waddell J, Meek E, Labow RS, Edwards V, Santerre JP. The effect of polyethylene particle chemistry on human monocyte-macrophage function in vitro. J Biomed Mater Res 2000;52(2):239-45.

113. Rubio MA, Lopez-Rodriguez C, Nueda A, Aller P, Armesilla AL, Vega MA, et al. Granulocyte-macrophage colony-stimulating factor, phorbol ester, and sodium butyrate induce the CD11c integrin gene promoter activity during myeloid cell differentiation. Blood 1995;86(10):3715-24.

114. Deszo EL, Brake DK, Cengel KA, Kelley KW, Freund GG. CD45 negatively regulates monocytic cell differentiation by inhibiting phorbol 12-myristate 13-acetate-dependent activation and tyrosine phosphorylation of protein kinase Cdelta. J Biol Chem 2001;276(13):10212-7.

115. Monick MM, Carter AB, Gudmundsson G, Geist LJ, Hunninghake GW. Changes in PKC isoforms in human alveolar macrophages compared with blood monocytes. Am J Physiol 1998;275(2 Pt 1):L389-97.

116. Dinnes DL, Santerre JP, Labow RS. The influence of biodegradable and non-degradable material surfaces on differentiating human monocyte-derived macrophages. Differentiation 2007;In press.

117. Hayman AR, Bune AJ, Bradley JR, Rashbass J, Cox TM. Osteoclastic tartrate-resistant acid phosphatase (Acp 5): its localization to dendritic cells and diverse murine tissues. J Histochem Cytochem 2000;48(2):219-28.

118. Hayman AR, Cox TM. Tartrate-resistant acid phosphatase knockout mice. J Bone Miner Res 2003;18(10):1905-7.

119. Schlesinger L, Musson RA, Johnston RB, Jr. Functional and biochemical studies of multinucleated giant cells derived from the culture of human monocytes. J Exp Med 1984;159(4):1289-94.

120. Brunstedt MR, Anderson JM, Spilizewski KL, Marchant RE, Hiltner A. In vivo leucocyte interactions on Pellethane surfaces. Biomaterials 1990;11(6):370-8.

121. Matheson LA, Jack Fairbank N, Maksym GN, Paul Santerre J, Labow RS. Characterization of the Flexcell Uniflex cyclic strain culture system with U937 macrophage-like cells. Biomaterials 2006;27(2):226-33.

122. Matheson LA, Maksym GN, Santerre JP, Labow RS. Cyclic biaxial strain affects U937 macrophage-like morphology and enzymatic activities. J Biomed Mater Res A 2006;76(1):52-62.

123. Zenni GC, Ellinger J, Lam TM, Greisler HP. Biomaterial-induced macrophage activation and monokine release. J Invest Surg 1994;7(2):135-41.

124. Matheson LA, Maksym GN, Santerre JP, Labow RS. The functional response of U937 macrophage-like cells is modulated by extracellular matrix proteins and mechanical strain. Biochem Cell Biol 2006;84(5):763-73.

125. Yan SF, Ramasamy R, Bucciarelli LG, Wendt T, Lee LK, Hudson BI, et al. RAGE and its ligands: a lasting memory in diabetic complications? Diab Vasc Dis Res 2004;1(1):10-20.

126. Kokkola R, Andersson A, Mullins G, Ostberg T, Treutiger CJ, Arnold B, et al. RAGE is the major receptor for the proinflammatory activity of HMGB1 in rodent macrophages. Scand J Immunol 2005;61(1):1-9.

127. Kalinina N, Agrotis A, Antropova Y, DiVitto G, Kanellakis P, Kostolias G, et al. Increased expression of the DNA-binding cytokine HMGB1 in human atherosclerotic lesions: role of activated macrophages and cytokines. Arterioscler Thromb Vasc Biol 2004;24(12):2320-5.

128. Li W, Sama AE, Wang H. Role of HMGB1 in cardiovascular diseases. Curr Opin Pharmacol 2006;6(2):130-5.

129. Jiang W, Pisetsky DS. Mechanisms of Disease: the role of high-mobility group protein 1 in the pathogenesis of inflammatory arthritis. Nat Clin Pract Rheumatol 2007;3(1):52-8.

130. Dong Xda E, Ito N, Lotze MT, Demarco RA, Popovic P, Shand SH, et al. High mobility group box I (HMGB1) release from tumor cells after treatment: implications for development of targeted chemoimmunotherapy. J Immunother (1997) 2007;30(6):596-606.

131. Choi YR, Kim H, Kang HJ, Kim NG, Kim JJ, Park KS, et al. Overexpression of high mobility group box 1 in gastrointestinal stromal tumors with KIT mutation. Cancer Res 2003;63(9):2188-93.

132. El Gazzar M. HMGB1 modulates inflammatory responses in LPS-activated macrophages. Inflamm Res 2007;56(4):162-7.

133. Tang D, Shi Y, Kang R, Li T, Xiao W, Wang H, et al. Hydrogen peroxide stimulates macrophages and monocytes to actively release HMGB1. J Leukoc Biol 2007;81(3):741-7.

134. Kim CH, Han SI, Lee SY, Youk HS, Moon JY, Duong HQ, et al. Protein kinase C-ERK1/2 signal pathway switches glucose depletion-induced necrosis to apoptosis by regulating superoxide dismutases and suppressing reactive oxygen species production in A549 lung cancer cells. J Cell Physiol 2007;211(2):371-85.

135. Zuckerman ST, Kao WJ. LC/MS identification of 12 intracellular cytoskeletal and inflammatory proteins from monocytes adherent on surface-adsorbed fibronectin-derived peptides. J Biomed Mater Res A 2007; e-pub Aug 29.

136. Li F, Hui DY. Modified low density lipoprotein enhances the secretion of bile salt-stimulated cholesterol esterase by human monocyte-macrophages. species-specific difference in macrophage cholesteryl ester hydrolase. J Biol Chem 1997;272(45):28666-71.

137. Khoo JC, Mahoney EM, Steinberg D. Neutral cholesterol esterase activity in macrophages and its enhancement by cAMP-dependent protein kinase. J Biol Chem 1981;256(24):12659-61.

138. Hoeg JM, Demosky SJ, Jr., Pescovitz OH, Brewer HB, Jr. Cholesteryl ester storage disease and Wolman disease: phenotypic variants of lysosomal acid cholesteryl ester hydrolase deficiency. Am J Hum Genet 1984;36(6):1190-203.

139. Patel D, Hooper NM, Scott CS. Subcellular fractionation studies indicate an intracellular localization for human monocyte specific esterase (MSE). Br J Haematol 1993;84(4):608-14.

140. Scott CS, Patel D, Keen JN. Purification of human monocyte-specific esterase (MSE): molecular and kinetic characteristics. Br J Haematol 1992;81(4):470-9.

141. Scott CS, Linch DC, Bynoe AG, Allen C, Hogg N, Ainley MJ, et al. Electrophoretic and cytochemical characterization of alpha-naphthyl acetate esterases in acute myeloid leukemia: relationships with membrane receptor and monocyte-specific antigen expression. Blood 1984;63(3):579-87.

142. Saboori AM, Newcombe DS. Human monocyte carboxylesterase. Purification and kinetics. J Biol Chem 1990;265(32):19792-9.

143. Boyle C, Cosby SL, Markey GM, Alexander HD, Morris TC. Quantitative deficiency of monocyte-specific esterase (MSE) mRNA in monocyte esterase deficiency (MED). Br J Haematol 2000;110(3):699-703.

144. Andrade LO, Andrews NW. The Trypanosoma cruzi-host-cell interplay: location, invasion, retention. Nat Rev Microbiol 2005;3(10):819-23.

145. Tardieux I, Webster P, Ravesloot J, Boron W, Lunn JA, Heuser JE, et al. Lysosome recruitment and fusion are early events required for trypanosome invasion of mammalian cells. Cell 1992;71(7):1117-30.

146. Rodriguez A, Samoff E, Rioult MG, Chung A, Andrews NW. Host cell invasion by trypanosomes requires lysosomes and microtubule/kinesin-mediated transport. J Cell Biol 1996;134(2):349-62.

147. Khan I, Smith N, Jones E, Finch DS, Cameron RE. Analysis and evaluation of a biomedical polycarbonate urethane tested in an in vitro study and an ovine arthroplasty model. Part I: materials selection and evaluation. Biomaterials 2005;26(6):621-31.

148. Khan I, Smith N, Jones E, Finch DS, Cameron RE. Analysis and evaluation of a biomedical polycarbonate urethane tested in an in vitro study and an ovine arthroplasty model. Part II: in vivo investigation. Biomaterials 2005;26(6):633-43.

149. Ratner BD, Gladhill KW, Horbett TA. Analysis of in vitro enzymatic and oxidative degradation of polyurethanes. J Biomed Mater Res 1988;22(6):509-27.

150. Stokes K, Urbanski P, Upton J. The in vivo auto-oxidation of polyether polyurethane by metal ions. J Biomater Sci Polym Ed 1990;1(3):207-30.

151. Christenson EM, Anderson JM, Hiltner A. Oxidative mechanisms of poly(carbonate urethane) and poly(ether urethane) biodegradation: In vivo and in vitro correlations. J Biomed Mater Res 2004;70A(2):245-55.

152. Labow RS, Tang Y, McCloskey CB, Santerre JP. The effect of oxidation on the enzyme-catalyzed hydrolytic biodegradation of poly(urethane)s. J Biomater Sci Polym Ed 2002;13(6):651-65.

153. Yu D, Imajoh-Ohmi S, Akagawa K, Kanegasaki S. Suppression of superoxide-generating ability during differentiation of monocytes to dendritic cells. J Biochem (Tokyo) 1996;119(1):23-8.

154. Naif HM, Li S, Ho-Shon M, Mathijs JM, Williamson P, Cunningham AL. The state of maturation of monocytes into macrophages determines the effects of IL-4 and IL-13 on HIV replication. J Immunol 1997;158(1):501-11.

155. Matheson LA, Labow RS, Santerre JP. Biodegradation of polycarbonate-based polyurethanes by the human monocytes-derived macrophage and U937 cell systems. J Biomed Mater Res 2002;61(4):505-13.

156. Ma N, Petit A, Yahia L, Huk OL, Tabrizian M. Cytotoxic reaction and TNF-alpha response of macrophages to polyurethane particles. J Biomater Sci Polym Ed 2002;13(3):257-72.

157. Hass R, Bartels H, Topley N, Hadam M, Kohler L, Goppelt-Strube M, et al. TPA-induced differentiation and adhesion of U937 cells: changes in ultrastructure, cytoskeletal organization and expression of cell surface antigens. Eur J Cell Biol 1989;48(2):282-93.

158. Ways DK, Dodd RC, Bennett TE, Hooker JL, Earp HS. Effect of retinoic acid on phorbol ester-stimulated differentiation and protein kinase C-dependent phosphorylation in the U937 human monoblastoid cell. Cancer Res 1988;48(20):5779-87.

159. Zhao QH, McNally AK, Rubin KR, Renier M, Wu Y, Rose-Caprara V, et al. Human plasma alpha 2-macroglobulin promotes in vitro oxidative stress cracking of Pellethane 2363-80A: in vivo and in vitro correlations. J Biomed Mater Res 1993;27(3):379-88.

160. Wiggins MJ, MacEwan M, Anderson JM, Hiltner A. Effect of soft-segment chemistry on polyurethane biostability during in vitro fatigue loading. J Biomed Mater Res A 2004;68(4):668-83.

161. Tanzi MC, Fare S, Petrini P. In vitro stability of polyether and polycarbonate urethanes. J Biomater Appl 2000;14(4):325-48.

162. Meijs GF, McCarthy SJ, Rizzardo E, Chen YC, Chatelier RC, Brandwood A, et al. Degradation of medical-grade polyurethane elastomers: the effect of hydrogen peroxide in vitro. J Biomed Mater Res 1993;27(3):345-56.

163. Labow RS, Meek E, Santerre JP. Differential synthesis of cholesterol esterase by monocyte-derived macrophages cultured on poly(ether or ester)-based poly(urethane)s. J Biomed Mater Res 1998;39(3):469-77.

164. Labow RS, Duguay DG, Santerre JP. The enzymatic hydrolysis of a synthetic biomembrane: a new substrate for cholesterol and carboxyl esterases. J Biomater Sci Polym Ed 1994;6(2):169-79.

165. Zheng YZ, Lan WS, Qiao CL, Mulchandani A, Chen W. Decontamination of vegetables sprayed with organophosphate pesticides by organophosphorus hydrolase and carboxylesterase (B1). Appl Biochem Biotechnol 2007;136(3):233-41.

166. Yourno J, Burkart P, Mastropaolo W, Lizzi F, Tartaglia A. Monocyte nonspecific esterase. Enzymologic characterization of a neutral serine esterase associated with myeloid cells. J Histochem Cytochem 1986;34(6):727-33.

167. Lee MJ, Waters HC, 3rd. Inhibition of monocyte esterase activity by organophosphate insecticides. Blood 1977;50(5):947-51.

168. Tang YW, Labow RS, Revenko I, Santerre JP. Influence of surface morphology and chemistry on the enzyme catalyzed biodegradation of polycarbonate-urethanes. J Biomater Sci Polym Ed 2002;13(4):463-83.

169. Dennis EA. Diversity of group types, regulation, and function of phospholipase A_2. J Biol Chem 1994;269(18):13057-60.

170. Brown RC, Poole A. Arachidonic acid release and prostaglandin synthesis in a macrophage-like cell line exposed to asbestos. Agents Actions 1984;15(3-4):336-40.

171. Dinnes DL, Santerre JP, Labow RS. Intracellular phospholipase A_2 expression and location in human macrophages: Influence of synthetic material surface chemistry. J Cell Physiol 2008;214:136-144.

172. Labow RS, Santerre JP, Waghray G. The effect of phospholipids on the biodegradation of polyurethanes by lysosomal enzymes. J Biomater Sci Polym Ed 1997;8(10):779-95.

173. Salacinski HJ, Tai NR, Carson RJ, Edwards A, Hamilton G, Seifalian AM. In vitro stability of a novel compliant poly(carbonate-urea)urethane to oxidative and hydrolytic stress. J Biomed Mater Res 2002;59(2):207-18.

174. Akiba S, Ohno S, Chiba M, Kume K, Hayama M, Sato T. Protein kinase Calpha-dependent increase in Ca2+-independent phospholipase A_2 in membranes and

arachidonic acid liberation in zymosan-stimulated macrophage-like P388D1 cells. Biochem Pharmacol 2002;63(11):1969-77.

175. Balsinde J, Balboa MA, Insel PA, Dennis EA. Differential regulation of phospholipase D and phospholipase A_2 by protein kinase C in P388D1 macrophages. Biochem J 1997;321 (Pt 3):805-9.

176. Clark JD, Lin LL, Kriz RW, Ramesha CS, Sultzman LA, Lin AY, et al. A novel arachidonic acid-selective cytosolic PLA_2 contains a Ca^{2+}-dependent translocation domain with homology to PKC and GAP. Cell 1991;65(6):1043-51.

177. Lin WW, Chen BC. Distinct PKC isoforms mediate the activation of $cPLA_2$ and adenylyl cyclase by phorbol ester in RAW264.7 macrophages. Br J Pharmacol 1998;125(7):1601-9.

178. Luo SF, Lin WN, Yang CM, Lee CW, Liao CH, Leu YL, et al. Induction of cytosolic phospholipase A_2 by lipopolysaccharide in canine tracheal smooth muscle cells: involvement of MAPKs and NF-kappaB pathways. Cell Signal 2006;18(8):1201-11.

179. Orzechowski A, Jank M, Gajkowska B, Sadkowski T, Godlewski MM, Ostaszewski P. Delineation of signalling pathway leading to antioxidant-dependent inhibition of dexamethasone-mediated muscle cell death. J Muscle Res Cell Motil 2003;24(1):33-53.

180. Pompeia C, Cury-Boaventura MF, Curi R. Arachidonic acid triggers an oxidative burst in leukocytes. Braz J Med Biol Res 2003;36(11):1549-60.

181. Sellmayer A, Obermeier H, Danesch U, Aepfelbacher M, Weber PC. Arachidonic acid increases activation of NADPH oxidase in monocytic U937 cells by accelerated translocation of $p47_{phox}$ and co-stimulation of protein kinase C. Cell Signal 1996;8(5):397-402.

182. Shmelzer Z, Haddad N, Admon E, Pessach I, Leto TL, Eitan-Hazan Z, et al. Unique targeting of cytosolic phospholipase A_2 to plasma membranes mediated by the NADPH oxidase in phagocytes. J Cell Biol 2003;162(4):683-92.

183. Someya A, Nagaoka I, Nunoi H, Yamashita T. Translocation of guinea pig $p40_{phox}$ during activation of NADPH oxidase. Biochim Biophys Acta 1996;1277(3):217-25.

184. Zhao X, Bey EA, Wientjes FB, Cathcart MK. Cytosolic phospholipase A_2 ($cPLA_2$) regulation of human monocyte NADPH oxidase activity. $cPLA_2$ affects translocation but not phosphorylation of $p67_{phox}$ and $p47_{phox}$. J Biol Chem 2002;277(28):25385-92.

185. Park JW, Jang MA, Lee YH, Passaniti A, Kwon TK. p53-independent elevation of p21 expression by PMA results from PKC-mediated mRNA stabilization. Biochem Biophys Res Commun 2001;280(1):244-8.

186. Kaneko YS, Ikeda K, Nakanishi M. Phorbol ester inhibits DNA damage-induced apoptosis in U937 cells through activation of protein kinase C. Life Sci 1999;65(21):2251-8.

187. Zhuang S, Demirs JT, Kochevar IE. Protein kinase C inhibits singlet oxygen-induced apoptosis by decreasing caspase-8 activation. Oncogene 2001;20(46):6764-76.

188. Meinhardt G, Roth J, Totok G. Protein kinase C activation modulates pro- and anti-apoptotic signaling pathways. Eur J Cell Biol 2000;79(11):824-33.

189. Basu A, Lu D, Sun B, Moor AN, Akkaraju GR, Huang J. Proteolytic activation of protein kinase C-epsilon by caspase-mediated processing and transduction of antiapoptotic signals. J Biol Chem 2002;277(44):41850-6.

190. Mellor H, Parker PJ. The extended protein kinase C superfamily. Biochem J 1998;332 (Pt 2):281-92.

191. Newton AC. Protein kinase C: structure, function, and regulation. J Biol Chem 1995;270(48):28495-8.

192. Ma HT, Lin WW, Zhao B, Wu WT, Huang W, Li Y, et al. Protein kinase C beta and delta isoenzymes mediate cholesterol accumulation in PMA-activated macrophages. Biochem Biophys Res Commun 2006;349(1):214-20.

193. Hecker E. Cell membrane associated protein kinase C as receptor of diterpene ester co-carcinogens of the tumor promoter type and the phenotypic expression of tumors. Arzneimittelforschung 1985;35(12A):1890-903.

194. Downey GP, Chan CK, Lea P, Takai A, Grinstein S. Phorbol ester-induced actin assembly in neutrophils: role of protein kinase C. J Cell Biol 1992;116(3):695-706.

195. Gladwin AM, Hassall DG, Martin JF, Booth RF. MAC-1 mediates adherence of human monocytes to endothelium via a protein kinase C dependent mechanism. Biochim Biophys Acta 1990;1052(1):166-72.

196. Okumura K, Shirasawa S, Nishioka M, Sasazuki T. Activated Ki-Ras suppresses 12-O-tetradecanoylphorbol-13-acetate-induced activation of the c-Jun NH2-terminal kinase pathway in human colon cancer cells. Cancer Res 1999;59(10):2445-50.

197. Toullec D, Pianetti P, Coste H, Bellevergue P, Grand-Perret T, Ajakane M, et al. The bisindolylmaleimide GF 109203X is a potent and selective inhibitor of protein kinase C. J Biol Chem 1991;266(24):15771-81.

198. Aiello LP. The potential role of PKC beta in diabetic retinopathy and macular edema. Surv Ophthalmol 2002;47 Suppl 2:S263-9.

199. Basu A, Woolard MD, Johnson CL. Involvement of protein kinase C-delta in DNA damage-induced apoptosis. Cell Death Differ 2001;8(9):899-908.

200. Nauseef WM, Volpp BD, McCormick S, Leidal KG, Clark RA. Assembly of the neutrophil respiratory burst oxidase. Protein kinase C promotes cytoskeletal and membrane association of cytosolic oxidase components. J Biol Chem 1991;266(9):5911-7.

201. Sathyamoorthy M, de Mendez I, Adams AG, Leto TL. $p40_{phox}$ down-regulates NADPH oxidase activity through interactions with its SH3 domain. J Biol Chem 1997;272(14):9141-6.

202. Halliwell B. Phagocyte-derived reactive species: salvation or suicide? Trends Biochem Sci 2006;31(9):509-15.

203. Nakagawara A, Nathan CF, Cohn ZA. Hydrogen peroxide metabolism in human monocytes during differentiation in vitro. J Clin Invest 1981;68(5):1243-52.

204. Seres T, Knickelbein RG, Warshaw JB, Johnston RB, Jr. The phagocytosis-associated respiratory burst in human monocytes is associated with increased uptake of glutathione. J Immunol 2000;165(6):3333-40.

2.0 MANUSCRIPT #1

The role of protein kinase C in the monocyte-derived macrophage-mediated biodegradation of polycarbonate-based polyurethanes

STATEMENT OF AUTHOR CONTRIBUTIONS

Joanne E. McBane was the primary author and sole contributor to the experimental data for this manuscript. **Dr. J. Paul Santerre** is a co-investigator of Dr. Rosalind S. Labow, and principal investigator on the CIHR operating grant that funded this research. Dr. Santerre's Polymer Chemistry laboratory at the University of Toronto synthesized the model PCNU materials used in the following study. He also aided in the editing of the manuscript. **Dr. Rosalind S. Labow** is the supervisor of Joanne E. McBane and contributed to both the experimental design and the editing of the manuscript.

SUMMARY

The following manuscript entitled "The role of protein kinase C in the monocyte-derived macrophage-mediated biodegradation of polycarbonate-based polyurethanes" was published in the Journal of Biomedical Materials Research [(2005) 74A: 1-11]. MDM have been found to cause the degradation of polyurethanes as assayed using ^{14}C-labeled polyurethanes *in vitro* [Labow RS *et al.* J Biomed Mater Res (2001) 54: 189-197]. CE and MSE have been found to be partially responsible for this degradation, however the mechanism of release of these enzymes is unknown [Labow RS *et al.* *Biomaterials* (2002) 23: 3969-3975]. PKC was studied to see if activation or inhibition of this enzyme would affect the production or release of esterase and subsequent MDM-mediated degradation.

Three model ^{14}C-PCNUs (HDI431, HDI31 and MDI321) were used so that MDM-mediated degradation could be measured in the supernatant. Esterase activity and MSE protein of lysates was also assayed. Phorbol myristate acetate was used to activate protein kinase C in MDM while protein kinase C inhibitor H-7 was used to inhibit basal and PMA-activated protein kinase C. Since the respiratory burst enzyme NADPH oxidase is a possible substrate for PKC the respiratory burst was inhibited using sodium azide. From these results, two different mechanisms of PCNU degradation by MDM were proposed depending on hard segment chemistry (hexane diisocyanate versus methylene bisphenyl diisocyanate).

ABSTRACT

Polycarbonate-polyurethanes (PCNUs) elicit a foreign body reaction during the initial tissue contact, partly mediated by the respiratory burst in monocytes, during which, protein kinase C (PKC) activates NADPH oxidase. Using an *in vitro* cell system, monocytes were differentiated into monocyte-derived macrophages (MDM) and then re-seeded onto three PCNUs (HDI431, HDI321 or MDI321): hexane (HDI) or 4,4'-methylene bis-phenyl (MDI) diisocyanates synthesized with poly (1,6-hexyl carbonate) diol (PCN) and ^{14}C-labeled butanediol (BD) in the ratios 4:3:1 or 3:2:1 (diisocyanate:PCN:BD). MDM-mediated degradation was assessed by radiolabel release in the presence of a PKC activator (phorbol ester, PMA), inhibitor (H7), and a catalase/peroxidase inhibitor (NaN_3). Activating PKC decreased biodegradation and esterase activity in MDM on HDI431 and HDI321 but not MDI321, whereas H7 and NaN_3 inhibited the MDM degradation of MDI321 only. Pretreatment of the PCNUs with H_2O_2 inhibited esterase-mediated radiolabel release from HDI431 and HDI321 but stimulated radiolabel release from MDI321. The difference in the effect of H_2O_2 on the HDI versus MDI PCNUs contributes to explaining the effect of PKC activation on material degradation. Understanding the mechanism by which this pathway is linked to PCNU chemistry may assist in designing materials with tailored biodegradation rates.

INTRODUCTION

Polyurethanes (PU)s have been proven to be versatile biocompatible materials[1] that have uses in implanted devices (pacemaker leads)[2] as well as in tissue scaffolding[3], bio-artificial liver support[4], and drug delivery systems[5]. In order to minimize the foreign body reaction (when PUs come into contact with tissues), efforts have been made to modify PU chemistry[6]. Polycarbonate-PUs (PCNU)s have been demonstrated superior to polyester- and polyether-PUs in terms of reduced environmental stress cracking (ESC) and metal ion oxidation, however, they have been shown to be very susceptible to hydrolysis[7,8]. Although ESC has invoked oxidation as the initiating mechanism in long term implant degradation[9] due to monocyte-derived macrophages (MDM) and foreign body giant cells, no study to date has investigated biological links between oxidation and the subsequent hydrolytic degradation that has been observed.

The mechanism of *in vivo* biodegradation of PCNUs and PUs is unknown, but it certainly is related in some way to white blood cell activation. Neutrophils and monocytes are the two major white blood cells involved, since both are recruited to the site of injury associated with an implanted foreign body, as a result of the inflammatory response[10]. Activated neutrophils proceed to release reactive oxygen species (ROS) and lysosomal hydrolases[11] as part of their phagocytic reaction to the foreign surface. However, when neutrophils were incubated with PUs, degradation only continued for 18 hours since cell viability then decreased past this time[12]. Monocytes migrate from the bloodstream to the site of inflammation, adhere to the implanted biomaterial and differentiate into MDM[10]. These MDM release enzymes during frustrated phagocytosis, where phagocytic cells

incapable of engulfing their target proceed to release cellular contents to degrade or kill the foreign body [13].

Cholesterol esterase (CE) and carboxyl esterase (CXE) are two candidate enzymes previously shown to elicit PU degradation that was dependent on surface chemistry[7]. MDM have previously been shown to synthesize CE[14] and monocyte specific esterase[15] (MSE, an esterase with specificity similar to CXE). Immunoblotting of MDM after PCNU incubation showed both CE and MSE were present in the cell supernatant[7,16]. The total esterase activity, *de novo* esterase synthesis and amount of both CE and MSE in MDM differed depending on the material surface[17].

The above studies clearly indicated that macrophages respond to small changes in polymer chemistry depending upon which PCNU is the seeding surface for the MDM; however, the mechanism of macrophage activation by these different materials is still unknown. One of the first responses associated with MDM that occurs with exposure to these materials is the respiratory burst, which is mediated to some extent by protein kinase C (PKC)[18,19]. After PKC is activated, it phosphorylates the p47-*phox* cytosolic subunit of nicotinamide adenine dinucleotide phosphate (NADPH) oxidase. This helps translocate the subunit to the membrane where it assembles to form the active NADPH oxidase complex[18]. NADPH oxidase catalyzes the formation of superoxide anion from oxygen (O_2) and initializes the respiratory burst cascade producing various ROS. Hydrogen peroxide (H_2O_2) is the predominant end product in the respiratory burst of MDM, whereas in neutrophils and monocytes, it is hypochlorous acid (HOCl)[19].

Catalase is an enzyme that produces H_2O and O_2 from H_2O_2 thereby removing H_2O_2 (H_2O_2 scavenger) but also producing O_2, which could reinitialize the respiratory burst. Sodium azide (NaN_3) has previously been used in the study of the neutrophil respiratory burst since NaN_3 is an inhibitor of peroxidase (i.e. myeloperoxidase or glutathione peroxidase) and catalase and thereby prevents the breakdown of H_2O_2 into other reactive oxygen species[20].

When assessing the effect of the PKC activator phorbol myristate acetate (PMA) on neutrophil-mediated biodegradation of model ^{14}C-radiolabeled poly (ester-urea-urethane)s[21] radiolabel release was inhibited, whereas the PKC inhibitor H7 and the peroxidase/catalase inhibitor NaN_3 had no effect. This inhibition in radiolabel release occurs with a simultaneous increase in H_2O_2 release followed by the formation of HOCl catalyzed by myeloperoxidase, known to be dependent on the activation of PKC. HOCl has been found to oxidize the surface of the PU affecting its subsequent susceptibility to hydrolytic degradation[22].

The three PCNUs used in this study differ in diisocyanate chemistry (hexane (HDI) or 4,4'-methylene bis-phenyl (MDI) diisocyanates) and stoichiometric ratio of diisocyanate:polycarbonate diol: butanediol (4:3:1 or 3:2:1). This work will assess how differences in material surface chemistry affect the activation of PKC, the respiratory burst, and the subsequent production of esterases leading to degradation.

MATERIALS AND METHODS

Isolation and culture of monocytes-Monocytes were isolated from whole blood (with the approval of the Research Ethics Committee of the University of Ottawa Heart Institute, UOHI 91-102, valid until Feb. 7, 2005) as previously described[23] by collecting approximately 120 mL of whole blood in EDTA-containing Vacutainers® and layering onto Histopaque 1077, then centrifuging at 1000*xg* followed by serial washing and centrifuging at 450*xg* (10 minutes with 5-6 washes). Monocytes were then seeded on tissue culture grade polystyrene (PS), incubated at 37°C/5% CO_2 and 100% humidity and fed three times a week with RPMI medium with 12.7 mM HEPES, 2.0 g/L sodium bicarbonate, with 10% fetal bovine serum (FBS), 2% penicillin/streptomycin, and 0.69 mM L-glutamine. Monocytes began to differentiate after 72 hours[24] and fully differentiated into MDM after two weeks. The mature MDM were trypsinized by a previously described method[12] where the MDM were treated with ethylenediaminetetraacetic acid disodium salt (EDTA) and 0.25 % trypsin for 5 minutes and then re-suspended in Hanks solution (5.4 mM KCl, 0.44 mM KH_2PO_4, 140 mM NaCl, 4.2 mM $NaHCO_3$, 3.4 mM Na_2HPO_4, and 5.5 mM glucose) with 5% FBS and centrifuged at 450x*g*. The MDM were then resuspended in the complete media in preparation for re-seeding. All cell culturing was done in the laminar flow hood under sterile conditions. Cell counts were performed using an automated Vi-Cell™ cell counter (Beckman Coulter; Miami, FL, USA).

Preparation of material surfaces- PCNUs used in this experiment were HDI431, HDI321 (hexane diisocyanate):poly (1,6-hexyl carbonate) diol (PCN):butanediol (BD) in

a 4:3:1 and a 3:2:1 stoichiometric ratio respectively and MDI321 (4,4'-methylene bis-phenyl diisocyanate:PCN:BD) in a 3:2:1 ratio synthesized with an unlabeled or ^{14}C-radiolabeled BD moiety for all three polymers (see Table 2.1) as described in detail previously[25,26]. In order to compare the different counts from the three polymers, the released radiolabel values were normalized to the specific radioactivity of HDI431. The solid polymer was dissolved in dimethylacetamide in a 10% (w/v) solution and filtered with a 45 μM PTFE (Teflon) Chromospec® syringe filter to remove any insoluble particles. Glass coverslips (15 mm) were aseptically coated with 100 μL of the polymer solution in a laminar flow hood, dried overnight at 55°C, then purged without vacuum at 50°C for 24 hours followed by drying in a vacuum oven (-100 kPa) for 48-72 hours at 50°C as described previously[12]. Coated slips were placed in 24-well tissue culture plates and hydrated with 1 mL of sterile Dulbecco's phosphate buffered saline (DPBS) solution in each well and incubated overnight at 37°C/5% CO_2 and 100% humidity (no more than 24 hours before the experiment) to equilibrate the slips with an aqueous environment.

Re-seeding of MDM on secondary PCNU surface- One million cells per mL (in complete medium) of the resuspended MDM were added to the sample wells and 1 mL of complete medium without cells was added to the control wells. Tissue culture plates were incubated for 1 hour at 37°C/5% CO_2 and 100% humidity. After 1 hour the supernatant was aspirated off and replaced with complete medium or with a specified inhibitor in complete medium. This plate (named T=48) was incubated for 48 hours at 37°C/5% CO_2 and 100% humidity. A plate labeled T=0 was made for each experiment and was treated similarly to the T=48 plate except that after the one hour incubation the

aspirated supernatant was replaced with 240 μL of 0.05% Triton-X 100 in order to lyse the cells for DNA analysis (see below).

TABLE 2.1

Model PCNU Chemistries

Polymer Name	Diisocyanate	Macrodiol	Chain Extender*	Specific Radioactivity (CPM/100mg)
HDI431	Hexane	poly (1,6-hexyl carbonate) diol	butanediol	$1.42x10^7$
HDI321	Hexane	poly (1,6-hexyl carbonate) diol	butanediol	$1.43x10^7$
MDI321	4,4'-Methylene bis-phenyl	poly (1,6-hexyl carbonate) diol	butanediol	$0.74x10^7$

*Radiolabeled polymers have ^{14}C-radiolabeled carbons in butanediol.

Preparation of enzyme solutions for radiolabel release experiments-CXE solutions were made by dissolving CXE in sterile 0.05 M sodium phosphate buffer (pH 7.0) as previously described[7]. The number of esterase units of CXE required to elicit maximal radiolabel release from the three different polymers was assessed using a concentration response protocol[7] and the esterase assay described below. The maximal response dose was used in further studies with this enzyme on PCNUs with or without H_2O_2 pretreatment.

H_2O_2 pretreatment studies of biodegradation-For H_2O_2 pretreatment, 600 μL of ~20% H_2O_2 solution (previously shown to decrease PU degradation[27]) was incubated on the ^{14}C-radiolabed PCNU slips at 37°C and replaced every day for 3 days. As a control, slips were incubated with 600 μL of de-ionized, distilled H_2O as above and replaced every day for three days.

Determination of ^{14}C-radiolabel release-After the 48 hour incubation period, 600 μL of the cell supernatant (releasate) was removed from each well and added to 10 mL of liquid scintillation cocktail for counting in a liquid scintillation counter (LKB Wallac 1219 RackBeta; Gaithersburg, MD, USA). Counts were normalized to the average DNA content of the sample from T=0 to T=48 (CPM per 10 μg DNA). For the CXE experiments coated slips were incubated with or without CXE at 37°C/5% CO_2 for 24 hours. After 24 hours, 800 μL of the buffer/enzyme solution was added to liquid scintillation cocktail and counted as above.

Preparation of cell lysates and releasates-Cell supernatants (releasates) were taken from the T=48 plate well and stored at –40°C until needed for enzyme activity assays. The medium was removed from a well and replaced with 0.05% Triton-X 100 lysis buffer in order to prepare cell lysates from T=48 plates for DNA analysis and enzyme activity assays (see below).

Assay of DNA content of cell lysates-The amount of DNA present in cell lysates was determined for an aliquot of cell lysate suspension using a modification of the assay

outlined previously[17]. Briefly 0.1% Hoescht Dye #33258 was diluted in 10% 10X buffer containing 0.10 M Trizma base, 2.0 M NaCl and 0.01 M EDTA (in de-ionized, distilled water (ddH_2O), pH 7.4) on the day of analysis. Cell lysate (15 μL) was added to the dye (100 μL) into a 96 well plate and read against a calf thymus DNA standard (100-300 ng) in a fluorescence microplate reader (POLARstar Galaxy, BMG Technologies; Durham, NC, USA).

Preparation of inhibitors and activators-H7 Dihydrochloride (PKC inhibitor) (5 mg/ml H_2O) was used at a concentration of 100 μM in complete medium. PMA (an activator of PKC) (1 mg/mL in dimethylsulfoxide) diluted 15.4 μL in 2.5 mL of DPBS was further diluted in complete MDM medium to give a final concentration of 10^{-7} M. NaN_3 was dissolved in complete medium to give a final concentration of $5x10^{-3}$ M solution. The concentration of all these reagents was selected based on those previously used in neutrophil experiments[21].

Assay of esterase activity in MDM cell lysates and releasates-The esterase activity of the cell lysates and releasates was assayed using a previously described protocol with p-nitrophenylbutyrate (PNB)[12]. After 30 minutes incubation at 37°C, the absorbance of each sample was read at 400.6 nm using a spectrophotometer. One esterase unit was defined as the release of 1 nmol/min of p-nitrophenol (PNP) (ε=16,300 $cm^{-1}M^{-1}$) at 37°C and normalized to 10 μg of DNA using the average value from T=0 to T=48.

SDS gel electrophoresis and immunoblotting-The cell lysate proteins were separated by polyacrylamide gel electrophoresis (PAGE) and immunoblotted as previously described[16]. The primary antibody used was rabbit anti-porcine esterase (reacts with MSE) or rabbit anti-CE (a gift from Dr. Hui, University of Cincinnati College of Medicine, Cincinnati, OH, USA). The secondary antibody used was goat anti-rabbit IgG conjugated to horseradish peroxidase. Protein bands were then visualized using the SuperSignal West Femto Maximum Sensitivity Substrate Enhanced Chemiluminescence Detection Kit and recorded on CL-Xposure X-ray film (both from Pierce; Rockland, IL, USA). The bands in the x-ray film were quantified with Quantity One Software® v.4.1[16] (Bio-Rad; Hercules, CA, USA).

Statistical analysis-The data were analyzed by 1 way and 2 way ANOVAs using SAS® version 8.2 with a significance value of $p<0.05$ adjusted for multiple comparisons ($p<0.0167$).

RESULTS

Monocyte and MDM behaviour can vary a great deal between donors[23]; therefore, to account for these differences, each of the experiments were related to their own media control. As well, the number of cells obtained for a given isolation varied. Due to these limitations only one surface could be assessed per isolation with the two inhibitors and one activator. The media controls and inhibitor values were first normalized to 10 μg of DNA, and the relative radiolabel release and esterase activity were calculated, with cells in media alone (i.e. no inhibitor or activator) being set at 100%. This method of

comparison eliminated the physiological variability in the absolute values obtained, and yielded similar effects for the specific treatment conditions. Figures 2.1-2.4 illustrate that by comparing radiolabel release and esterase activity to the cells in media only control, the relative inhibition or activation of radiolabel release and esterase activity was reproducible with the standard error being less than 10 % for these values.

Effect of material surface chemistry on the biodegradation and esterase activity elicited by MDM in the presence of a PKC activator- Figure 2.1 shows that PMA significantly inhibited the radiolabel release elicited by MDM on the two HDI PCNUs by ~40% ($p<0.0001$) but no effect was observed for MDI321. Figure 2.1 also shows that the esterase activity elicited by MDM re-seeded on HDI PCNUs was significantly inhibited by ~40% ($p<0.0001$). Again no significant change in esterase activity was observed for MDM re-seeded on MDI321.

Effect of material surface chemistry on the amount of MSE protein produced in MDM re-seeded in the presence or absence of a PKC activator-Since activating PKC had different effects on esterase activity based on material surface, the total amount of MSE was determined in order to see if the protein itself was reduced by PKC activation or if the downstream effects of PKC activation inhibited esterase activity. The amount of MSE produced in cell lysates of MDM re-seeded on the three surfaces with or without PMA as assessed by immunoblotting analysis is shown in Figure 2.2. The graph shows the relative amount of MSE produced by the PMA treated MDM on the three surfaces as a percent of the MDM in media only control.

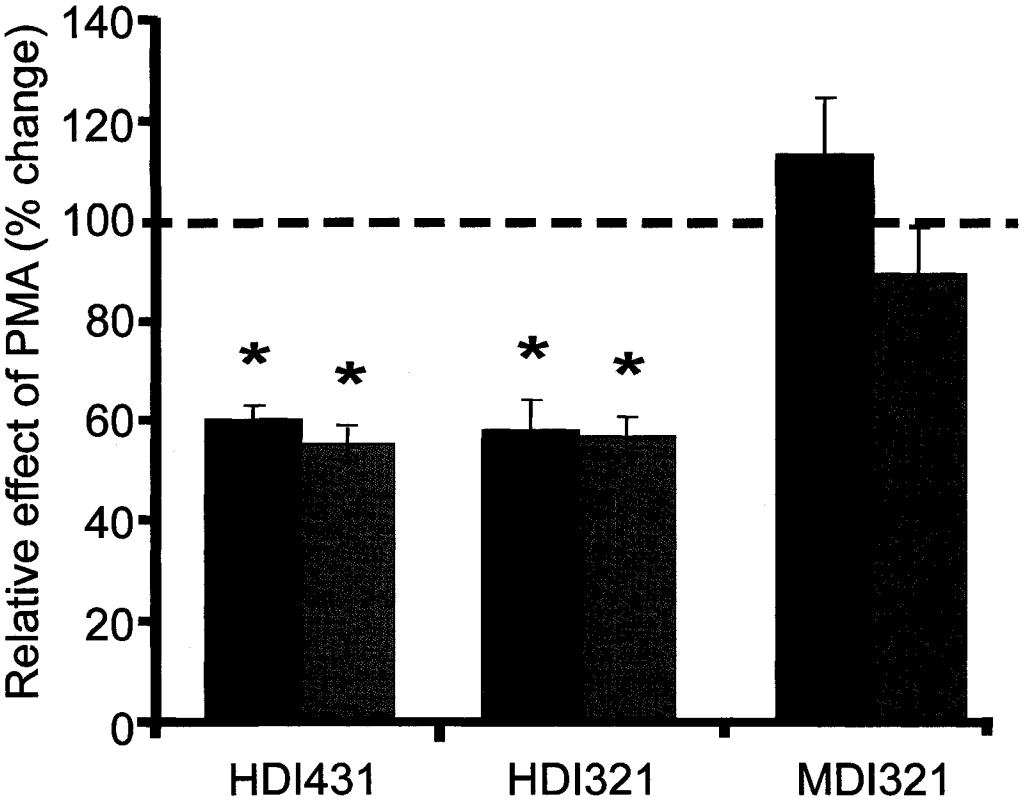

Figure 2.1: Effect of PMA on MDM-mediated biodegradation and esterase activity. Radiolabel release (red bar) and esterase activity (blue bar) was calculated for MDM differentiated on PS and re-seeded on ^{14}C-labeled HDI431, HDI321 and MDI321 PCNUs compared to cells in media only control and given in CPM per 10 μg of DNA or nmol/min per 10 μg of DNA (respectively). *There was a significant inhibition versus media control. **There is a significant difference in % original radiolabel release or % original esterase activity between the two polymers (n=3).

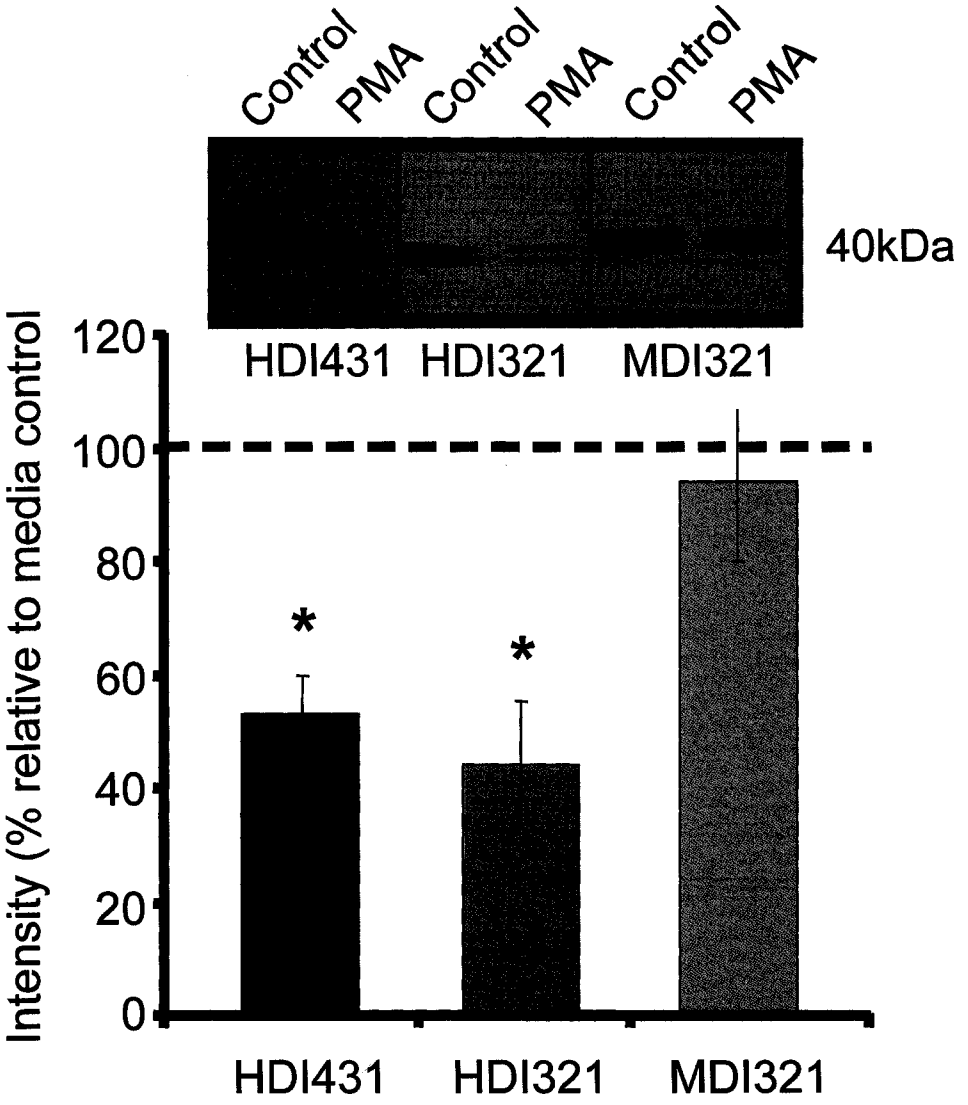

Figure 2.2: Effect of PMA on the amount of MSE in MDM re-seeded on the three different material surfaces. MDM cell lysates were immunoblotted using anti-MSE antibody and quantified. The blot shown is representative of all blots and the boxed area shows the 40kDa doublets that were quantified on the three surfaces with or without PMA (media only control). The cell lysates were obtained from monocytes differentiated to MDM on PS and re-seeded on HDI431 (red bar), HDI321 (blue bar) and MDI321 (green bar) in the presence of PMA given as intensity in percent relative to cells in media only control. *There is a significant inhibition of the amount of MSE present in the PMA treated sample relative to the media control (n=4).

There were two other bands at 57 and 64 kDa in addition to the 40 kDa doublet shown in Figure 2.2. These data were not shown since at the level of sensitivity used to detect the difference in the 40 kDa doublet, no difference was observed in these other two bands between the surfaces due to saturation. HDI431 and HDI321 lysates treated with PMA had significantly less MSE than the media control with relative intensities of 53% ($p<0.0001$) and 44% ($p<0.0001$) respectively. This agreed with the radiolabel release inhibition and the esterase activity inhibition in Figure 2.1. There was no decrease in the amount of MSE produced in the cell lysates of MDM re-seeded on MDI321. This also agreed with the lack of inhibition of radiolabel release and esterase activity observed for PMA treated MDI321 re-seeded cells (Figure 2.1). Gels were run in parallel and immunoblotted with anti-CE however no significant difference was seen between PMA and control MDM cell lysates (data not shown).

Effect of material surface chemistry on the biodegradation and esterase activity elicited by MDM in the presence of a PKC activator and a peroxidase/catalase inhibitor-In order to determine if the above inhibition of biodegradation and esterase was caused by activation of the respiratory burst, NaN_3, an inhibitor of peroxidase and catalase and therefore an inhibitor of the respiratory burst, was tested with the cell system in the presence or absence of PMA. Figure 2.3a shows the radiolabel release data reported as % change in radiolabel release. The NaN_3 treated cells showed an interesting material surface difference where the MDI321 re-seeded MDM cells had a radiolabel release inhibition of ~60%. This was significantly greater than the radiolabel release inhibition for HDI431 ($p<0.0001$) or HDI321 ($p<0.0001$) (Figure 2.3a). In order to determine if the

inhibition of radiolabel release and esterase activities for PMA and NaN_3 occurred though the same mechanism, both PMA and NaN_3 were added to the same MDM in media. Radiolabel release data shown in Figure 2.3a suggest that both HDI PCNUs could have their PMA radiolabel release inhibition (as seen in Figure 2.1) slightly reversed by combing NaN_3 with PMA. HDI431 radiolabel release was reversed significantly by ~30% from the PMA treatment alone ($p=0.003$). The MDM re-seeded on MDI321 had a different pattern where adding PMA and NaN_3 to the media inhibited the radiolabel release by ~80%, more than with either reagent by itself (Figures 2.1 and 2.3a).

Figure 2.3b shows that the esterase activity relative to media control (set at 100%) was inhibited significantly for NaN_3 treated MDM on all three surfaces ($p<0.0001$ for all three) with inhibitions of ~30% for the two HDI PCNUs and ~50% for MDI321 (Figure 2.3b). However the effect of the material surface difference was maintained with the esterase activity of NaN_3 treated MDMs on MDI321 being inhibited significantly more ($p=0.0043$ and $p=0.0040$ respectively) than on the HDI PCNUs (Figure 2.3b). With the combined PMA and NaN_3 treatment the esterase activity for the HDI431 re-seeded cells was not significantly different from the PMA treated cells alone (Figures 2.3b and 2.1 respectively). HDI321 esterase activity inhibition was slightly reversed ($p=0.0002$)) when PMA was combined with NaN_3 (Figure 2.3b) versus PMA alone (Figure 2.1). MDI321 re-seeded MDM esterase activity for the combined treatment was inhibited more than for the PMA alone treated cells (Figure 2.1) but not significantly more than the esterase activity for the NaN_3 treated cells (Figure 2.3b).

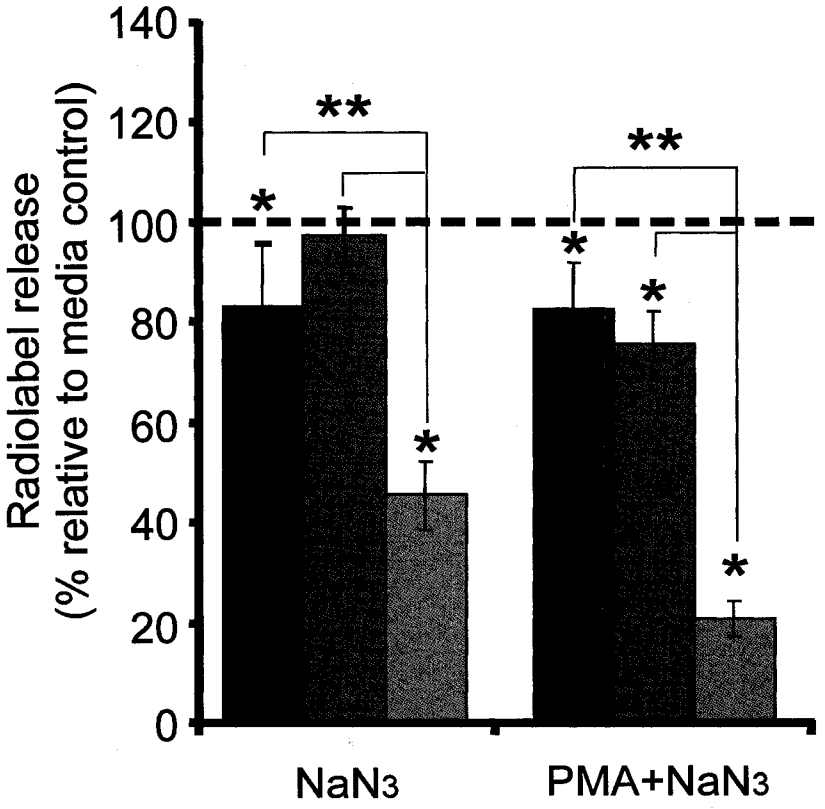

Figure 2.3a: Effect of NaN_3 on the PMA inhibition of MDM-mediated biodegradation of PCNUs. Radiolabel release was calculated for MDM differentiated on PS and re-seeded on ^{14}C-labeled HDI431 (red bar), HDI321 (blue bar) and MDI321 (green bar) PCNUs compared to cells in media only control calculated as CPM per 10 μg of DNA in the sample. *There was a significant inhibition of radiolabel release. **There was a significant difference in % original radiolabel release between these two polymers (n=3).

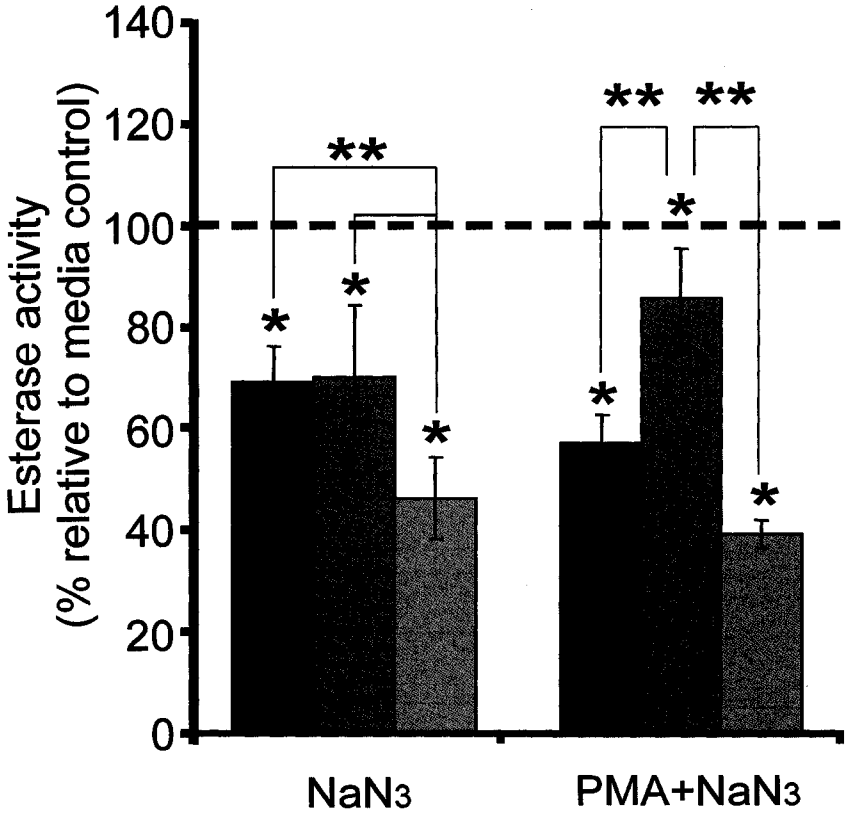

Figure 2.3b: Effect of NaN_3 on the PMA inhibition of the esterase activity in MDM re-seeded on PCNUs. Esterase activity was calculated for MDM differentiated on PS and re-seeded on ^{14}C-labeled HDI431 (red bar), HDI321 (blue bar) and MDI321 (green bar) PCNUs compared to cells in media only cell control and given in nmol/min per 10 μg of DNA in the sample. *There was a significant inhibition of esterase activity. **There was a significant difference in % original esterase activity between these two polymers (n=3).

Effect of material surface chemistry on biodegradation and esterase activity elicited by MDM in the presence of a PKC activator and inhibitor–The PKC inhibitor H7 was tested to see if the PKC activation by PMA could be reversed. Figure 2.4a shows the % change in radiolabel release when treating the MDM with H7 or PMA and H7. HDI431 re-seeded cells had a 25% inhibition of radiolabel release ($p=0.0004$) (Figure 2.4a) when treated with H7 whereas HDI321 re-seeded cells had no significant inhibition of radiolabel release (Figure 2.4a). The radiolabel release elicited by re-seeding MDM on MDI321 was significantly more inhibited when treated with H7, than the two HDI PCNUs, with only about 20% original radiolabel release remaining ($p<0.0001$) compared to cells in media only control and both HDI PCNUs).

Combinations of PMA and H7 were assessed to see if the effect on radiolabel release or esterase activity could be reversed on any of the surfaces. Figure 2.4a confirms that treatment of HDI431 re-seeded MDM with PMA and H7 completely reversed the PMA induced radiolabel release inhibition ($p<0.0001$) (Figure 2.4a and 2.1). MDM re-seeded on HDI321 and treated with the combination of PMA and H7 also had no significant inhibition of radiolabel release, which differed from the PMA induced inhibition (Figures 2.4a and 2.1). MDI321 re-seeded cells had a partial reversal of the radiolabel release inhibition when treated with PMA and H7 (40% inhibition of radiolabel release) versus H7 alone (80% inhibition radiolabel release) ($p<0.0001$).

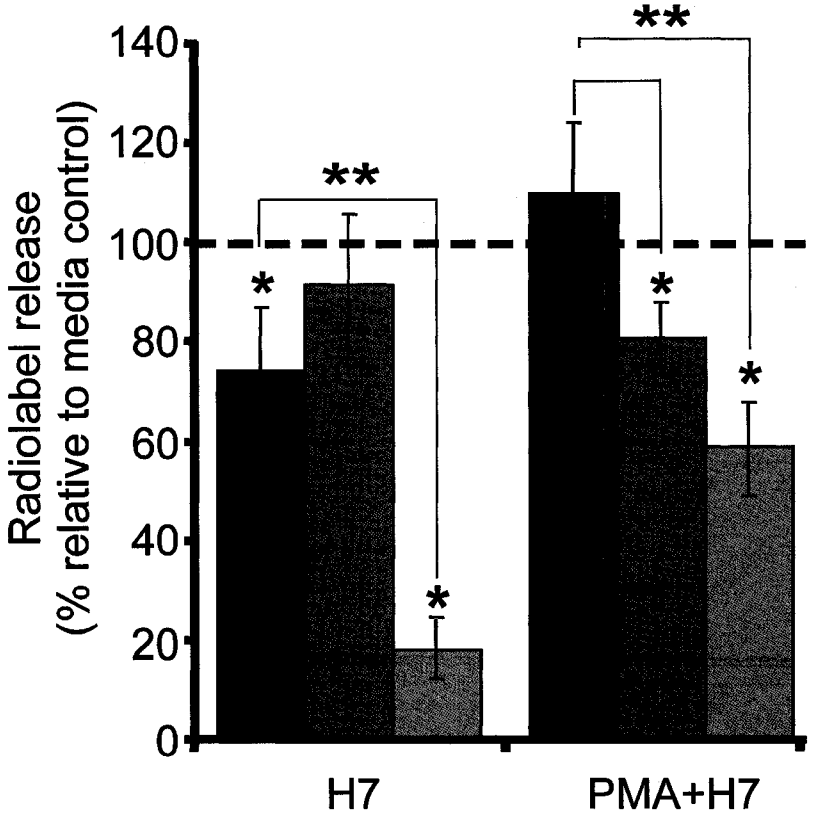

Figure 2.4a: Effect of H7 on the PMA inhibition of MDM-mediated biodegradation of PCNUs. Radiolabel release was calculated for MDM differentiated on PS and re-seeded on ^{14}C-labeled HDI431 (red bar), HDI321 (blue bar) and MDI321 (green bar) PCNUs compared to cells in media only control and given in CPM per 10 μg of DNA in the sample. Esterase activity was calculated for MDM differentiated on PS and re-seeded on ^{14}C-labeled HDI431 (red bar), HDI321 (blue bar) and MDI321 (green bar) PCNUs compared to cells in media only control and given in nmol/min per 10 μg of DNA in the sample. *There was a significant inhibition of radiolabel release. **There was a significant difference in % original radiolabel release between the two polymers (n=3).

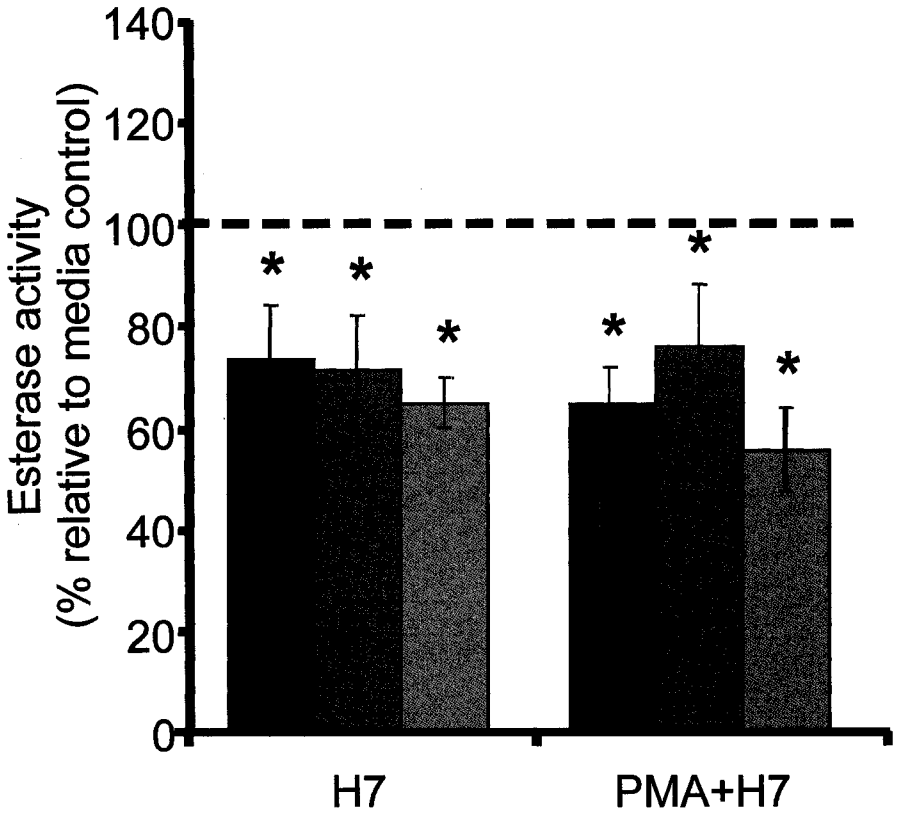

Figure 2.4b: Effect of H7 on the PMA inhibition of the esterase activity in MDM on PCNUs. Esterase activity was calculated for MDM differentiated on PS and re-seeded on ^{14}C–radiolabeled HDI431 (red bar), HDI321 (blue bar) and MDI321 (green bar) PCNUs compared to cells in media only control and given in nmol/min per 10 μg of DNA in the sample. *There was a significant inhibition of esterase activity (n=3).

Esterase activity for H7 treated cells was significantly inhibited on all three surfaces by about 25% ($p<0.0001$) (Figure 2.4b) with no significant material surface difference. With the combined treatment of H7 and PMA the HDI431 and HDI321 treated cells both had significantly inhibited esterase activities but neither was significantly different from the PMA or H7 alone treated cells' esterase activities (Figures 2.1 and 2.4b). The esterase activity of the MDI321 re-seeded cells was also inhibited about 40% when PMA and H7 treatment was combined ($p<0.0001$) (Figure 2.4b), which was not significantly different from the H7 treated cells but significantly different from the PMA alone treated cells (Figure 2.1).

Effect of material surface chemistry on the hydrolysis of PCNUs pretreated with H_2O_2- H_2O_2 is the final product of the respiratory burst in MDM. In order to assay the effect of over-stimulating the respiratory burst on PCNU hydrolytic biodegradation, PCNUs were pretreated with H_2O_2 for three days (or ddH_2O for control slips) and then incubated with CXE for 24 hours. Figure 2.5 shows that H_2O_2 pretreatment inhibited the release of product from HDI431 and HDI321 by CXE (~10-13% $p=0.01$, $p=0.002$ respectively) but increased the biodegradation of MDI321 by CXE (~13%, $p=0.001$). Incubation with CE post-H_2O_2 treatment did not have any significant effect (Data not shown).

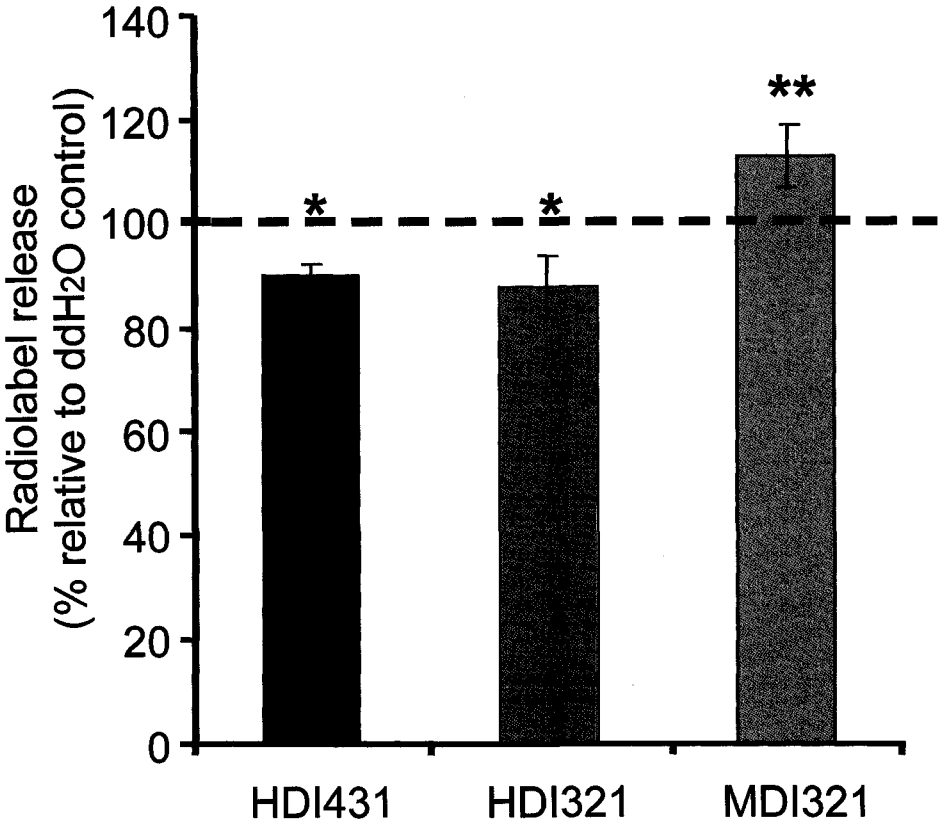

Figure 2.5: Effect of H_2O_2 pretreatment on the carboxyl esterase (CXE) elicited biodegradation of PCNUs. Radiolabel release was calculated for ^{14}C-radiolabeled HDI431 (red bar), HDI321 (blue bar) and MDI321 (green bar) incubated with CXE for 24 hours post 3-day H_2O_2 pretreatment in percent relative to ddH_2O pretreated slips. *There was a significant inhibition of radiolabel release. **There was a significant increase in radiolabel release. (n=2)

DISCUSSION

One possible mechanism by which PKC could affect biodegradation of PCNUs by MDM is through activation of the respiratory burst. PKC phosphorylation of NADPH oxidase initiates the cascade, which produces various ROS[18,19] that react with the material surfaces differently based on their diisocyanate chemistry (Figure 2.5). This would explain why Figure 2.1 shows an inhibition of radiolabel release for the HDI re-seeded MDMs in the presence of PMA whereas MDI321 was unaffected. If this were the sole mechanism controlling the biodegradation character of both polymers, then inhibiting PKC or the respiratory burst would reverse the radiolabel release inhibition by PMA on the HDI PCNUs. Comparing Figure 2.3a to Figure 2.1 suggests that inhibiting the production of ROS with NaN_3 can at least partially reverse the effects of PKC activation since the radiolabel release from HDI PCNUs was less inhibited.

However, the radiolabel release elicited by the MDM on MDI321 was inhibited by the combined treatment of NaN_3 and PMA. This implies that the oxidant plays a role in allowing biodegradation to proceed in MDI321 and rationalizes why the biodegradation of MDI321 by CXE was increased with H_2O_2 pretreatment (Figure 2.5). The fact that azide inhibited MDI321 degradation in the absence of PMA would suggest that MDI321 itself activates the oxidative pathway. Since much lower reductions in radiolabel release were observed for the HDI polymers (Figure 2.3a) these materials may not be activating the release of ROS to the same extent as MDI321. The inhibitor of PKC, H7, showed a similar pattern when the effect of H7 and PMA were combined (Figure 2.4a).

The fact that the MDI321 surface did not show inhibition of radiolabel release by the PMA treatment is believed to reflect the unique nature of the surface chemistry, which is substantially different from that of the HDI PCNUs[25,28]. MDI321 is very well phase mixed with extensive hydrogen (H)-bonding between the carbonate and urethane groups at the surface when compared to the HDI polymers[25]. Therefore H_2O_2, the ROS released from MDM, will be reacting with MDI segments in MDI321, whereas the carbonate groups will be readily exposed for reaction with H_2O_2 in the well phase-separated HDI polymers. Oxidation of the MDI moieties will disrupt the H-bonding shielding of MDI321 and allow for subsequent hydrolysis of the soft segment backbone with subsequent radiolabel release. Reaction of the carbonate with H_2O_2 will generate some chain scission, but will also promote cross-linking, which will delay product release when subsequent hydrolysis reactions are catalyzed by MSE. This explanation is confirmed by the observation that HDI PCNUs pretreated with H_2O_2 and incubated with CXE overnight showed a significant inhibition of biodegradation whereas MDI321 showed a significant increase in hydrolytic biodegradation as assayed by radiolabel release (Figure 2.5).

Although esterase activity has been linked to biodegradation in the MDM cell systems[7,12], a direct correlation between radiolabel release and specific esterase activity has not yet been obtained. Using PNB esterase hydrolysis as a measure of esterase activity is non-specific. This assay quantifies MSE, CE and any other enzyme with esterolytic activity in the sample, such as serine proteases. Immunoblotting of specific esterases was required in order to confirm the induction or suppression of the esterase(s) concerned.

Although the immunoblotting analysis using the antibody to MSE showed single bands at higher molecular weights around 57kDa and 64kDa, only the 40 kDa doublet showed sensitivity to the inhibitor and/or activator treatments. It should be noted that the 40 kDa doublet may not represent all the activity measured by the PNB assay and may not be responsible for all the degradation observed (Figure 2.1). Previously, it was shown that the 57 kDa band was the prominent band, with significantly more of this isoform visible from MDM on HDI431 than on MDI321[17]. However, the 40 kDa doublet was below detectable limits in the latter study, and therefore by using the more sensitive femto substrate in this study it was possible to visualize the 40 kDa doublet and show the effect of PMA.

A proposed mechanism for HDI PCNU degradation, based on the results from this study, has been generated and is detailed in Figure 2.6. The fact that the amount of MSE (Figure 2.2) produced in the lysates of HDI431 and HDI321 re-seeded MDM was inhibited by PMA treatment suggests that esterase production itself is influenced by PKC activation. A recent study found that sodium fluoride, an inhibitor of MSE, inhibited the radiolabel release from MDM re-seeded on all three PCNU surfaces[29]. The same study showed that sodium taurocholate (NaT), a known CE inhibitor, had no significant effect on the radiolabel release from MDM re-seeded on HDI431 or HDI321. NaT added to incubation with CXE on the two HDI PCNUs could inhibit radiolabel release suggesting that CE was stimulated to compensate for an inhibited MSE in the MDM[29].

Figure 2.6: Proposed mechanism of HDI PCNU biodegradation. *(a)* MSE synthesis is stimulated by the HDI PCNU surface, increasing radiolabel release (RLR) and esterase activity. *(b)* PMA stimulates synthesis of c-Jun mRNA and p44/42 mitogen-activated protein kinase, leading to the inhibition of MSE gene transcription which in turn inhibits biodegradation RLR and esterase activity (Figures 1 and 2). *(c)* H7 by inhibiting PKC partially reverses this inhibition of MSE production. However, since it does not completely inhibit c-Jun[31] there would not be a full restoration of esterase activity (Figure 4b). *(d)* ROS (i.e. H_2O_2) production in the MDM causes a decrease in RLR since the PCNU surface is protected from hydrolysis (most likely by cross-linking polymer chains, Figure 5). *(e)* PMA activates NADPH oxidase, which helps stimulate the respiratory burst and decrease RLR through ROS reacting with the HDI PCNU surface (Figure 1). *(f)* H7 and NaN_3 block the stimulation of the respiratory burst by (fully or partially) reversing the activation of PKC and/or the respiratory burst respectively (Figures 3 and 4). *(g)* CE is another candidate enzyme released by MDM in the inflammatory response to a biomaterial which may account for some of the esterase activity and RLR elicited by the MDM re-seeded on the HDI PCNUs; however it is unaffected by PMA activation of PKC.

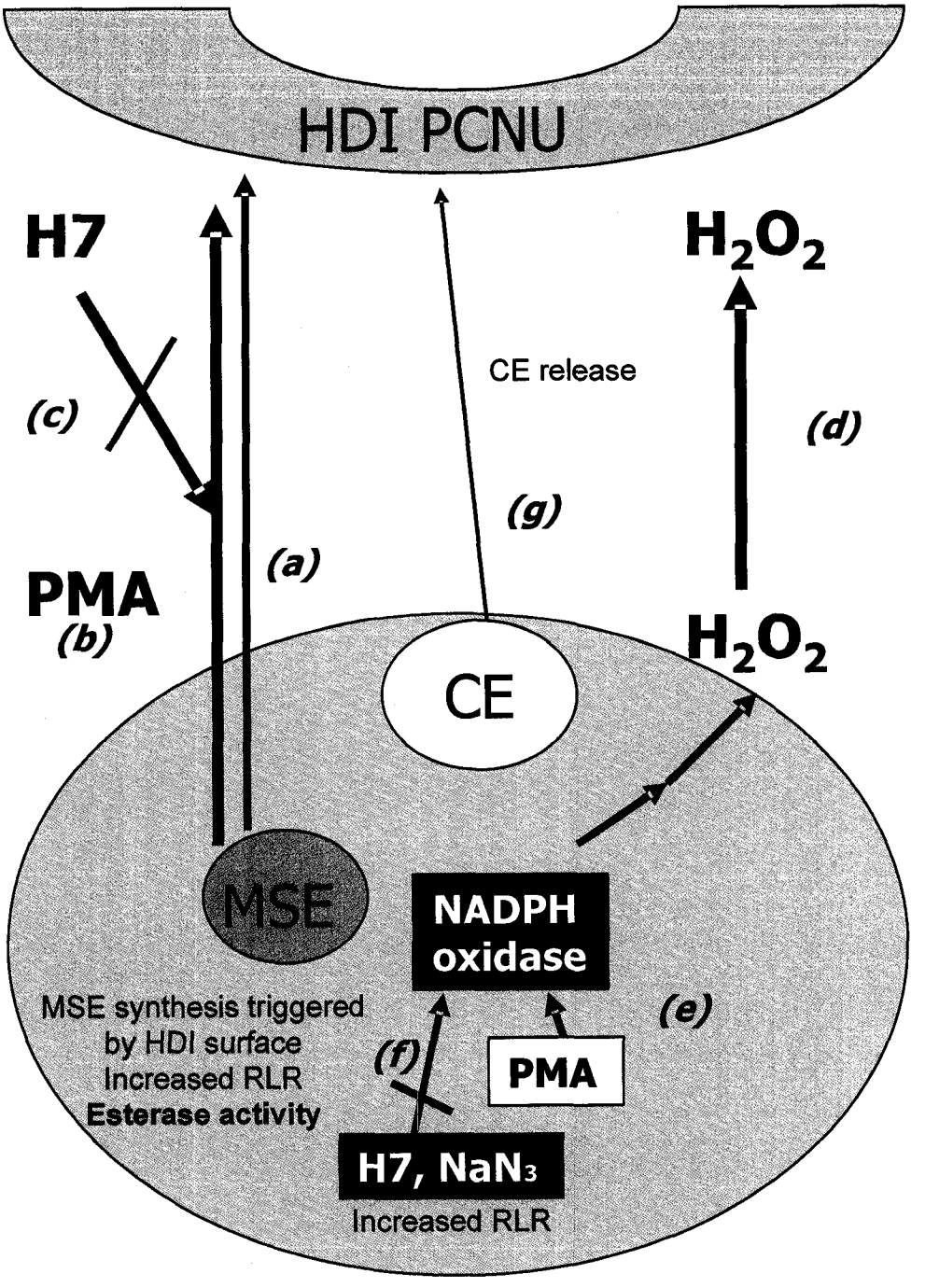
HDI PCNU
H7
(c)
PMA
(b)
(a)
CE release
(g)
H_2O_2
(d)
H_2O_2
CE
MSE
NADPH oxidase
(e)
PMA
(f)
H7, NaN_3
Increased RLR
MSE synthesis triggered by HDI surface
Increased RLR
Esterase activity

It is possible that the esterase (MSE) inhibition phenomenon was a downstream effect of an earlier PKC phosphorylation event leading to a decreased amount of esterase being produced. A recent study using surfactant protein A found that PMA could down-regulate surfactant protein A mRNA and protein via inhibition of gene transcription[30]. PKC activation caused phosphorylation of p44/42 mitogen-activated protein kinase and c-Jun-NH(2)-terminal kinase which were found to be directly involved in the gene expression of surfactant protein A[30].

Another study suggests that c-Jun-NH(2)-terminal kinase activation by PMA cannot be fully reversed by H7 but could be reversed by PKC inhibitor GF109203X suggesting that the PKC isoforms involved in its activation are not inhibited by H7[31]. The fact that there was a material surface chemistry difference in the amount of MSE produced (Figure 2.2) suggests that the pathway for MSE release is controlled by PKC activation to varying degrees depending upon MDM activation by the PCNUs. In addition, it is possible that the esterase activity itself was inhibited directly by PKC phosphorylation of the serine in its active site[32], likely the site involved in PU biodegradation[33].

Figure 2.7: Proposed mechanism of MDI PCNU biodegradation. *(a)* MSE is synthesized due to the general inflammatory response to a biomaterial but is not stimulated by the MDI PCNU surface as much as with HDI PCNUs[17]. *(b)* Since MDI321 does not stimulate synthesis of MSE, PMA does not affect MSE gene transcription or MSE protein (40 kDa doublet, see Figure 2). *(c)* ROS production in the MDM causes an increase in RLR since oxidation makes the surface more susceptible to biodegradation. MDI segments which shield carbonate groups from hydrolysis[25] are readily oxidized and disrupt carbonate shielding, rendering the latter soft segment more susceptible to hydrolysis by esterase (MSE and CE) activity. *(d)* PMA activates NADPH oxidase which helps stimulate the respiratory burst (ROS do not react with MDI PCNUs in a similar manner to HDI PCNUs, therefore there is no decrease in RLR) (Figure 1). *(e)* H7 and NaN_3 block the stimulation of the respiratory burst by both MDI321 and PMA thereby decreasing biodegradation (Figures 3 and 4). *(f)* CE is synthesized by MDM re-seeded on MDI321 and accounts for some of the RLR and esterase activity however is unaffected by PMA activation of PKC.

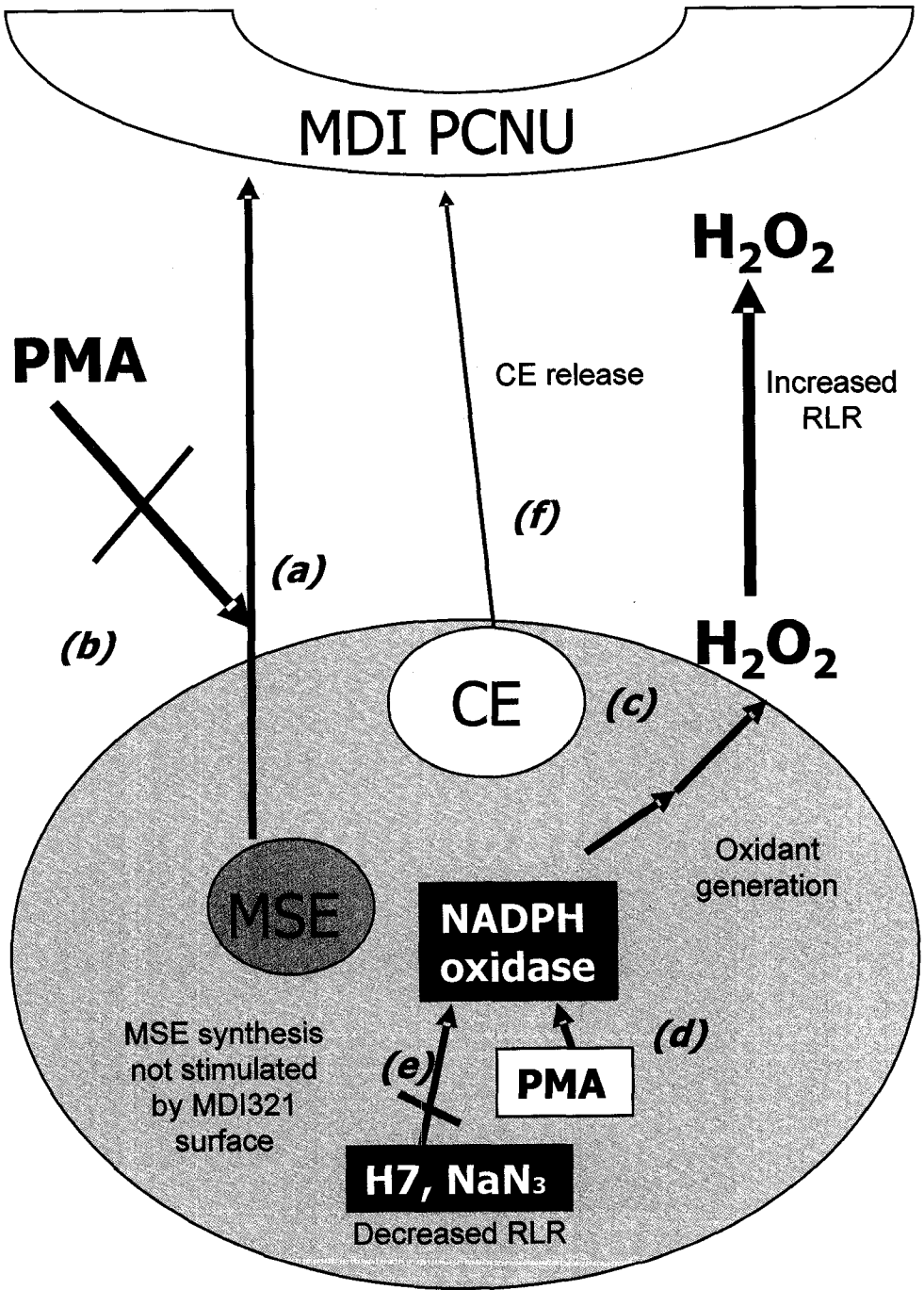
MDI PCNU
H_2O_2
PMA
CE release
Increased RLR
(f)
(a)
(b)
H_2O_2
CE
(c)
Oxidant generation
MSE
NADPH oxidase
MSE synthesis not stimulated by MDI321 surface
(e)
PMA
(d)
H7, NaN_3
Decreased RLR

Figure 2.7 shows a proposed mechanism for the MDM elicited degradation of MDI321. It differs from the HDI mechanism in several ways. A recent study showed that when NaT was added to MDM re-seeded on MDI321 an increase in radiolabel release was observed[29]. Therefore CE (although unaffected by PMA) may be more involved in MDI321 degradation than for the HDI PCNUs, and MSE synthesis may not be stimulated by the MDI321 surface whereas CE may be. This may explain why PMA does not affect the amount of MSE for MDM on MDI321 (Figure 2.2). Oxidant generation is showing an opposite effect to that of the HDI polymers since H_2O_2 treatment of the MDI surface increased radiolabel release (Figure 2.5). Phorbol ester treatment enhances the respiratory burst, maintaining the radiolabel release or increasing it. Inhibiting PKC or the respiratory burst decreases radiolabel release because there is a decrease in oxidant generation (Figures 2.3a and 2.4a).

H7 and NaN_3 treatments both of which inhibit ROS release, decreased the esterase activity measured by the PNB assay for MDM on MDI321 but had less of an effect on the HDI PCNUs (Figure 2.3b and 2.4b). This suggests that MSE (or CE) in MDM on MDI321 was affected by the respiratory burst pathway, either by decreased synthesis or inhibition of esterase activity by ROS. Therefore MDI321 itself must activate ROS production and the PKC activator provides little more in terms of change to radiolabel release since the ROS response is already exhibited when cells contact MDI321. This explains why Figure 2.1 shows no significant increase in radiolabel release whereas Figure 2.5 does. In Figure 2.5 the H_2O_2 pretreatment overrides the material's control of

ROS whereas in Figure 2.1, the material is controlling the ROS release in the absence of the PKC activator.

The results of this study suggest that PKC has an important role in the MDM-mediated biodegradation of PCNUs and most likely biomaterials in general. This finding is one of the first studies to clearly link material surface and cell membrane activation with the oxidative and hydrolytic mechanisms of PU degradation. Figures 2.6 and 2.7 illustrate the proposed mechanisms for HDI versus MDI PCNU biodegradation respectively based on PKC activation of the respiratory burst. It is possible that the release of oxygen species by PKC activation alters the surfaces in different ways therefore perturbing the surface chemistry and influencing subsequent hydrolysis by enzymes released from MDM. Another role for PKC would be inactivation of the active site of serine esterases and proteases known to degrade PCNUs. Thirdly, inhibition of esterase production by inhibiting *de novo* synthesis pathways may also be involved. By understanding the effect that material surface differences have on cell signaling pathways, the mechanism(s) of biodegradation may be elucidated and ultimately controlled by tailoring material chemistry leading to the exploitation of the knowledge for the design of bio-responsive polymers.

ACKNOWLEDGEMENTS

The polymers were synthesized by Dr. Meilin Yang, Faculty of Dentistry, University of Toronto, ON. These studies were funded by the Canadian Institutes for Health Research (CIHR) and the MSH Foundation, Montreal, QC.

REFERENCES

1. Zdrahala RJ, Zdrahala IJ. Biomedical applications of polyurethanes: a review of past promises, present realities, and a vibrant future. J Biomater Appl 1999;14(1):67-90.

2. Hauser RG, Cannom D, Hayes DL, Parsonnet V, Hayes J, Ratliff N, 3rd, Tyers GF, Epstein AE, Vlay SC, Furman S and others. Long-term structural failure of coaxial polyurethane implantable cardioverter defibrillator leads. Pacing Clin Electrophysiol 2002;25(6):879-82.

3. Grad S, Kupcsik L, Gorna K, Gogolewski S, Alini M. The use of biodegradable polyurethane scaffolds for cartilage tissue engineering: potential and limitations. Biomaterials 2003;24(28):5163-71.

4. Linti C, Zipfel A, Schenk M, Dauner M, Doser M, Viebahn R, Becker HD, Planck H. Cultivation of porcine hepatocytes in polyurethane nonwovens as part of a biohybrid liver support system. Int J Artif Organs 2002;25(10):994-1000.

5. Yang M, Santerre JP. Utilization of quinolone drugs as monomers: characterization of the synthesis reaction products for poly(norfloxacin diisocyanatododecane polycaprolactone). Biomacromolecules 2001;2(1):134-41.

6. Ma N, Petit A, Yahia L, Huk OL, Tabrizian M. Cytotoxic reaction and TNF-alpha response of macrophages to polyurethane particles. J Biomater Sci Polym Ed 2002;13(3):257-72.

7. Labow RS, Meek E, Matheson LA, Santerre JP. Human macrophage-mediated biodegradation of polyurethanes: assessment of candidate enzyme activities. Biomaterials 2002;23(19):3969-75.

8. Tang YW, Labow RS, Santerre JP. Enzyme induced biodegradation of polycarbonate-polyurethanes: dose dependence effect of cholesterol esterase. Biomaterials 2003;24(12):2003-11.

9. Stokes K, McVenes R, Anderson JM. Polyurethane elastomer biostability. J Biomater Appl 1995;9(4):321-54.

10. Marchant RE, Miller KM, Anderson JM. In vivo biocompatibility studies. V. In vivo leukocyte interactions with Biomer. J Biomed Mater Res 1984;18(9):1169-90.

11. Anderson JM. Mechanisms of inflammation and infection with implanted devices. Cardiovasc Pathol 1993;2(3):33S-41S.

12. Labow RS, Meek E, Santerre JP. Model systems to assess the destructive potential of human neutrophils and monocyte-derived macrophages during the acute and chronic phases of inflammation. J Biomed Mater Res 2001;54(2):189-97.

13. Cannon GJ, Swanson JA. The macrophage capacity for phagocytosis. J Cell Sci 1992;101 (Pt 4):907-13.

14. Li F, Hui DY. Modified low density lipoprotein enhances the secretion of bile salt-stimulated cholesterol esterase by human monocyte-macrophages. species-specific difference in macrophage cholesteryl ester hydrolase. J Biol Chem 1997;272(45):28666-71.

15. Saboori AM, Newcombe DS. Human monocyte carboxylesterase. Purification and kinetics. J Biol Chem 1990;265(32):19792-9.

16. Matheson LA, Labow RS, Santerre JP. Biodegradation of polycarbonate-based polyurethanes by the human monocytes-derived macrophage and U937 cell systems. J Biomed Mater Res 2002;61(4):505-13.

17. Matheson LA, Santerre JP, Labow RS. Changes in macrophage function and morphology due to biomedical polyurethane surfaces undergoing biodegradation. J Cell Physiol 2004;199(1):8-19.

18. Jackson SH, Gallin JI, Holland SM. The p47phox mouse knock-out model of chronic granulomatous disease. J Exp Med 1995;182(3):751-8.

19. Thomas EL, Fishman M. Oxidation of chloride and thiocyanate by isolated leukocytes. J Biol Chem 1986;261(21):9694-702.

20. Walrand S, Valeix S, Rodriguez C, Ligot P, Chassagne J, Vasson MP. Flow cytometry study of polymorphonuclear neutrophil oxidative burst: a comparison of three fluorescent probes. Clin Chim Acta 2003;331(1-2):103-10.

21. Labow RS, Meek E, Santerre JP. Neutrophil-mediated biodegradation of medical implant materials. J Cell Physiol 2001;186(1):95-103.

22. Labow RS, Tang Y, McCloskey CB, Santerre JP. The effect of oxidation on the enzyme-catalyzed hydrolytic biodegradation of poly(urethane)s. J Biomater Sci Polym Ed 2002;13(6):651-65.

23. Labow RS, Meek E, Santerre JP. Differential synthesis of cholesterol esterase by monocyte-derived macrophages cultured on poly(ether or ester)-based poly(urethane)s. J Biomed Mater Res 1998;39(3):469-77.

24. Boynton EL, Waddell J, Meek E, Labow RS, Edwards V, Santerre JP. The effect of polyethylene particle chemistry on human monocyte-macrophage function in vitro. J Biomed Mater Res 2000;52(2):239-45.

25. Tang YW, Labow RS, Santerre JP. Enzyme-induced biodegradation of polycarbonate-polyurethanes: dependence on hard-segment chemistry. J Biomed Mater Res 2001;57(4):597-611.

26. Tang YW, Labow RS, Santerre JP. Enzyme-induced biodegradation of polycarbonate polyurethanes: dependence on hard-segment concentration. J Biomed Mater Res 2001;56(4):516-28.

27. Schubert MA, Wiggins MJ, Anderson JM, Hiltner A. The effect of strain state on the biostability of a poly(etherurethane urea) elastomer. J Biomed Mater Res 1997;35(3):319-28.

28. Tang YW, Labow RS, Revenko I, Santerre JP. Influence of surface morphology and chemistry on the enzyme catalyzed biodegradation of polycarbonate-urethanes. J Biomater Sci Polym Ed 2002;13(4):463-83.

29. Labow RS, Sa D, Matheson LA, Santerre JP. Polycarbonate-urethane hard segment type influences esterase substrate specificity for human macrophage mediated biodegradation. J Biomater Sci Polym Ed 2005;Accepted.

30. Miakotina OL, Snyder JM. Signal transduction events involved in TPA downregulation of SP-A gene expression. Am J Physiol Lung Cell Mol Physiol 2004;286(6):L1210-9.

31. Okumura K, Shirasawa S, Nishioka M, Sasazuki T. Activated Ki-Ras suppresses 12-O-tetradecanoylphorbol-13-acetate-induced activation of the c-Jun NH2-terminal kinase pathway in human colon cancer cells. Cancer Res 1999;59(10):2445-50.

32. Newton AC. Protein kinase C: structure, function, and regulation. J Biol Chem 1995;270(48):28495-8.

33. Labow RS, Duguay DG, Santerre JP. The enzymatic hydrolysis of a synthetic biomembrane: a new substrate for cholesterol and carboxyl esterases. J Biomater Sci Polym Ed 1994;6(2):169-79.

3.0 MANUSCRIPT #2

The interaction between hydrolytic and oxidative pathways in macrophage-mediated polyurethane degradation

STATEMENT OF AUTHOR CONTRIBUTIONS

Joanne E. McBane was the primary author and sole contributor to the experimental data for this manuscript. **Dr. J. Paul Santerre** is a co-investigator of Dr. Rosalind S. Labow, and principal investigator on the CIHR operating grant that funded this research. Dr. Santerre's Polymer Chemistry laboratory at the University of Toronto synthesized the model PCNU materials used in the following study. He also aided in the editing of the manuscript. **Dr. Rosalind S. Labow** is the supervisor of Joanne E. McBane and contributed to both the experimental design and the editing of the manuscript.

SUMMARY

The following manuscript entitled "The interaction between hydrolytic and oxidative pathways in macrophage-mediated polyurethane degradation" was published in the Journal of Biomedical Materials Research [(2007) 82(4): 984-994]. Manuscript#1 focused on assessing the effect of PMA on MDM-mediated PCNU degradation proposed NADPH oxidase as a possible substrate for the PMA-activated PKC in MDM; however, the respiratory burst was not assayed.

Manuscript#2 proposes NADPH oxidase as a target for the PMA-activated PKC. Also, this manuscript attempts to link the oxidative and hydrolytic pathways of MDM-mediated PCNU degradation. The effect of surface oxidation on subsequent hydrolytic degradation

was assayed. The effect of PCNU oxidation by hydrogen peroxide on cell morphology was shown by scanning electron microscopy.

ABSTRACT

Although relatively resistant to oxidation, polycarbonate-based polyurethanes (PCNU)s are degraded by monocyte-derived macrophages (MDM) by a co-mediated mechanism involving both hydrolytic and oxidative pathways. Since a previous study showed that PCNU pretreatment with H_2O_2 modulated degradation by esterases, human MDM were used to further elucidate this dual pathway mechanism of degradation for ^{14}C-radiolabeled PCNU (synthesized with 1,6-hexane diisocyanate: polycarbonate-diol: butanediol with different stoichiometry (HDI431 and HDI321) or another diisocyanate 4,4'-methylene bisphenyl diisocyanate (MDI321)). Scanning electron microscopy of PCNU slips pretreated with 20% H_2O_2 showed that HDI431 had visible holes with more radiolabel release than from the other PCNUs. When MDM were seeded on H_2O_2-treated PCNUs, degradation of HDI321 and MDI321, but not HDI431 was decreased. Esterase activity was inhibited in MDM on all surfaces except MDI321, whereas inhibition of acid phosphatase occurred on all surfaces. The material surface itself, induced H_2O_2 release from live MDM, with more H_2O_2 elicited by phorbol myristate acetate treated MDM when cultured on HDI431 but not the other materials. H_2O_2 pretreatment affected cell function by chemically altering the material surface and MDM-mediated degradation, known to be dependent on surface chemistry. The findings highlight that both oxidative and hydrolytic mechanisms need to be understood in order to tailor material chemistry to produce desired cell responses for *in vivo* applications.

INTRODUCTION

For many years the synthesis of biomaterials for use in implanted medical devices focused on modifications that would decrease *in vivo* degradation by both oxidative and hydrolytic mechanisms. With the introduction of drug-eluting stents and tissue regeneration applications, the ability to create biomaterials with controlled rates of degradation has become increasingly important. Polyurethanes (PU)s and specifically polycarbonate-based PUs (PCNUs) are useful materials for both types of research since they have been proven to be biocompatible[1] and easily tailored by changing hard segment concentrations or hard segment chemistries[2,3] so that the cell response can be modulated for the intended function of the device. In terms of soft segment chemistries, PCNUs have been proven superior to polyester- and polyether-PUs especially in terms of reduced environmental stress cracking (ESC) and metal ion oxidation; however, they have been shown to be susceptible to hydrolysis[4,5].

The *in vivo* mechanism of PCNU biodegradation, although not completely elucidated, has been linked to white blood cell activation. *In vivo* testing using the cage-implant system has shown that neutrophils come first to the implanted biomaterial followed by monocytes that adhere to the surface and differentiate to monocyte-derived macrophages (MDM)[6], that over time fuse to form multi-nucleated foreign body giant cells[7]. One of the earliest events that occurs in the innate immune response is the respiratory burst resulting in the release of reactive oxygen species (ROS). Protein kinase C (PKC) activation results in the phosphorylation of the p47-*phox* cytosolic subunit of nicotinamide adenine dinucleotide phosphate (NADPH) oxidase (NADPH oxidase)[8,9],

translocating the cytosolic subunit to the plasma membrane to form the active NADPH oxidase complex. Activated NADPH oxidase catalyzes the formation of superoxide anion from oxygen[8]. Neutrophils and monocytes release hypochlorous acid (HOCl)[9] and lysosomal hydrolases[10] as part of their reaction to the foreign surface; however their role diminishes over time. *In vitro* testing has shown that neutrophils incubated with PUs only degraded the surface for 18 hours post-seeding due to decreased viability[11]. As the foreign body reaction progresses, activated MDM produce ROS in response to the material surface[7] and in this case the end product is hydrogen peroxide (H_2O_2).

ESC, the hallmark of long-term implant *in vivo* degradation, has invoked oxidation as the initiating mechanism[12] due to MDM and foreign body giant cells. Various groups have looked into *in vitro* methods for studying ESC using accelerated testing techniques. Several studies have shown that *in vivo* ESC of PUs could be mimicked *in vitro* using concentrated H_2O_2 (10-25%) treatment with or without cobalt chloride[13,14,15]. Differences in the susceptibility to oxidative degradation were found between Elasthane 80A (a polyether-PU) and the PCNU, Bionate 80A[16] using this type of accelerated oxidation system[17,18].

With regard to MDM activation and hydrolytic degradation, cholesterol esterase (CE) and carboxyl esterase (CXE) are two candidate hydrolytic enzymes previously shown to degrade PUs by varying degrees depending on material surface chemistry[4]. Model PCNUs used in previous studies differed in their diisocyanate chemistry (hexane (HDI)- or 4,4'-methylene bis-phenyl (MDI) diisocyanate) and the stoichiometric ratio of

diisocyanate:1,6-hexyl polycarbonate diol (PCN): butanediol (BD) (4:3:1 or 3:2:1) (referred to as HDI431, HDI321 or MDI321). Each PCNU differed in terms of hard segment concentration as well, with HDI431, HDI321 and MDI321 having increasing hard segment concentrations of 20%, 23% and 30% respectively. Previously it has been found that increasing hard segment concentration increases the resistance of a PCNU to hydrolytic degradation by CE[3]. This agreed with *in vitro* data showing that HDI431 was the most susceptible to degradation by MDMs, followed by HDI321 and MDI321[19,20]. CE[21] and monocyte specific esterase[22] (MSE, an esterase with specificity similar to CXE) in MDM were synthesized *de novo* post-re-seeding on the most degradable PCNU, HDI431[20]. Immunoblotting of the conditioned medium of MDM after culturing on the above 3 different PCNU surfaces, showed that both CE and MSE were present, but in significantly different amounts in the cell supernatants from the three surfaces[4,23]. The total esterase activity, *de novo* esterase synthesis and amount of both CE and MSE in MDM differed depending on the material surface chemistry and morphology[20].

Few studies have investigated the link between hydrolytic and oxidative degradation of PCNUs. Pretreatment of aliphatic PCNUs with HOCl caused inhibition of the hydrolytic degradation by CE, whereas MDI321 degradation was slightly increased[24]. In a recent study, it was shown that H_2O_2 pretreatment of the two HDI PCNUs inhibited subsequent CXE-mediated degradation, whereas pretreatment of MDI321 did not reduce degradation[25]. When MDM were cultured with phorbol myristate acetate (PMA), MDM-mediated degradation of HDI PCNUs was inhibited; however, the degradation of MDI321 was unaffected[25]. It was suggested that PMA activation of PKC was responsible for this result since the release of ROS might inhibit susceptibility to hydrolysis of the

HDI PCNUs due to oxidation of the surface. These studies suggest that oxidation of the material can alter the surface chemistry making fewer or more susceptible bonds available for hydrolytic cleavage, or perhaps modulating the MDM response to the altered surface.

Although it appeared in the previous study that oxidation of the surface affected subsequent hydrolysis[25], no determination of the ROS released from MDM on the different materials was made. For the first time, this study quantified the ROS produced by MDM in response to the PCNU surfaces with and without the PMA activation of PKC, and these findings were discussed in terms of structural changes to the surfaces following treatment with H_2O_2, the latter being the end product of the respiratory burst in MDM. In addition, the functional response of MDM to the altered surfaces was assessed by measuring esterase and acid phosphatase (AP) activities.

MATERIALS AND METHODS

Isolation and culture of monocytes-Monocytes were isolated from whole blood (with the approval of the Research Ethics Committee of the University of Ottawa Heart Institute, UOHI 2005-161, valid until Feb. 18, 2007) as previously described[26] by collecting approximately 120 mL of whole blood in EDTA-containing Vacutainers® and layering onto Histopaque 1077, then centrifuging at 1000*xg* followed by serial washing and centrifuging at 450*xg* (10 minutes with 5-6 washes). Monocytes were then seeded on tissue culture polystyrene (TCPS), incubated at 37°C/5% CO_2 and 100% humidity and fed three times a week with RPMI medium with 12.7 mM HEPES, 2.0 g/L sodium

bicarbonate, with 10% fetal bovine serum (FBS), 2% penicillin/streptomycin, and 0.69 mM L-glutamine (complete medium). The mature MDM were trypsinized and re-suspended in complete media by a previously described method[11]. All cell culturing was done in the laminar flow hood under sterile conditions. Cell counts were performed using an automated Vi-Cell™ cell counter (Beckman Coulter; Miami, FL, USA).

Preparation of material surfaces- PCNUs used in this experiment were those described above (HDI431, HDI321 and MDI321) synthesized with an unlabeled or ^{14}C-radiolabeled BD moiety for all three polymers (see Table 3.1)[2,3]. A 10% (w/v) polymer in dimethylacetamide solution was filtered with a 45 μM PTFE (Teflon) Chromospec® syringe filter and glass coverslips (15 mm diameter) were aseptically coated with 100 μL of the polymer solution in a laminar flow hood as described previously[11].

H_2O_2 degradation of PCNUs- The three model PCNUs were incubated at 37°C with 600 μL of 20% H_2O_2 or de-ionized, distilled water (ddH_2O) 24 hours or 72 hours (replacing solution every day). The solution containing the radioactivity released from the PCNUs (600 μL) was removed from each well and added to 10 mL of liquid scintillation cocktail for counting in a liquid scintillation counter (LKB Wallac 1219 RackBeta; Gaithersburg, MD, USA) as previously described[11]. The cumulative counts are given in counts per minute (CPM) per 1 mL of solution less the ddH_2O control. Experiments were repeated at least three times with three replicates within each experiment.

TABLE 3.1

Model PCNU Chemistries

Polymer Name	Diisocyanate	Macrodiol	Chain Extender*	Specific Radioactivity (CPM/100mg)
HDI431	Hexane	poly (1,6-hexyl carbonate) diol	butanediol	1.26×10^7
HDI321	Hexane	poly (1,6-hexyl carbonate) diol	butanediol	1.43×10^7
MDI321	4,4'-Methylene bis-phenyl	poly (1,6-hexyl carbonate) diol	butanediol	1.02×10^7

*Radiolabeled polymers have ^{14}C-radiolabeled carbons in butanediol.

H_2O_2 effect on MDM-mediated biodegradation of PCNUs- For H_2O_2 pretreatment, ~20% H_2O_2 solution (600 μL) or ddH_2O was incubated on the ^{14}C-radiolabeled PCNU slips at 37°C for 24 hours. Prior to re-seeding, each well was washed three times with sterile phosphate buffered saline (PBS: 0.00268 M KCl, 0.00147 M KH_2PO_4, 0.137 M NaCl, 0.00806 M Na_2HPO_4) and this PBS was assayed for H_2O_2 as previously described[27]. If residual H_2O_2 was left additional washes were carried out to prevent cells being exposed to H_2O_2, thereby affecting viability. One million cells per mL (in complete medium) of the re-suspended MDM were added to the sample wells and 1 mL of complete medium without cells was added to the control wells as previously described[11].

After reseeding, the MDM were incubated for 1 hour at 37°C/5% CO_2 and 100% humidity. After 1 hour the supernatant was aspirated off and replaced with complete medium. This plate of cells (named T=48) was incubated for 48 hours at 37°C/5% CO_2 and 100% humidity. Cell supernatants (releasates) were taken from the T=48 plate well and an aliquot removed for counting for radioactivity released as described above. The remainder of the cell supernatant was stored at –80°C until needed for enzyme activity assays. The medium was removed from a well and replaced with 240 μL of lysis buffer (0.05% Triton-X100, 50 mM EDTA in PBS) in order to prepare cell lysates from T=48 plates for DNA analysis and enzyme activity assays (see below). A plate labeled T=0 was made for each experiment and was treated similarly to the T=48 plate except that after the one hour incubation the aspirated supernatant was replaced with the lysis buffer as for the T=48 plates. Radioactivity released and enzyme activity were normalized to the average DNA content of the sample from T=0 to T=48 (CPM per 10 μg DNA or units of enzyme activity per 10 μg DNA) respectively. Experiments were repeated at least three times with three replicates within each experiment.

Assay of DNA content of cell lysates-The amount of DNA present in cell lysates was determined for an aliquot of cell lysate suspension using a modification of the assay outlined previously[20]. Briefly 0.1% Hoescht Dye #33258 was diluted in 10% 10X buffer containing 0.10 M Trizma base, 2.0 M NaCl and 0.01 M EDTA (in ddH_2O), pH 7.4) on the day of analysis. Cell lysate (15 μL) was added to the dye (100 μL) into a 96 well plate and read against a calf thymus DNA standard (100-300 ng) in a fluorescence microplate reader (POLARstar Galaxy, BMG Technologies; Durham, NC, USA).

Assay of acid phosphatase (AP) and esterase activity in MDM cell lysates and releasates- After the 48 hour incubation period, the cell supernatant and the cell lysate of adherent U937 cells were assayed for esterase and AP activities using the substrates p-nitrophenylbutyrate (PNB) and p-nitrophenylphosphate (PNP)[11,28], respectively. One unit of activity was defined as the release of 1 nmol of p-nitrophenol (γ = 16 300 $cm^{-1}M^{-1}$) per minute at 37°C at pH 7.0 and 400.6 nm (PNB) or 410 nm (PNP), as previously described [11,29]. The activities with PNB and PNP substrates were normalized to 10 μg of DNA using the average value from T=0 to T=48 as described above.

Preparation of PKC activator- PMA (1 mg/mL in dimethylsulfoxide) was diluted 15.4 μL in 2.5 mL of PBS solution (pH 7.2) and further diluted in complete MDM medium to give a final concentration of 100 nM, a concentration used previously to measure HOCl production in neutrophils[30].

Dihydroethidium to measure ROS in live MDM: Live cell microscopy with blue fluorescent dihydroethidium (HET) was used to measure ROS in the adherent MDM with an adapted protocol. HET is the chemically reduced form of the commonly used DNA dye ethidium bromide. In the cell cytoplasm HET fluoresces blue (absorption emission: 355nm/420nm); however upon oxidation by superoxide anion and DNA intercalation[31], it becomes red fluorescent ethidium (absorption/emission: 518nm/605nm). PCNU coated glass coverslips were placed in 24-well tissue culture plates and hydrated with 1 mL of sterile PBS solution in each well and incubated overnight at 37°C/5% CO_2 and 100% humidity (no more than 24 hours before the experiment) to equilibrate the slips with an

aqueous environment. MDM were re-seeded on HDI431, HDI321 or MDI321 surfaces, allowed to adhere for one hour as described above and then incubated with 5 μM HET in the presence or absence of 100 nM PMA for 15 minutes before visualizing by excitation at 547nm[32]. Briefly, coverslips were mounted in an aluminum chamber with MDM medium and live images taken using an Olympus IX70 inverted microscope using a Polychrome IV monochrometer and an IMAGO CCD camera from TillPhotonics (GmBH). The cells were maintained at 37°C and images were taken initially and then one and two hours post chamber assembly at various areas of interest. Experiments were repeated at least three times with eight pictures taken at each time point.

Scanning electron microscopy: Cells were fixed in 3% glutaraldehyde in PBS, post fixed in 1% osmium tetroxide, and followed by a series of ethanol washes prior to critical point drying as previously described in detail[26]. The samples were analyzed and photographed using a Hitachi S 2500 Scanning Electron Microscope (Hitachi Ltd., Mito City, Japan) at an operating voltage of 10 kV in the Faculty of Dentistry, University of Toronto.

Statistical analysis-The data were analyzed by either 1 way or 2 way ANOVA using SAS® version 9.0 with a significance value of $p<0.05$ adjusted for multiple comparisons. All data were normalized for differences in specific radioactivity of the polymers, and where appropriate, for differences in cell number.

RESULTS

Effect of H_2O_2 treatment on the degradation of PCNU surfaces- Previously it has been shown that the three model PCNUs used in this study have different susceptibilities to enzymatic[2,3], U937 macrophage-like cells or MDM-mediated degradation[19]. However the susceptibility of these PCNUs to degradation by H_2O_2 oxidation had yet to be characterized. Figure 3.1 shows that by incubating PCNU-coated coverslips with 20% H_2O_2 for 24 hours, the surface can be degraded more than by incubating with ddH_2O. There was a material surface difference whereby the aliphatic PCNUs suffered significantly more degradation with the 24-hour 20% H_2O_2 treatment than MDI321 ($p<0.001$). However, this difference was no longer apparent at 72 hours. SEM analysis of the 24-hour treated slips showed a deepening of crevasses or pitting and holes formed on HDI431 following H_2O_2 treatment compared to the ddH_2O treated surface (Figures 3.2a and 3.2b). HDI321 did not show the same visual differences between the two treatments (Figures 3.3a and 3.3b), even though similar levels of degradation were recorded by ^{14}C release that followed H_2O_2 treatment (Figure 3.1). H_2O_2 treated MDI321 slips showed increased cracking in the material surface compared to ddH_2O treatment (Figures 3.4a and 3.4b) rather than holes for HDI431 (Figures 3.2a and 3.2b) suggesting that the surface had a different sensitivity to the oxidant. The appearance of deep holes (Figure 3.4c and 3.4d) within the cracked regions after 24 hours in 20% H_2O_2 and 48 hours in media parallels the significant increase in ^{14}C release (Figure 3.1) for MDI321 at 72 hours post-treatment.

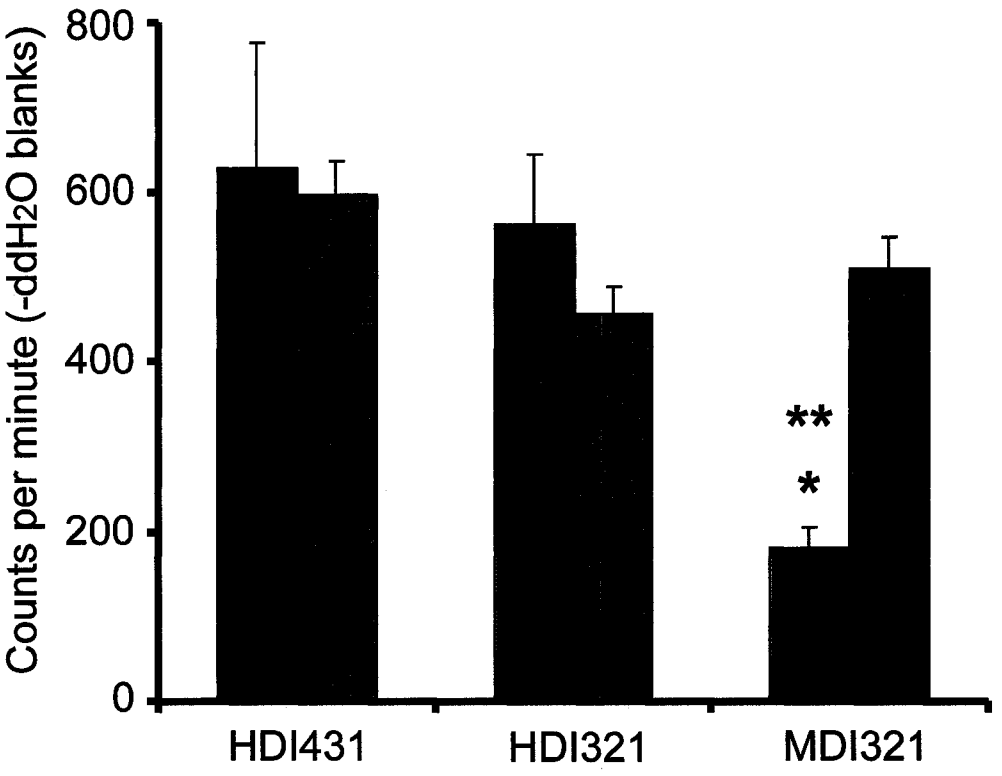

Figure 3.1: Effect of H_2O_2 treatment on the degradation of PCNU surfaces. The ^{14}C-labeled HDI431, HDI321 or MDI321 PCNU coated slips were treated with ddH_2O or 20% H_2O_2 in ddH_2O for 24 hours (red bar) or 72 hours (blue bar) with solutions counted and replaced every day as described in detail in Materials and Methods. Cumulative counts are expressed in counts per minute (CPM) less the ddH_2O control samples. *There was a significant difference between counts taken from MDI321 slips treated for 24 hours (with H_2O_2) compared to MDI321 slips treated for 72 hours. **MDI321 slips treated for 24 hours had significantly less radiolabel release than HDI431 or HDI321 slips. n=3 and data are reported with standard errors of the mean.

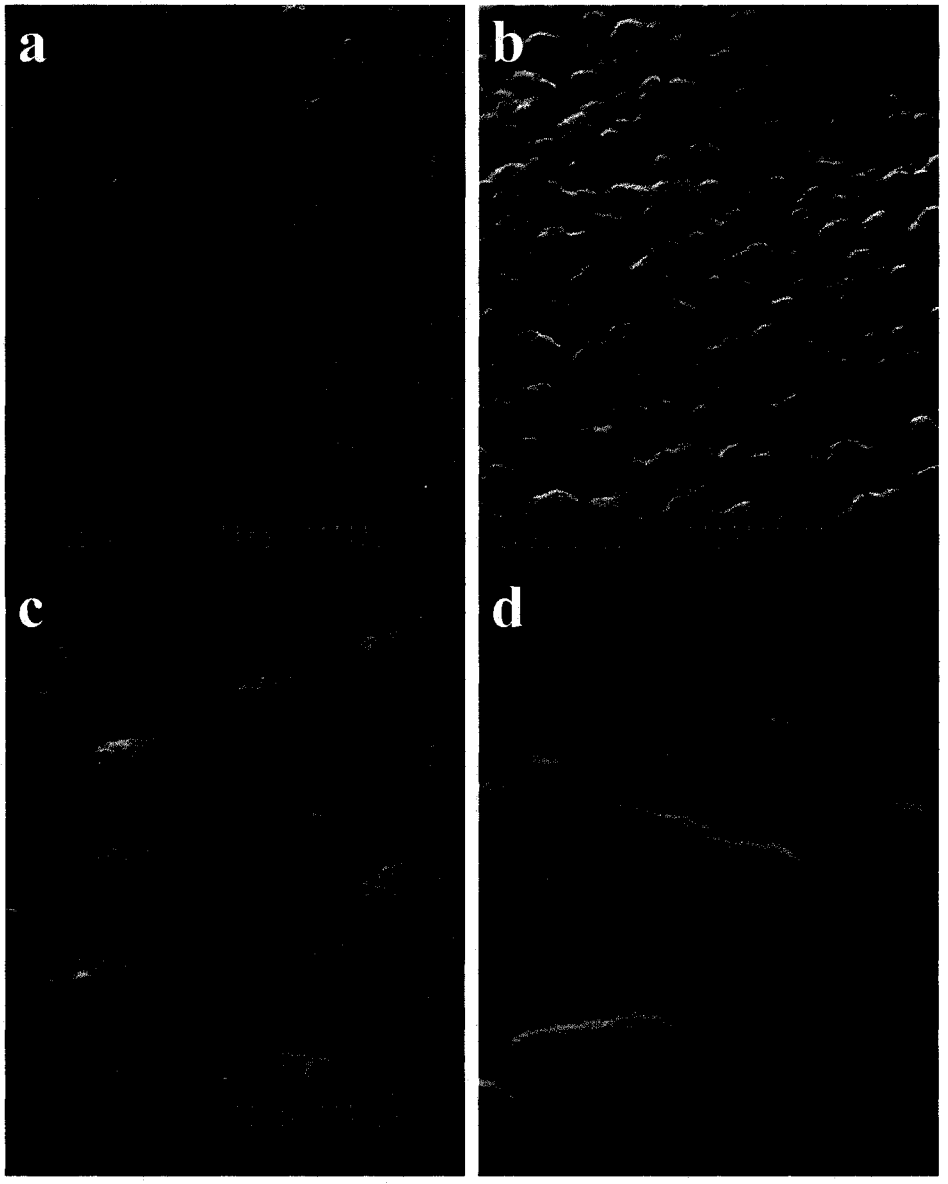

Figure 3.2: Effect of 20% H_2O_2 pretreatment on the surface of HDI431. HDI431 coated coverslips were pretreated for 24 hours with either ddH_2O (a, c) or 20% H_2O_2 (b, d) prior to incubation with complete medium for 48 hours. Slips were then analyzed by SEM as described in detail in Materials and Methods.

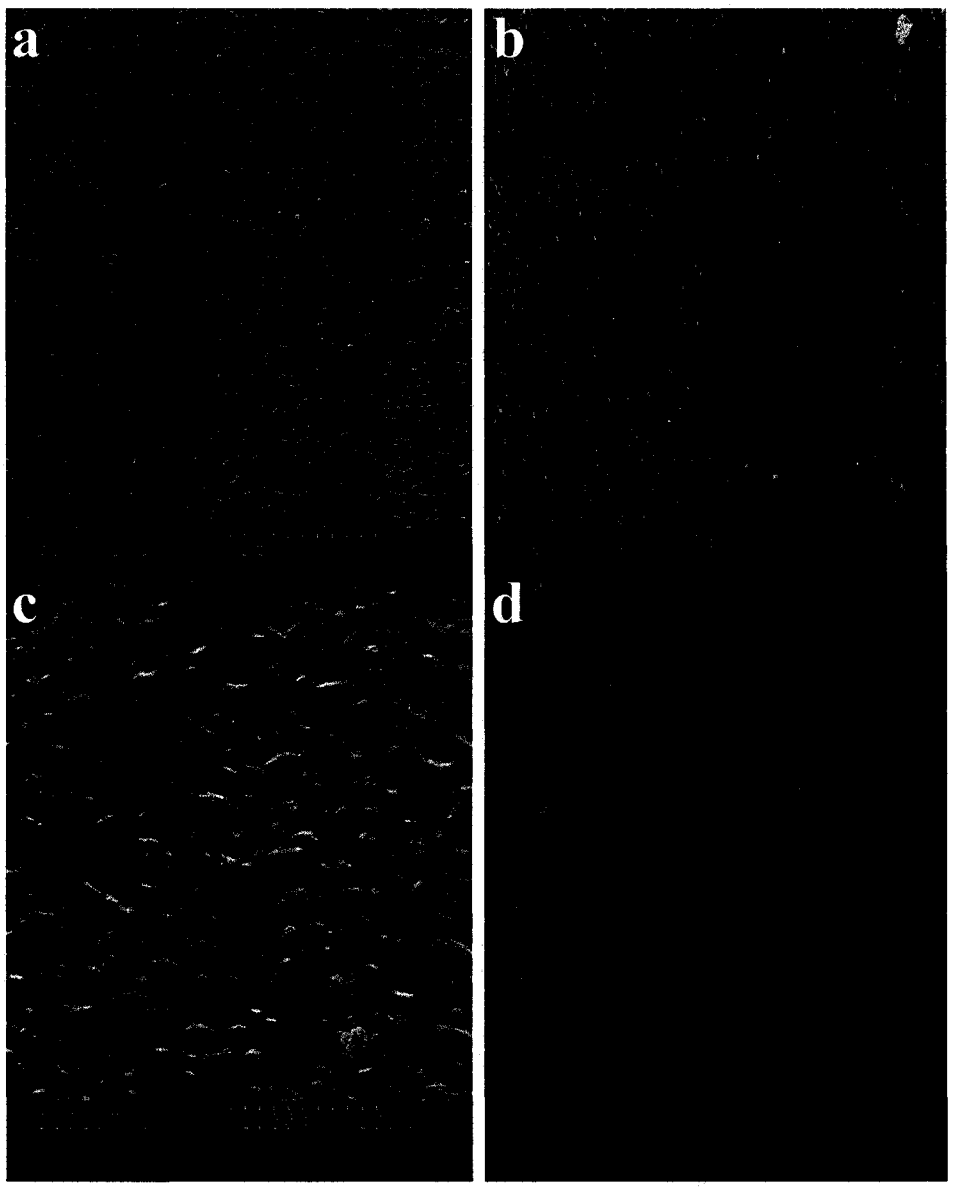

Figure 3.3: Effect of 20% H_2O_2 pretreatment on the surface of HDI321. HDI321 coated coverslips were pretreated for 24 hours with either ddH_2O (a, c) or 20% H_2O_2 (b, d) prior to incubation with complete medium for 48 hours. Slips were then analyzed by SEM as described in detail in Materials and Methods.

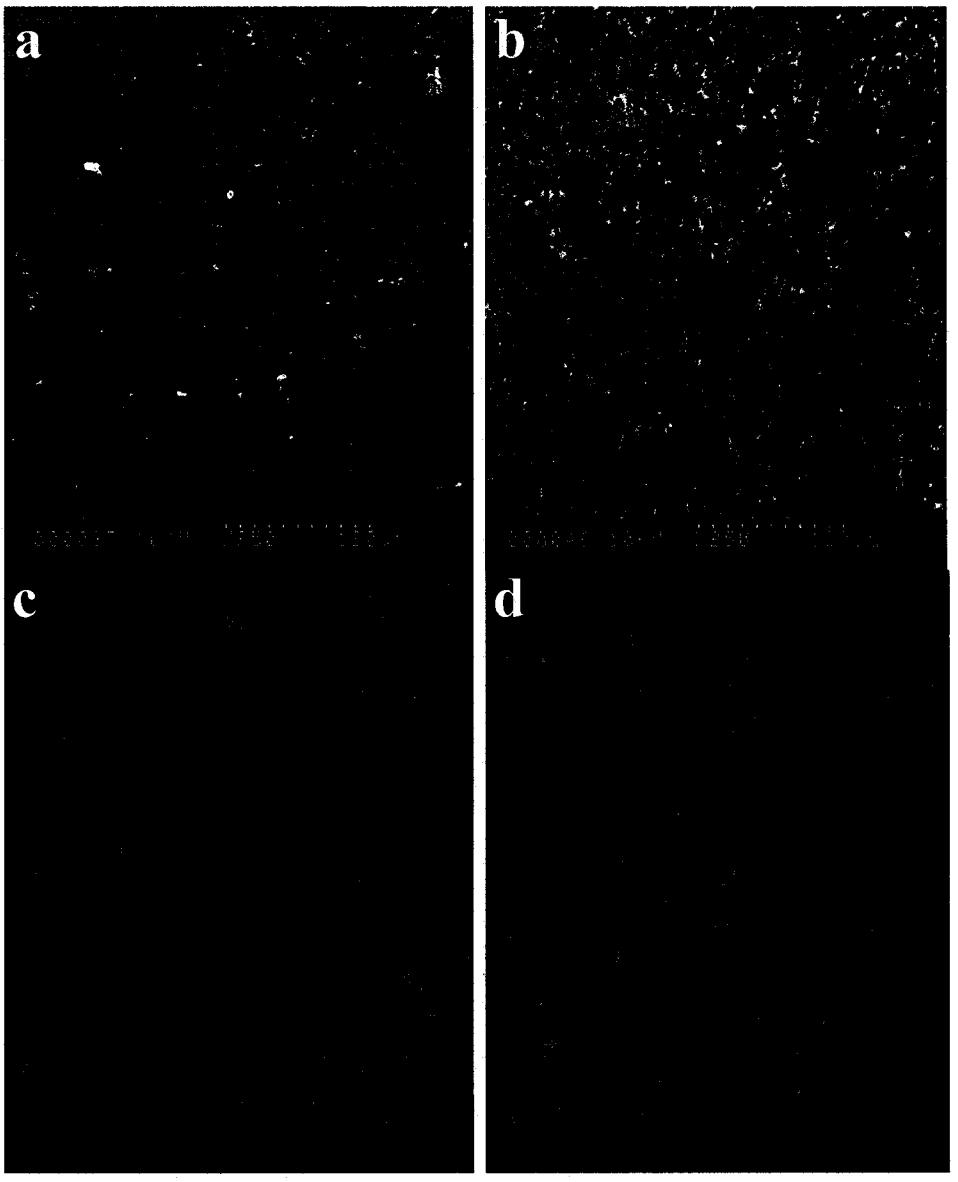

Figure 3.4: Effect of 20% H_2O_2 pretreatment on the surface of MDI321. MDI321 coated coverslips were pretreated for 24 hours with either ddH_2O (a, c) or 20% H_2O_2 (b, d) prior to incubation with complete medium for 48 hours. Slips were then analyzed by SEM as described in detail in Materials and Methods.

Effect of H_2O_2 pretreatment on MDM-mediated degradation of PCNUs- To test the MDM-mediated biodegradation of PCNUs following surface oxidation, PCNUs were treated with 20% H_2O_2 for 24 hours prior to re-seeding with MDM. Figure 3.5 shows that HDI321 and MDI321 slips pretreated with H_2O_2 showed a significant (50%) inhibition (both $p<0.001$) of biodegradation by MDM relative to MDM seeded on slips pretreated with ddH_2O. The degradation of HDI431 was not significantly inhibited by pretreatment with H_2O_2 maintaining a greater degree of degradation than the other surfaces (Figure 3.5, $p<0.001$).

A material surface difference was also seen in terms of esterase activity. The lysates of MDM that were re-seeded on the two HDI PCNUs showed significant inhibition of esterase activity when these slips had been pretreated with H_2O_2 ($p<0.001$). No inhibition of esterase activity was seen for the MDM re-seeded on pretreated MDI321 (Figure 3.5). There was an inhibition of AP activity for cells re-seeded on all the H_2O_2 pretreated surfaces compared to the ddH_2O treated surfaces. Even though significantly inhibited relative to ddH_2O pretreatment, cells re-seeded on HDI431 had significantly more AP activity remaining than the MDM on the other surfaces (Figure 3.5).

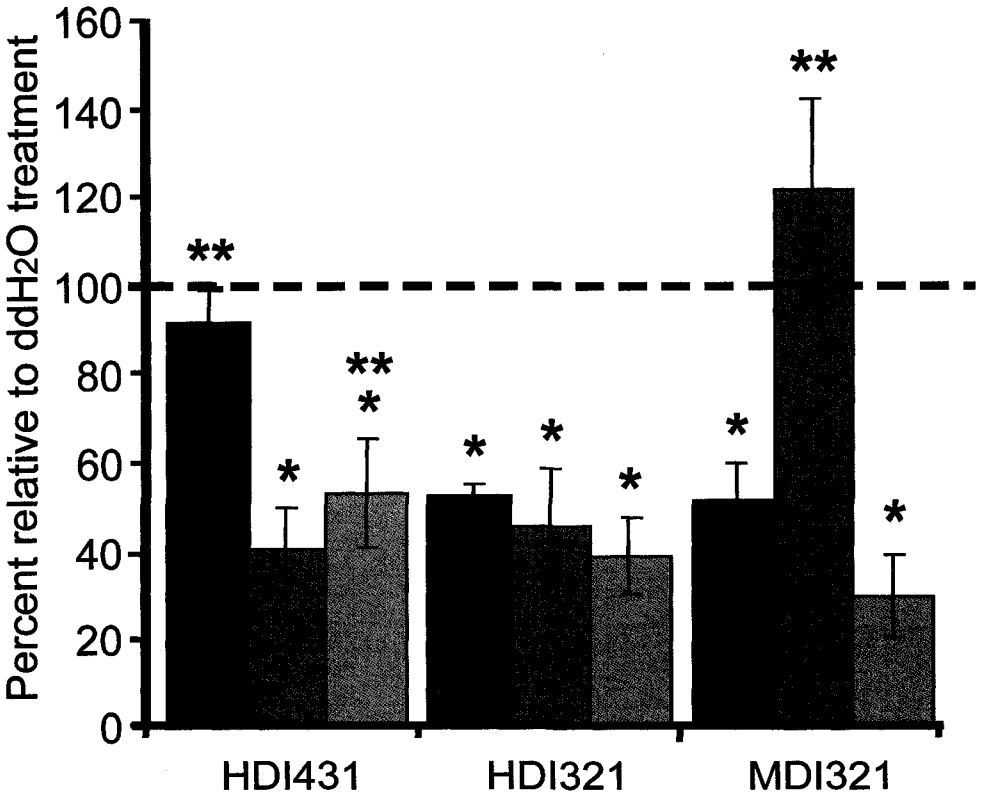

Figure 3.5: Effect of H_2O_2 pretreatment on MDM-mediated biodegradation, esterase, and AP activities following re-seeding on the PCNU surfaces. ^{14}C-labeled PCNU-coated slips were pretreated for 24 hours with 20% H_2O_2 or ddH_2O prior to re-seeding with MDM for 48 hours as described in detail in Materials and Methods. Wells were analyzed for radiolabel release (red bar), esterase activity (EA, blue bar) and AP activity (green bar). *There was a significant inhibition compared to ddH_2O treated slips. ** There was a material surface difference where the indicated surface was significantly higher than the other surfaces. n=3 and data are reported with standard errors of the mean.

Although there were significant differences in the SEMs of the H_2O_2 treated PCNUs compared to ddH_2O treatment (Figure 3.2), SEM analysis of MDM re-seeded on the three PCNUs that had been treated showed that there was no significant morphological difference between cells on ddH_2O pretreated slips versus H_2O_2 pretreated slips (Figures 3.6-3.8). However, the morphological differences seen previously[20] between MDM re-seeded on the HDI PCNUs (Figures 3.6 and 3.7) compared to MDI321 (Figure 3.8) were maintained on the pretreated PCNUs. MDM re-seeded on HDI PCNUs appeared less spread out and more three-dimensional (Figures 3.6 and 3.7) than those re-seeded on MDI321 that tended to be more flat (Figure 3.8). The latter again reflecting important differences in surface chemistry and morphology, reported on previously by Labow and Santerre[33,34].

Effect of material surface chemistry and PKC activation on the ROS production in MDM- To measure the ROS produced in live MDM re-seeded on different material surfaces, blue fluorescent HET was added to MDM medium with or without PMA for 15 minutes prior to imaging. Figure 3.9 is the quantification of these images taken on all three surfaces. Using this method, the ROS produced in cells could successfully be visualized even in the absence of a PKC activator like PMA. ROS production in MDM, in the absence of PMA, was similar on all three surfaces (Figure 3.9). Interestingly, in the presence of PMA the ROS production in MDM on HDI431 was significantly higher than on all the other surfaces (Figure 3.9, $p<0.001$).

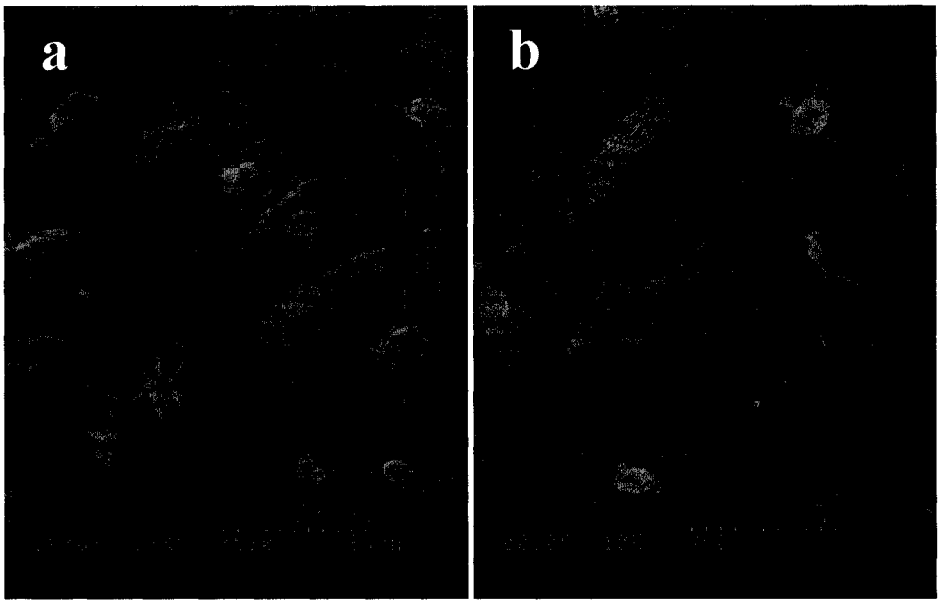

Figure 3.6: Effect of 20% H_2O_2 pretreatment on the surface of HDI431 incubated with MDM. HDI431 coated coverslips were pretreated for 24 hours with either ddH_2O (a) or 20% H_2O_2 (b) prior to incubation with MDM in complete medium for 48 hours. Slips were then analyzed by SEM as described in detail in Materials and Methods.

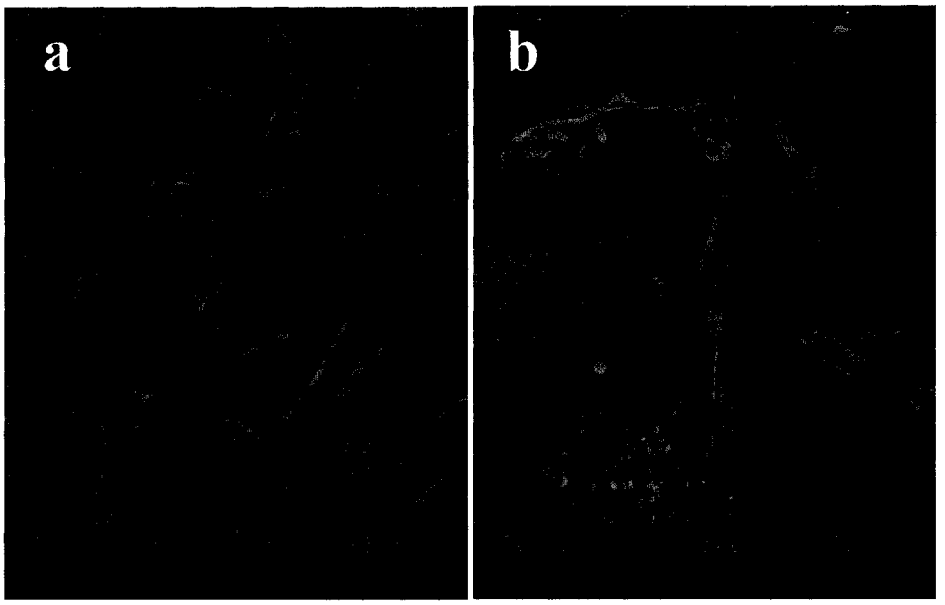

Figure 3.7: Effect of 20% H_2O_2 pretreatment on the surface of HDI321 incubated with MDM. HDI321 coated coverslips were pretreated for 24 hours with either ddH_2O (a) or 20% H_2O_2 (b) prior to incubation with MDM in complete medium for 48 hours. Slips were then analyzed by SEM as described in detail in Materials and Methods.

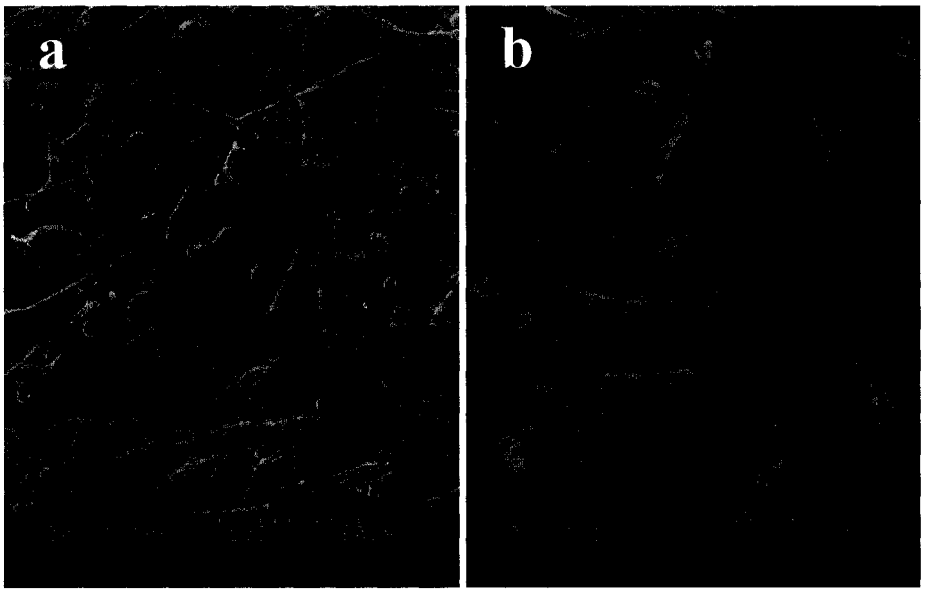

Figure 3.8: Effect of 20% H_2O_2 pretreatment on the surface of MDI321 incubated with MDM. MDI321 coated coverslips were pretreated for 24 hours with either ddH_2O (a) or 20% H_2O_2 (b) prior to incubation with MDM in complete medium for 48 hours. Slips were then analyzed by SEM as described in detail in Materials and Methods.

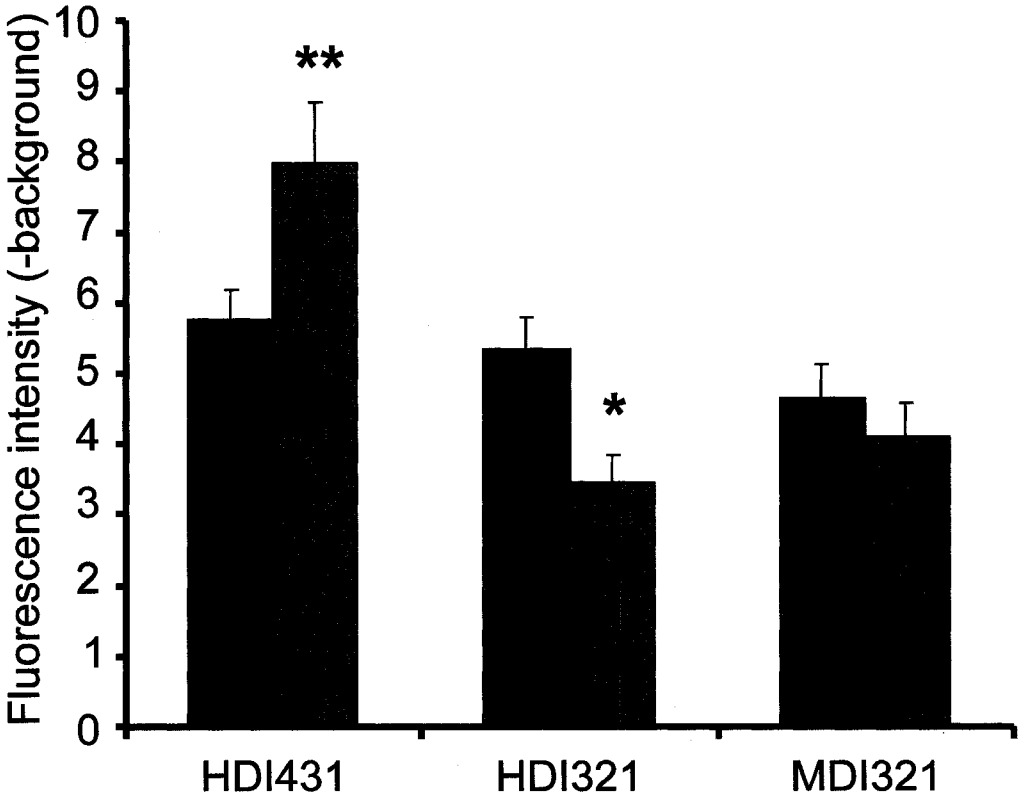

Figure 3.9: Effect of PMA on the amount of ROS produced in MDM re-seeded on HDI431, HDI321 or MDI321 coated slips. MDM were re-seeded onto surfaces for 1h prior to incubation with 5μM HET without PMA (red bar) or with 100nM PMA (blue bar) for 15 minutes as described in detail in Materials and Methods. Live cell fluorescent images (547nm) taken at start, 1h and 2h timepoints were quantified as the sum of pixel intensity per cell minus the background. *Significant inhibition of ROS production with PMA treated cells compared to cells in media only. **Significantly greater ROS than cells on the other surfaces. n=3 and all data are reported with standard error of the mean.

No significant difference in ROS production was seen between MDM re-seeded on MDI321 in the presence or absence of PMA. PMA had a negative effect on the ROS production of MDM re-seeded on HDI321 (Figure 3.9, p=0.003, p=0.005, respectively).

DISCUSSION

The results of this study have shown for the first time that changes in surface state, generated by oxidation, affected cellular responses ultimately leading to differences in the mechanism and degree of material degradation especially hydrolysis (Figure 3.5). Although a previous study comparing the oxidation of polyether PUs to a commercial MDI-containing PCNU showed the latter to be more resistant to oxidation both chemically (less chain scission and cross-linking) and physically (less pitting)[35], the present study found that changes in surface structures did occur following treatment with 20% H_2O_2. Therefore, degradation must always be discussed in the context of specific PUs and not PUs in general. The use of 20% H_2O_2 was justified in previous accelerated studies as being physiologically relevant because it mimics the oxidative environment created at the cell-material interface[17,18] and was used here for comparative purposes to earlier data only.

The degree of degradation following treatment of the surfaces with 20% H_2O_2 measured by radiolabel release agreed with what was observed with SEM analysis (Figures 3.1-3.4). HDI431 slips treated with H_2O_2 were degraded significantly more than the other PCNUs (Figure 3.1). The SEMs showed that the surface of HDI431 was pitted and had visible holes (Figures 3.2 and 3.6) on the order of 5-10 μm, whereas the surface of

MDI321 had cracks (Figures 3.4 and 3.8). The cracking in MDI321 may be due to the unique surface features presented by this material that have been reported on elsewhere by the authors[33,34]. MDI321 forms big domains of MDI hard segment H-bonded to polycarbonate segments. Chemical hydrolysis of the carbonate groups can only readily occur around the rim of these domains. This would account for the slower release of hard segment components during oxidative degradation of MDI321 (Figure 3.1) and the fact that these sites appear as cracks surrounding plaques of non-degraded polymer (Figure 3.4). Previously an investigation on the degradation of Biomer™ fractions (a polyether PU) showed that both the hard segment (MDI) aromatic urethane bond and soft segment could undergo oxidative attack[36]. It is well known that aromatic urethanes are more sensitive to oxidation than are aliphatic PUs[37] and therefore the extensive surface deformation of MDI321 in comparison to the HDI polymers most likely reflects the attack of aromatic hard segments. Hence, the chemical structures at the surfaces of HDI431, HDI321 and MDI321 differed sufficiently[33,34] to exhibit variation in the mechanism of biodegradation caused by the oxidation with H_2O_2.

Degradation by MDM is believed to involve both oxidation and hydrolytic degradation. However, the dominance of one mechanism over the other appears to be dictated in a significant manner by the specific chemical and surface morphological features of a particular PU. A recent study by the Hiltner group suggested that oxidation was a more important mechanism of degradation of PCNUs than hydrolytic degradation by enzymes such as CE[38]. The MDI-based PCNU used in that study showed minimal degradation by CE when compared to the degradation caused by 20% H_2O_2 and cobalt chloride

treatment[38]. Previous characterization of the PCNUs used in this study suggest that the HDI based PCNUs are more susceptible to hydrolytic degradation by CE than MDI321[2,3,5]; as well, *in vitro* characterization has shown that the synthesis of CE and MSE can be stimulated more by re-seeding cells onto different surfaces[20]. For instance, MDM re-seeded on non-degradable TCPS have previously been found to produce more esterase activity than MDM re-seeded on the three PCNUs tested in this study[19]. Another study of these PCNUs showed that MDM-mediated degradation of HDI431 was affected differently from the degradation of HDI321 (after the addition of the PKC inhibitor H-7)[25]. These studies suggest that MDM can differentiate and react differently to material surfaces that have identical chemical moieties and differ by only 3% in hard segment concentration[3]. Therefore, although other studies have suggested that oxidation is the most dominant activity in the degradation of PUs[38], this does not hold true for PUs in general and even for specific classes of PUs (i.e. polyether-PUs, PCNUs, etc.) but rather the mechanism is tied to specific chemistry and its intermolecular assembly. What the cell is stimulated to produce and how that activity alters the material surface are important factors that need to be considered in order to determine whether oxidative or hydrolytic means of PU degradation will prevail.

Even though MDM may be stimulated to produce certain activities when re-seeded on a surface, the susceptibility of the surface to degradation by that activity is dependent on the chemistry of the material surface itself. Since MDI321 has an increase in the amount of hydrogen bonding between the carbonate and urethane bonds[2] it was more stable than the HDI-based PCNUs. This was probably due to the fact that MDI321 is phase mixed

whereas the HDI PCNUs are phase-separated. Therefore, different products were produced since different bonds were susceptible to cleavage by CE[39]. Methylene dianiline was found to be a product from CE-mediated MDI321 degradation, but hexamethylene diamine was not one of the products of HDI321[39]. It was suggested that for HDI321 the carbonate soft segment and carbonate bonds adjacent to the urethane linkage were more susceptible to hydrolysis, but for MDI321 the urethane bond was the most susceptible[39], with the carbonate bonds being stabilized[2] to a greater extent than similar bonds in the HDI polymers due to shielding by the aromatic hard segment.

Since esterases (CE and MSE) in MDM have been associated with hydrolytic degradation of PCNUs, exhibiting differences in the amount synthesized and secreted when adherent to the different surfaces, it was of interest to assess the effect of the oxidized surfaces on both degradation and the esterase activity in the adherent MDM. Previously, oxidation of a PCNU by H_2O_2 pretreatment did show changes in its susceptibility to hydrolytic cleavage by CXE[25]. Since neutrophils, monocytes and MDM all release ROS it is possible *in vivo* for an MDM to attach to an implanted material that has previously been oxidized. There were significant differences in the response of the MDM adherent to the oxidized PCNUs. HDI431 MDM-mediated degradation was not altered by H_2O_2 pretreatment, whereas the degradation of HDI321 and MDI321 was inhibited (Figure 3.6). This suggests that oxidation can degrade HDI431 without hindering the subsequent MDM-mediated degradation. The differences seen with the various materials strongly indicated that degradation by the MDM must proceed through multiple pathways, some of which interfere with each other, or others that are additive.

In addition to significant differences in degradation post-oxidation of 3 PCNUs, the amount of esterase activity in the MDM adherent to the oxidized surfaces also was significantly different (Figure 3.5). The esterase activity in MDM adherent to MDI321 was significantly greater than the other 2 surfaces. Previously, esterase activity has been found to be an indicator of the degradative potential of macrophages towards PCNUs[4,23]. Although not a classical marker of the immune response, esterases have been associated with many pathological conditions. MSE has been shown to increase in leukemias[40] or be deficient in other malignancies as well as autoimmune diseases[41]. Recently, MSE has been shown to be a marker of HL60 differentiation that requires retinoblastoma protein and Vitamin D_3[42]. Therefore, increased esterase activity in the MDM adherent to the MDI321 surface may be a sign of cell activation. In a previous study, in which monocytes were differentiated on MDI321, more CE protein was measured post re-seeding on HDI431[43], suggesting the MDM had been differentiated to an "activated" phenotype.

In addition to ROS and esterase activity an additional marker of the foreign body reaction to a biomaterial may be AP, a lysosomal enzyme that has been shown to be associated with MDM activation[44]. In another study, AP activity in MDM was influenced by the material surface it was re-seeded on, with non-degradable polydimethylsiloxane re-seeded MDM having significantly greater activity than those re-seeded on PCNU surfaces[19]. In addition, there was significantly more AP protein in MDM re-seeded on PCNUs than those re-seeded on TCPS[19]. Since AP activity was inhibited in all cells re-seeded on the H_2O_2 pretreated PCNU surfaces (Figure 3.5), it is tempting to say that these

surfaces became less activating following oxidation. However, the most degradable PCNU, HDI431, with the least inhibition by oxidation, had significantly more AP activity in the adherent MDM even though it was significantly decreased relative to ddH_2O pretreated controls.

After determining the effect of PCNU oxidation on MDM-mediated biodegradation and induced enzymatic activities the next step was to determine if the production of ROS in MDM was affected by material surface chemistry. MDM re-seeded on HDI431 in the presence of PMA had the greatest overall production of ROS (Figure 3.9), which agrees with HDI431 being an activating, degradable substrate. A previous study using peritoneal and bone-marrow derived macrophages from tartrate-resistant AP deficient mice showed that PMA-induced superoxide anion production was increased in these cells, possibly due to an increase in pro-inflammatory cytokines[44]. So, even though AP activity was not increased in MDM re-seeded on HDI431 over the other surfaces[19], it was possible that inflammatory cytokines induced by PMA may have caused cell activation, eliciting the greater release of ROS from cells on HDI431.

Although PMA could activate ROS production in MDM re-seeded on HDI431 this was not the case for MDM on all surfaces. A previous study using a luminol-chemiluminescence assay with synovial macrophage-like cells found that PMA was required to measure ROS production[45]. However, this study found that PMA was not required for intracellular ROS production on all the surfaces (Figure 3.9). It was surprising to note that the addition of PMA did not stimulate, but significantly inhibited

ROS production in MDM re-seeded on HDI321 (Figure 3.9). HDI321 surface chemistry could be initiating the respiratory burst and PMA may compete and inhibit the production of ROS in these MDM. This result may explain why adding PMA to MDM re-seeded on HDI321 could inhibit degradation of the surface. However, PMA also inhibited biodegradation of MDM re-seeded on HDI431[25]. In this case, esterase activity was also inhibited in the MDM re-seeded on HDI431 in the presence of PMA[25]. Therefore it is possible that PMA inhibiting esterase activity by an unknown mechanism was more detrimental to the MDM-mediated degradation of HDI431 than the increase in ROS production (Figure 3.9). Perhaps in MDM-mediated degradation of HDI431, hydrolytic degradation is equally or more important than oxidative degradation, therefore highlighting once again the caution required when projecting biodegradation findings to a large family of polymers with diverse chemistries. Since MDM re-seeded on MDI321 showed no difference in ROS production, with or without PKC activation, it suggests that the material surface itself maximally triggered the respiratory burst in these cells. This agrees with previous findings that showed that the MDM-mediated degradation of MDI321 was not affected by PMA activation[25].

CONCLUSIONS

This study has shown for the first time that oxidation of PU surfaces can alter MDM functional responses, with respect to material degradation mechanisms. During the foreign body reaction to a biomaterial surface, both hydrolytic and oxidative activities may be triggered by the contact of the material with the surrounding tissue. By altering material chemistry either hydrolytic or oxidative mechanisms of degradation may be

preferred. In addition, the MDM functional responses, as assessed by esterase and AP activities reflected the changes in the material surfaces. Ultimately our understanding of the material activation of MDM pathways, leading to degradation, will help in the creation of materials that elicit the desired response from MDM *in vivo*, eliminating deleterious effects observed due to the foreign body reaction.

ACKNOWLEDGEMENTS

Thanks to Sarah McDonald and Katherine Suter who helped perform esterase and AP activity assays. The polymers were synthesized by Dr. Meilin Yang, Faculty of Dentistry, University of Toronto (Toronto, ON). The authors are grateful to Dr. Heidi McBride and Margaret Neuspiel from the University of Ottawa Heart Institute for advice and technical assistance with the live-cell microscopy experiments. Thanks to Robert Chernecky at the University of Toronto who performed all SEM analysis. JE McBane was partially funded by a CIHR Strategic Training Fellowship for Cell Signaling in Mucosal Inflammation and Pain (STP-53877) and by an Ontario Graduate Scholarship in Science and Technology. These studies were funded by a grant from the Canadian Institutes for Health Research (CIHR).

REFERENCES

1. Zdrahala RJ, Zdrahala IJ. Biomedical applications of polyurethanes: a review of past promises, present realities, and a vibrant future. J Biomater Appl 1999;14(1):67-90.

2. Tang YW, Labow RS, Santerre JP. Enzyme-induced biodegradation of polycarbonate-polyurethanes: dependence on hard-segment chemistry. J Biomed Mater Res 2001;57(4):597-611.

3. Tang YW, Labow RS, Santerre JP. Enzyme-induced biodegradation of polycarbonate polyurethanes: dependence on hard-segment concentration. J Biomed Mater Res 2001;56(4):516-28.

4. Labow RS, Meek E, Matheson LA, Santerre JP. Human macrophage-mediated biodegradation of polyurethanes: assessment of candidate enzyme activities. Biomaterials 2002;23(19):3969-75.

5. Tang YW, Labow RS, Santerre JP. Enzyme induced biodegradation of polycarbonate-polyurethanes: dose dependence effect of cholesterol esterase. Biomaterials 2003;24(12):2003-11.

6. Marchant R, Hiltner A, Hamlin C, Rabinovitch A, Slobodkin R, Anderson JM. In vivo biocompatibility studies. I. The cage implant system and a biodegradable hydrogel. J Biomed Mater Res 1983;17(2):301-25.

7. Marchant RE, Miller KM, Anderson JM. In vivo biocompatibility studies. V. In vivo leukocyte interactions with Biomer. J Biomed Mater Res 1984;18(9):1169-90.

8. Jackson SH, Gallin JI, Holland SM. The p47phox mouse knock-out model of chronic granulomatous disease. J Exp Med 1995;182(3):751-8.

9. Thomas EL, Fishman M. Oxidation of chloride and thiocyanate by isolated leukocytes. J Biol Chem 1986;261(21):9694-702.

10. Anderson JM. Mechanisms of inflammation and infection with implanted devices. Cardiovasc Pathol 1993;2(3):33S-41S.

11. Labow RS, Meek E, Santerre JP. Model systems to assess the destructive potential of human neutrophils and monocyte-derived macrophages during the acute and chronic phases of inflammation. J Biomed Mater Res 2001;54(2):189-97.

12. Stokes K, McVenes R, Anderson JM. Polyurethane elastomer biostability. J Biomater Appl 1995;9(4):321-54.

13. Meijs GF, McCarthy SJ, Rizzardo E, Chen YC, Chatelier RC, Brandwood A, Schindhelm K. Degradation of medical-grade polyurethane elastomers: the effect of hydrogen peroxide in vitro. J Biomed Mater Res 1993;27(3):345-56.

14. Zhao QH, McNally AK, Rubin KR, Renier M, Wu Y, Rose-Caprara V, Anderson JM, Hiltner A, Urbanski P, Stokes K. Human plasma alpha 2-macroglobulin promotes in vitro oxidative stress cracking of Pellethane 2363-80A: in vivo and in vitro correlations. J Biomed Mater Res 1993;27(3):379-88.

15. Martin DJ, Warren LA, Gunatillake PA, McCarthy SJ, Meijs GF, Schindhelm K. New methods for the assessment of in vitro and in vivo stress cracking in biomedical polyurethanes. Biomaterials 2001;22(9):973-8.

16. Christenson EM, Anderson JM, Hiltner A. Oxidative mechanisms of poly(carbonate urethane) and poly(ether urethane) biodegradation: In vivo and in vitro correlations. J Biomed Mater Res 2004;70A(2):245-55.

17. Schubert MA, Wiggins MJ, Anderson JM, Hiltner A. Role of oxygen in biodegradation of poly(etherurethane urea) elastomers. J Biomed Mater Res 1997;34(4):519-30.

18. Schubert MA, Wiggins MJ, Schaefer MP, Hiltner A, Anderson JM. Oxidative biodegradation mechanisms of biaxially strained poly(etherurethane urea) elastomers. J Biomed Mater Res 1995;29(3):337-47.

19. Matheson LA, McBane JE, Malowany JI, Santerre JP, Labow RS. A comparison of the effects of degradable and non-degradable polymers on U937 cell morphology and function. in preparation 2006.

20. Matheson LA, Santerre JP, Labow RS. Changes in macrophage function and morphology due to biomedical polyurethane surfaces undergoing biodegradation. J Cell Physiol 2004;199(1):8-19.

21. Li F, Hui DY. Modified low density lipoprotein enhances the secretion of bile salt-stimulated cholesterol esterase by human monocyte-macrophages. species-specific difference in macrophage cholesteryl ester hydrolase. J Biol Chem 1997;272(45):28666-71.

22. Saboori AM, Newcombe DS. Human monocyte carboxylesterase. Purification and kinetics. J Biol Chem 1990;265(32):19792-9.

23. Matheson LA, Labow RS, Santerre JP. Biodegradation of polycarbonate-based polyurethanes by the human monocytes-derived macrophage and U937 cell systems. J Biomed Mater Res 2002;61(4):505-13.

24. Labow RS, Tang Y, McCloskey CB, Santerre JP. The effect of oxidation on the enzyme-catalyzed hydrolytic biodegradation of poly(urethane)s. J Biomater Sci Polym Ed 2002;13(6):651-65.

25. McBane JE, Santerre, J.P., Labow, R.S. Winner of the Student Research Award in the Master's Degree Candidate Category, 30th Annual Meeting of the Society for Biomaterials, Memphis, Tennessee, April 27-30, 2005: Role of protein kinase C in the monocyte-derived macrophage-mediated biodegradation of polycarbonate-based polyurethanes. J Biomed Mater Res 2005;74A:1-11.

26. Labow RS, Meek E, Santerre JP. Differential synthesis of cholesterol esterase by monocyte-derived macrophages cultured on poly(ether or ester)-based poly(urethane)s. J Biomed Mater Res 1998;39(3):469-77.

27. Pick E, Keisari Y. A simple colorimetric method for the measurement of hydrogen peroxide produced by cells in culture. J Immunol Methods 1980;38(1-2):161-70.

28. Hayman AR, Warburton MJ, Pringle JA, Coles B, Chambers TJ. Purification and characterization of a tartrate-resistant acid phosphatase from human osteoclastomas. Biochem J 1989;261(2):601-9.

29. Akisaka T, Subita GP, Kawaguchi H, Shigenaga Y. Different tartrate sensitivity and pH optimum for two isoenzymes of acid phosphatase in osteoclasts. An electron-microscopic enzyme-cytochemical study. Cell Tissue Res 1989;255(1):69-76.

30. Labow RS, Meek E, Santerre JP. Neutrophil-mediated biodegradation of medical implant materials. J Cell Physiol 2001;186(1):95-103.

31. Rothe G, Valet G. Flow cytometric analysis of respiratory burst activity in phagocytes with hydroethidine and 2',7'-dichlorofluorescin. J Leukoc Biol 1990;47(5):440-8.

32. Neuspiel M, Zunino R, Gangaraju S, Rippstein P, McBride H. Activated mitofusin 2 signals mitochondrial fusion, interferes with Bax activation, and reduces susceptibility to radical induced depolarization. J Biol Chem 2005;280(26):25060-70.

33. Tang YW, Labow RS, Revenko I, Santerre JP. Influence of surface morphology and chemistry on the enzyme catalyzed biodegradation of polycarbonate-urethanes. J Biomater Sci Polym Ed 2002;13(4):463-83.

34. Revenko I, Tang YW, Santerre JP. Surface structure of polyurethanes visulaized by atomic force microscopy. Surface Science 2001;491(3):346-354.

35. Wiggins MJ, MacEwan M, Anderson JM, Hiltner A. Effect of soft-segment chemistry on polyurethane biostability during in vitro fatigue loading. J Biomed Mater Res A 2004;68(4):668-83.

36. Tyler BJ, Ratner BD. Oxidative degradation of Biomer fractions prepared by using preparative-scale gel permeation chromatography. J Biomater Sci Polym Ed 1994;6(4):359-73.

37. Lelah MD, Cooper SL. Polyurethanes in Medicine. Boca Raton, FL: CRC Press; 1986.

38. Christenson EM, Patel S, Anderson JM, Hiltner A. Enzymatic degradation of poly(ether urethane) and poly(carbonate urethane) by cholesterol esterase. Biomaterials 2006;27(21):3920-6.

39. Tang YW, Labow RS, Santerre JP. Isolation of methylene dianiline and aqueous-soluble biodegradation products from polycarbonate-polyurethanes. Biomaterials 2003;24(17):2805-19.

40. Uphoff CC, Drexler HG. Biology of monocyte-specific esterase. Leuk Lymphoma 2000;39(3-4):257-70.

41. Boyle C, Cosby SL, Markey GM, Alexander HD, Morris TC. Quantitative deficiency of monocyte-specific esterase (MSE) mRNA in monocyte esterase deficiency (MED). Br J Haematol 2000;110(3):699-703.

42. Ji Y, Studzinski GP. Retinoblastoma protein and CCAAT/enhancer-binding protein beta are required for 1,25-dihydroxyvitamin D3-induced monocytic differentiation of HL60 cells. Cancer Res 2004;64(1):370-7.

43. Labow RS, Sa D, Matheson LA, Dinnes DL, Santerre JP. The human macrophage response during differentiation and biodegradation on polycarbonate-based polyurethanes: dependence on hard segment chemistry. Biomaterials 2005;26(35):7357-66.

44. Bune AJ, Hayman AR, Evans MJ, Cox TM. Mice lacking tartrate-resistant acid phosphatase (Acp 5) have disordered macrophage inflammatory responses and reduced clearance of the pathogen, Staphylococcus aureus. Immunology 2001;102(1):103-13.

45. Tanabe T, Otani H, Mishima K, Ogawa R, Inagaki C. Phorbol 12-myristate 13-acetate (PMA)-induced oxyradical production in rheumatoid synovial cells. Jpn J Pharmacol 1997;73(4):347-51.

4.0 MANUSCRIPT #3

The effects of phorbol ester activation, inhibition and reactive oxygen species scavengers on the macrophage-mediated foreign body reaction to polyurethanes

---

STATEMENT OF AUTHOR CONTRIBUTIONS

Joanne E. McBane was the primary author and major contributor to the experimental data for this manuscript. **Dr. Loren A. Matheson** is a former graduate student supervised by Dr. R.S. Labow and currently a post-doctoral fellow in the department of Pediatrics, University of Saskatchewan, funded by the Canadian Arthritis Network. In an ongoing collaboration assessing HMGB1 activation as a marker of MDM activation, she performed the HMGB1 westerns in Figures 4.5 and 4.6 along with helping in manuscript editing. **Dr. J. Paul Santerre** is a co-investigator of Dr. Rosalind S. Labow, and principal investigator on the CIHR operating grant that funded this research. Dr. Santerre's Polymer Chemistry laboratory at the University of Toronto synthesized the model PCNU materials used in the following study. He also aided in the editing of the manuscript. **Dr. Rosalind S. Labow** is the supervisor of Joanne E. McBane and contributed to both the experimental design and the editing of the manuscript.

SUMMARY

The following manuscript entitled "The effect of phorbol ester activation, inhibition and reactive oxygen species scavengers on the macrophage-mediated foreign body reaction to polyurethanes" has been submitted to the *Biochemistry and Cell Biology* and is currently under review (December 2007). This paper addressed questions asked by both

manuscripts#1 and #2. Manuscript#1 suggested PKC had a role in the MDM-mediated degradation of HDI PCNUs, moreso than for MDI321. However, the PKC inhibitor H-7 was found to inhibit other protein kinases besides PKC, and treatment with H-7 yielded MDM with low cell viability. Therefore, the PMA effect on MDM-mediated PCNU degradation required further scrutiny. Manuscript#3 describes the use of a more specific inhibitor of PKC (bisindolylmaleimide I) and an analogue of PMA that does not activate PKC (4αPMA) in order to confirm that the effect of PMA was due to PKC activation and not another effect due to phorbol ester activation.

Manuscript#2 proposed that the material surface could trigger ROS without PMA activation. Manuscript#3 describes the use of scavengers of ROS with or without PMA to see how this affected subsequent MDM-mediated degradation and esterase/HMGB1 levels. Recently, HMGB1 has been investigated as a late inflammatory cytokine released by activated MDMs. However, this is one of the few studies evaluating HMGB1 protein as a marker of activation of MDM on different polyurethanes. Radiolabel release, cell viability, esterase activity, MSE protein, and HMGB1 protein were assayed in MDM on three model PCNU surfaces. MDM morphology on these surfaces (with or without PMA) was assayed by scanning electron microscopy.

ABSTRACT

Previously it was found that the foreign body response (FBR) of monocyte-derived macrophages (MDM) in the presence of protein kinase C (PKC) activator phorbol myristate acetate (PMA) differed between aliphatic and aromatic polycarbonate-based polyurethanes (PCNUs). PMA inhibited the MDM-mediated degradation of aliphatic PCNUs (HDI), but had no effect on the aromatic PCNU (MDI). To further investigate the material dependence of PKC activation by PMA, PKC inactive 4αPMA, a PKC inhibitor (BIM) and reactive oxygen species scavengers, catalase plus superoxide dismutase (CAT+SOD), were added to MDM cultured on PCNU surfaces. In MDM on HDI, esterase activity (linked to degradation and inflammation) was reduced by PMA+CAT+SOD, but not by 4αPMA. BIM reversed PMA inhibition of both degradation and esterase activity. Secretion of the pro-inflammatory high mobility group box 1 protein (HMGB1) was inhibited by PMA, resulting in more intracellular HMGB1, whereas CAT+SOD reduced intracellular HMGB1 levels +/-PMA. Conversely, in MDM on MDI, BIM+PMA, 4αPMA and CAT+SOD increased degradation. Less HMGB1 was secreted from MDM on MDI than MDM on HDI; however, intracellular and secreted HMGB1 were not inhibited by PMA and CAT+SOD+PMA increased intracellular HMGB1. Although exogenous agents can be used to delineate the signaling pathways (PKC) involved in the FBR of MDM to PCNUs, it is the material surface chemistry itself that dictates the activation of oxidative and/or hydrolytic degradative pathways.

INTRODUCTION

It has become increasingly important to understand the foreign body reaction (FBR) due to the interaction of monocyte-derived macrophages (MDM) with materials used in medical devices. The inflammatory activities of MDM, released by a phagocytic-like mechanism (Cannon and Swanson 1992, Marchant et al. 1984), have been implicated in the *in vivo* degradation of polyurethanes (PUs) (Labow et al. 2001a, Labow et al. 2001b). However, there are other aspects to the MDM FBR to PU that may influence the cells' ability to degrade certain materials. Recently, activation of signaling pathways in MDM, such as phospholipase A_2 and protein kinase C (PKC) were shown to be dependent on the chemistry of the polycarbonate-based PU (PCNU) material surfaces, with a range of consequences that have not been fully elucidated (Dinnes et al. 2005, McBane et al. 2005, McBane et al. 2007). This is true of the release of hydrolytic enzymes (esterases, e.g, cholesterol esterase (CE) and monocyte-specific esterase (MSE)) (Labow et al. 2002, Labow et al. 2005b, Matheson et al. 2004) as well as the release of reactive oxygen species (ROS) (Christenson et al. 2004, McBane et al. 2007, Schubert et al. 1997).

Recent work has established links between material oxidation and subsequent MDM-mediated hydrolytic degradation which may be both material (i.e. PCNU) and PKC dependent (McBane et al. 2005, McBane et al. 2007). The *in vivo* respiratory burst, partially mediated by PKC, is one of the first cellular responses to a biomaterial during the FBR, which leads to the production of hydrogen peroxide and other reactive oxygen species (ROS) in MDM (Jackson et al. 1995, Thomas and Fishman 1986). The effect of phorbol myristate acetate (PMA), a phorbol ester that activates conventional and novel

PKC isoforms and stimulates the respiratory burst, was studied using model PCNUs that differed in diisocyanate chemistry (hexane (HDI) or 4,4'-methylene bis-phenyl (MDI) diisocyanates) and stoichiometric ratios of diisocyanate:(1,6-hexyl polycarbonate) diol (PCN): butanediol (BD) (4:3:1 or 3:2:1) (Table 4.1). HDI431 was the most degradable by MDM, followed by HDI321 and MDI321 (Matheson et al. 2007, McBane et al. 2005). These findings agreed with hydrolytic degradation studies of the PCNUs by CE (Tang et al. 2001a, Tang et al. 2001b) and carboxyl esterase (CXE), a commercially available esterase with the same specificity as MSE (Labow et al. 2002, Labow et al. 2005b). An earlier study showed that PMA treatment of MDM caused an inhibition of esterase activity, MSE protein and MDM-mediated degradation of HDI PCNUs (McBane et al. 2005). However, this earlier work did not determine whether it was oxidation via ROS release and/or another action pathway of MDM following the PKC activation by PMA that specifically affected the subsequent hydrolytic degradation. This uncertainty arose from the fact that the MDM-mediated degradation of MDI321 was unaffected by PMA, therefore suggesting that multiple material-related pathways may be involved (McBane et al. 2005).

Sodium azide, an inhibitor of the respiratory burst, significantly inhibited MDI321 degradation whereas it only partially reversed the PMA-mediated inhibition of HDI PCNU degradation by MDM (McBane et al. 2005). In order to assess if the differences found for the effect of PMA and PMA with sodium azide were related in part to oxidation pathways, the PCNUs were pre-oxidized with 20% hydrogen peroxide and then assessed for their susceptibility to degradation. Both MDM- (McBane et al. 2007) and CXE-

mediated degradation (McBane et al. 2005) of PCNU surfaces were affected differentially, depending on the material surface chemistry. Moreover, when the production of ROS was measured in MDM adherent to the different PCNU surfaces, there were significant changes in intracellular ROS production in the presence of PMA that were also dependent on the PCNU surface (McBane et al. 2007). These findings along with the fact that the PKC and protein kinase A inhibitor 1-[5-isoquinolinylsulfonyl]-2 methylpiperazine (H7) could partially reverse the PMA effect on biodegradation suggested that PMA might be acting on the MDM-mediated biodegradation of PCNUs through the PKC pathway (McBane et al. 2005).

As a result of the above observations, the current study was designed to further define the role of PKC in MDM-material interactions using a PKC inactive phorbol ester isoform (C-4 hydroxyl in the α-position (Hecker 1985)) and the PKC specific inhibitor bisindolylmaleimide I (BIM). BIM was developed by chemically modifying the general kinase inhibitor, staurosporine, in order to make it more selective for PKC (Toullec et al. 1991). Since one action of PMA is to stimulate the respiratory burst through activation of PKC, this study investigated the effect of scavenging ROS (agents that have been shown to contribute to the biodegradation of PUs), the products generated by NADPH oxidase in activated MDM. Superoxide dismutase (SOD) converts superoxide anion ($O_2^{\cdot -}$) to H_2O_2, which catalase (CAT) then converts to water and oxygen (Ding et al. 2007). By the addition of CAT+SOD with and without PMA to the MDM on the PCNU surfaces, it may be possible to better understand the role of oxidation in the MDM FBR, one that may direct activation of specific pathways leading to material degradation.

A sensitive marker of inflammation is necessary in order to better understand the MDM FBR to specific material surfaces. High mobility group box 1 chromosomal protein (HMGB1) is a nuclear protein that is widely distributed in many cells, and acts as a pro-inflammatory mediator of inflammation when secreted from activated MDM. HMGB1 causes elevation in the secretion of tumor necrosis factor (TNF)-α, interleukin (IL)-1β as well as other macrophage inflammatory proteins. Early on it was shown that PMA causes a release of HMGB1 from murine erythroleukemia cells suggesting that PKC activation leads to its secretion (Passalacqua et al. 1997). Recently, PKC inhibition with BIM was shown to attenuate the cytokine induced HMBG1 secretion from THP-1 monocyte-macrophages (Kalinina et al. 2004). In addition, when glucose depleted A549 cells were treated with CAT, the secretion of HMGB1 was significantly reduced.

By using the PKC inhibitor BIM, and PKC inactive 4αPMA, PKC involvement in both the oxidative and hydrolytic pathways of MDM-mediated degradation of PCNUs could be confirmed. In addition, by relating the effect of ROS scavengers (CAT+SOD) to the pro-inflammatory mediator HMGB1, and PCNU degradation measurement, it may be possible to identify what key actions determine the activation pathway(s) for PCNU induced FBR as well as define the preferred pathway(s) of biodegradation for different PCNUs.

MATERIALS AND METHODS

Isolation and culture of monocytes- Monocytes were isolated from whole blood (with the approval of the Research Ethics Committee of the University of Ottawa Heart Institute, UOHI 2005-161, valid until Feb. 18, 2008) as previously described (Labow et al. 1998) by collecting approximately 120 mL of whole blood in EDTA-containing Vacutainers® and layering onto Histopaque 1077, then centrifuging at 1000x*g* followed by serial washing and centrifuging at 450x*g*. Monocytes were then seeded on tissue culture grade polystyrene (TCPS), incubated at 37°C/5% CO_2 and 100% humidity and fed three times a week with RPMI medium made up using 12.7 mM HEPES, 2.0 g/L sodium bicarbonate, with 10% fetal bovine serum (FBS), 2% penicillin/streptomycin, and 0.69 mM L-glutamine (complete medium). After 14 days the mature MDM were trypsinized and re-suspended in complete media by a previously described method (Labow et al. 2001b). All cell culturing was done in a laminar flow hood under sterile conditions. Cell counts were performed using an automated Vi-Cell™ cell counter (Beckman Coulter; Miami, FL, USA).

Preparation of material surfaces- PCNUs used in this experiment were HDI431, HDI321 and MDI321 synthesized with an unlabeled or ^{14}C-radiolabeled BD moiety for all three polymers (see Table 4.1) as described in detail previously (Tang et al. 2001a, Tang et al. 2001b). A 10% (w/v) polymer in dimethylacetamide solution was filtered with a 45 μM PTFE (Teflon) Chromospec® syringe filter and glass coverslips (15 mm

diameter) were aseptically coated with 100 μL of the polymer solution in a laminar flow hood as described previously (Labow et al. 2001a, Labow et al. 2001b).

TABLE 4.1

Model PCNU Chemistries

Polymer Name	Diisocyanate	Macrodiol	Chain Extender*	Specific Radioactivity (CPM/100mg)
HDI431	Hexane	poly (1,6-hexyl carbonate) diol	butanediol	$1.26x10^7$
HDI321	Hexane	poly (1,6-hexyl carbonate) diol	butanediol	$1.43x10^7$
MDI321	4,4'-Methylene bis-phenyl	poly (1,6-hexyl carbonate) diol	butanediol	$1.02x10^7$

*Radiolabeled polymers have ^{14}C-radiolabeled carbons in butanediol

MDM-mediated biodegradation of PCNUs- One million cells per mL (in complete medium) of the re-suspended MDM were added to the sample wells and 1 mL of complete medium without cells was added to the control wells as previously described (Labow et al. 2001b). TCPS plates (24 well) lined with the PCNU coated slips were incubated with media or MDM for 1 hour at 37°C/5% CO_2 and 100% humidity. After 1 hour the supernatant was aspirated off and replaced with complete medium with or without treatment reagents. This plate (named T=48) was incubated for 48 hours at 37°C/5% CO_2 and 100% humidity. A parallel plate T=0 was treated the same as the

T=48 plate with the exception that the supernatant was aspirated at 1h of incubation and the cells lysed in 250 μL of 0.05% Triton X-100 for immediate DNA analysis (see below). For the FBS-free samples (HMGB1 analysis), complete medium was replaced with FBS-free medium, incubated for a further 24h and otherwise treated as described above.

Preparation of phorbol esters and PKC inhibitor- The PKC activator PMA (1 mg/mL in dimethylsulfoxide) was diluted 15.4 μL in 2.5 mL of phosphate buffered saline (PBS) solution (pH 7.2) (10 μM) and further diluted in complete MDM medium to give a final concentration of 100 nM. The concentration was similar to that used in previous MDM-mediated PCNU degradation studies (McBane et al. 2005, McBane et al. 2007). 4αPMA (PKC inactive) was prepared as detailed above to a concentration of 100 nM. PKC inhibitor BIM was prepared by making a 2 mM solution in dimethylsulfoxide and then diluting to a final concentration of 2 μM in complete medium as previously established, (Labow et al. 2001c) based on the IC_{50} for inhibiting the PMA induced respiratory burst in alveolar macrophages (Forman et al. 1998).

Preparation of ROS scavengers- SOD was dissolved in sterile PBS at a concentration of 1000 units/mL (1 unit will inhibit the rate of reduction of cytochrome C by 50% in a coupled system with xanthine and xanthine oxidase at pH 7.8 at 25°C in a 3 mL reaction volume according to the manufacturer) and diluted in complete medium to a final concentration of 200 units/mL. Catalase was dissolved in sterile PBS at a concentration of 6000 units/mL and then diluted to a final concentration of 1000 units/mL in complete

medium (1 unit as assayed by manufacturer will decompose 1.0 μmol of H_2O_2 per minute at pH 7.0 at 25°C, while the H_2O_2 concentration falls from 10.3 to 9.2 mM, measured by the rate of decrease of A_{240}).

Determination of ^{14}C-radiolabel release from polymers-After the 48 hour incubation period, 600 μL of the cell supernatant was removed from each well and added to 10 mL of liquid scintillation cocktail for counting (LKB Wallac 1219 RackBeta; Gaithersburg, MD, USA) (Labow et al. 2001b). Counts were normalized to the average DNA content of the sample from T=0 to T=48 (CPM per 10 μg DNA).

Preparation of cell lysates and supernatants-After 48 hours, samples of conditioned media were taken from the T=48 plate well and stored at –80°C until assayed for enzyme activity. The medium was removed from a well and replaced with 0.05% Triton X-100, 10mM EDTA in PBS (lysis buffer) in order to prepare cell lysates from T=48 plates for DNA analysis, enzyme activity and protein assays (see below).

Assay of DNA content of cell lysates and cell viability-The amount of DNA present in cell lysates was determined for an aliquot of cell lysate suspension using a modification of the assay outlined previously (Matheson et al. 2004). Briefly 0.1% Hoescht Dye #33258 was diluted in buffer containing 0.10 M Trizma base, 2.0 M NaCl and 0.01 M EDTA (in de-ionized, distilled water (ddH_2O), pH 7.4) on the day of analysis. Cell lysate (15 μL) was added to the dye (100 μL) into a 96 well plate and read against a calf thymus

DNA standard (100-300 ng) in a fluorescence microplate reader (POLARstar Galaxy, BMG Technologies; Durham, NC, USA).

DNA measurement as a means of assessing live adherent cell number was validated by comparing the latter with data from the Vi-Cell™ cell counter automated trypan blue exclusion assay for one set of experiments where in cell viability was assessed after a 48 hour incubation period of MDM on HDI431 in the presence or absence of PMA, 4αPMA, BIM or BIM+PMA. There was no significant difference between DNA and cell viability, and hence normalizing measurements to 10μg DNA was used for reporting the data for all parameters (Table 4.2).

TABLE 4.2

Effect of PKC activators or inhibitors on MDM viability and the amount of DNA attached to HDI431.

Treatment	PMA	4αPMA	BIM	BIM+PMA*
Viability	100.4 ± 5.5	104.1 ± 4.0	109.6 ± 3.8	118.0 ± 14.2
DNA	109.5 ± 1.3	106.0 ± 2.0	104.8 ± 1.4	105.6 ± 1.0

* There was a significant increase compared to cells in media only (100%). n=3 and data are reported with standard errors of the mean.

Assay of esterase activity in MDM cell lysates and supernatants- After the 48 hour incubation period, MDM cell supernatants and lysates were assayed for esterase activity using the substrate p-nitrophenylbutyrate (PNB). One unit of activity was defined as the release of 1 nmol of p-nitrophenol (γ = 16 300$cm^{-1}M^{-1}$) per minute at 37°C at pH 7.0 and

400.6 nm as previously described (Labow et al. 2001b). The activity was normalized to 10 μg of DNA using the average value from T=0 to T=48, in order to account for cell number changes over the 48-hour period.

Polyacrylamide gel electrophoresis (PAGE) and immunoblotting analysis of MSE-Cell lysate proteins were separated by SDS-PAGE on a 12% polyacrylamide gel (acrylamide:N,N'-methylene bisacrylamide, 29:1) using a mini PROTEAN II electrophoresis module (Bio-Rad Laboratories; Mississauga, ON) as previously described (Matheson et al. 2002). Briefly, SDS-PAGE gels used for immunoblotting analysis were transferred to a nitrocellulose membrane (Bio-Rad), followed by incubation with the rabbit anti-porcine esterase (reacts with MSE) and then secondary goat anti-rabbit immunoglobulin G antibody conjugated to horseradish peroxidase. Protein bands were then visualized with an enhanced chemiluminescence detection system and recorded on CL-XPosure X-ray film (Pierce, Rockford, IL, USA). Densitometry analysis of bands on the x-ray film was quantified with Quantity One Software® v.4.1 (Bio-Rad) (Matheson et al. 2002).

PAGE and immunoblotting analysis of HMGB1- FBS-free conditioned media samples and their corresponding lysates were used for analysis of released HMGB1. HMGB1 analysis was also performed on cell lysates with treatment of CAT+SOD and CAT+SOD+PMA. Aliquots of medium or cell lysate were separated by SDS-PAGE as described above. SDS-PAGE gels used for immunoblotting analysis were transferred to a BioTrace® nitrocellulose membrane (VWR), followed by incubation with mouse anti-

human HMGB1 (Sigma; 1:1000 in 1% BSA) overnight at 4°C. Blots were washed and incubated with secondary goat anti-mouse immunoglobulin G antibody conjugated to horseradish peroxidase (Sigma, 1:5000 in 1% BSA). Protein bands were visualized with an enhanced chemiluminescence detection system (Immobilon, Millipore) and recorded on Kodak X-ray film (Fisher Scientific). Densitometry analysis of bands on the x-ray film was quantified with Image J Software® v.1.38x (NIH).

Scanning electron microscopy (SEM)- Cells were fixed in 3% glutaraldehyde in PBS, post fixed in 1% osmium tetroxide, followed by a series of ethanol washes prior to critical point drying as previously described (Labow et al. 1998). The samples were analyzed and photographed using a Hitachi S 2500 Scanning Electron Microscope (Hitachi Ltd., Mito City, Japan) at an operating voltage of 10 kV in the Faculty of Dentistry, University of Toronto.

Laser scanning confocal microscopy (LSCM)- After 48 hours in the presence or absence of PMA, MDM on the three PCNU surfaces were prepared for LSCM as described previously (Dinnes et al. 2008). Briefly, cells on PCNU coated slips were washed with PBS, fixed in 4% paraformaldehyde in PBS and permeabilized with lysis buffer prior to incubating with 1:50 dilution of rhodamine phalloidin (Molecular Probes, Eugene, OR, USA) in PBS for 30 minutes to stain for filamentous actin (F-actin) and then counterstained with 1:1000 dilution of Biostatus DRAQ5™ (Alexis Biochemicals, San Diego, CA, USA) in PBS for 5 minutes to stain cells for DNA. Cells on slips were then washed with PBS prior to mounting on slides with 90% glycerol as mounting solution.

An Olympus 100X oil immersion objective with a numerical aperture of 1.4, on an Olympus IX80 laser scanning confocal microscope operated by FV1000 software (version 1.4a) was used to visualize the cells. Rhodamine phalloidin (543 nm line of the Helium /Neon green laser) and DRAQ5™ (633 nm line of the Helium /Neon red laser) fluorochromes were excited with appropriate lasers and images (at eight different areas) were taken of cells on each surface with or without PMA, 4αPMA or BIM+PMA. For quantification purposes images from each of three donors were analyzed for cell size in pixels and the size of the cells treated with PMA was expressed as a percent relative to MDM on that particular surface in media only.

Statistical analysis-The data were analyzed by either 1 way or 2 way ANOVA using SAS® version 9.0 with a significance value of $p<0.05$ adjusted for multiple comparisons.

RESULTS

Effect of PKC activation or inhibition on the degradation of PCNU surfaces– The three model PCNUs used in this study (Table 4.1) have been shown to have different susceptibilities to MDM-mediated degradation (Matheson et al. 2007). Degradation of the HDI PCNUs was inhibited by PMA whereas there was no effect on MDI321 degradation (Figure 4.1, $p<0.001$). However, 4αPMA treatment of MDM on MDI321 caused a significant increase in radiolabel release with no effect on the MDM-mediated degradation of the HDI PCNUs (Figure 4.2a, $p<0.001$). Although BIM, an inhibitor of PKC, had little effect on the MDM-mediated radiolabel release from the three PCNUs, a combination of BIM+PMA reversed the inhibition of radiolabel release observed with

PMA alone with cells reseeded on HDI431 (Figure 4.2a) ($p<0.001$) and HDI321 ($p=0.009$).

Effect of ROS scavengers on the degradation of PCNU surfaces- The effect of ROS scavengers on the aromatic MDI321 was opposite to their effect on the aliphatic HDI PCNUs. When CAT+SOD was added to the culture medium, there was a significant increase in MDM-mediated degradation of MDI321 ($p<0.001$), whereas MDM-mediated degradation of HDI321 was inhibited (Figure 4.2b). The inhibition of MDM-mediated degradation of HDI431 and HDI321 by PMA was not reversed by CAT+SOD. When PMA was added to CAT+SOD the MDM responded similarly to all 3 PCNUs with a significant inhibition of degradation of all 3 PCNUs (Figure 4.2b).

Effect of PKC activation or inhibition on the esterase activity elicited by MDM re-seeded on PCNU surfaces- The effect of PMA on total esterase activity from MDM cultured on the different PCNUs was similar to the radiolabel release data (Figure 4.1). MDM incubated with PMA on the HDI PCNUs also demonstrated a significant inhibition of total esterase activity (Figure 4.1, $p<0.001$) whereas there was no effect on the esterase in MDM on MDI321. All other PKC related treatments showed no significant change in esterase activity when compared to their respective MDM in media controls (Figure 4.3a).

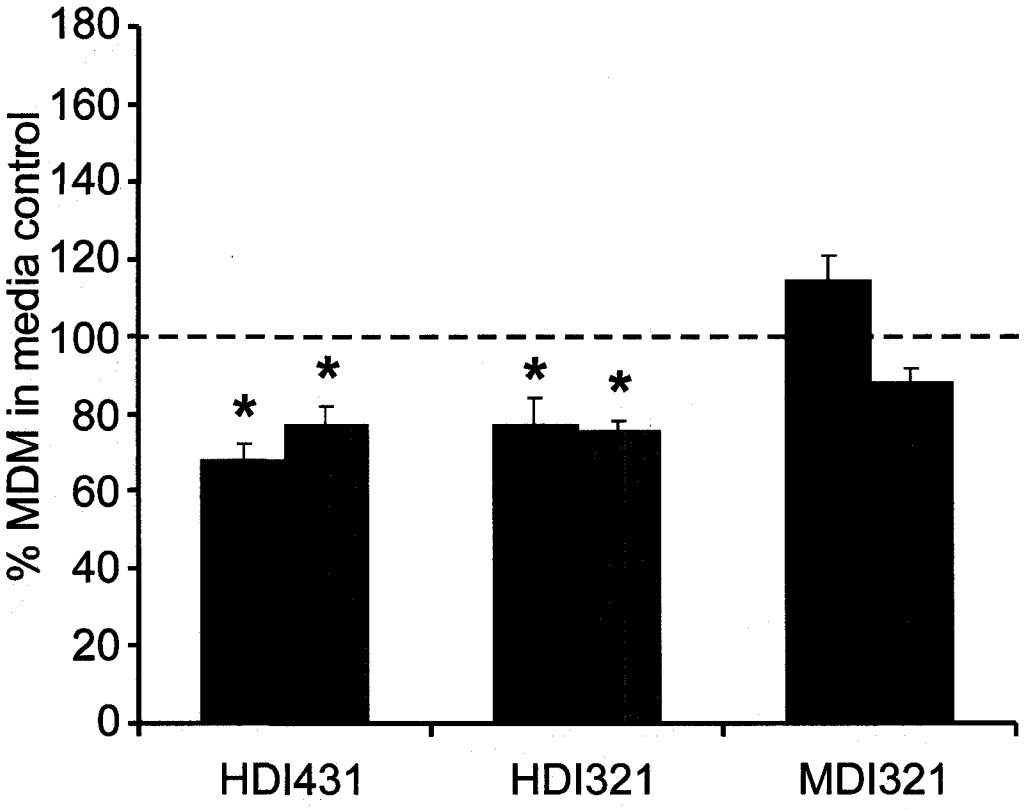

Figure 4.1: Effect of PMA on MDM-mediated radiolabel release from PCNUs and esterase activity in MDM lysates. Monocytes were differentiated to MDM for 14 days on TCPS prior to re-seeding onto ^{14}C-labeled: HDI431, HDI321 or MDI321 PCNU coated slips in the presence or absence of PMA in complete medium. After 48 hours, wells were analyzed for radiolabel release (red bar) and esterase activity (blue bar). n=3 and data are reported with standard errors of the mean. * There was a significant inhibition compared to cells in media only.

Figure 4.2: Effect of PKC activation or inhibition and ROS scavengers on the degradation of PCNU surfaces. Monocytes were differentiated to MDM for 14 days on TCPS prior to re-seeding onto ^{14}C-labeled: HDI431 (red bar), HDI321 (blue bar) or MDI321 (green bar) PCNU coated slips in the presence or absence of (a) 4αPMA, BIM or BIM+PMA in complete medium or (b) CAT+SOD or CAT+SOD+PMA. After 48 hours cell supernatants were counted for radiolabel release. n=3 and data are reported with standard errors of the mean. * There was a significant inhibition compared to cells in media only. ** There was a significant increase compared to cells in media only.

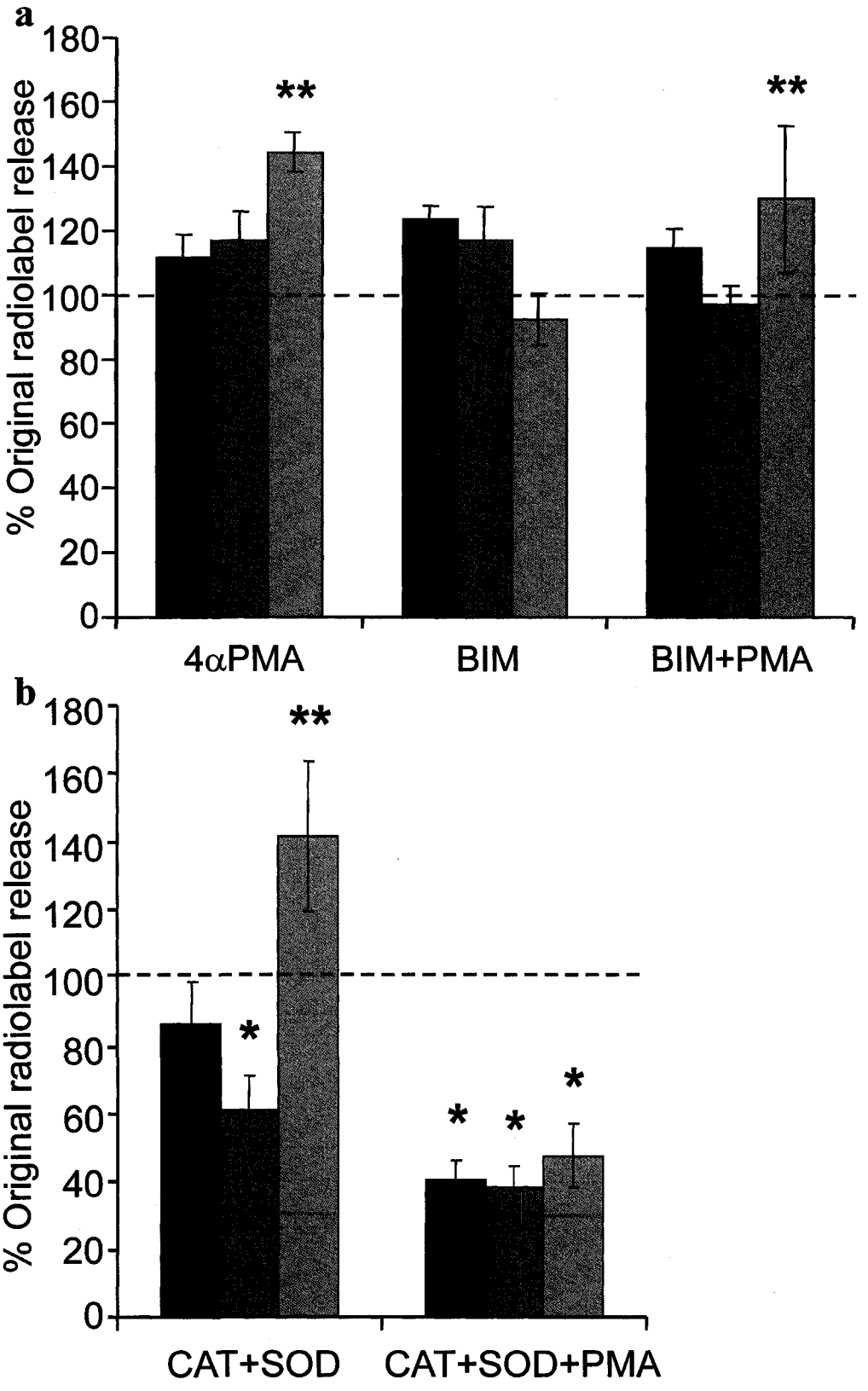
a
% Original radiolabel release
180
160
140
120
100
80
60
40
20
0
**
**
4αPMA
BIM
BIM+PMA
b
% Original radiolabel release
180
160
140
120
100
80
60
40
20
0
**
*
*
*
*
CAT+SOD
CAT+SOD+PMA

Figure 4.3: Effect of PKC activation or inhibition and ROS scavengers on the esterase activity elicited by MDM re-seeded on PCNU surfaces. Monocytes were differentiated to MDM for 14 days on TCPS prior to re-seeding onto ^{14}C-labeled: HDI431 (red bar), HDI321 (blue bar) or MDI321 (green bar) PCNU coated slips in the presence or absence of (a) 4αPMA, BIM or BIM+PMA in complete medium or (b) CAT+SOD or CAT+SOD+PMA. After 48 hours cell lysates and supernatants were assayed for esterase activity. n=3 and data are reported with standard errors of the mean. * There was a significant inhibition compared to cells in media only.

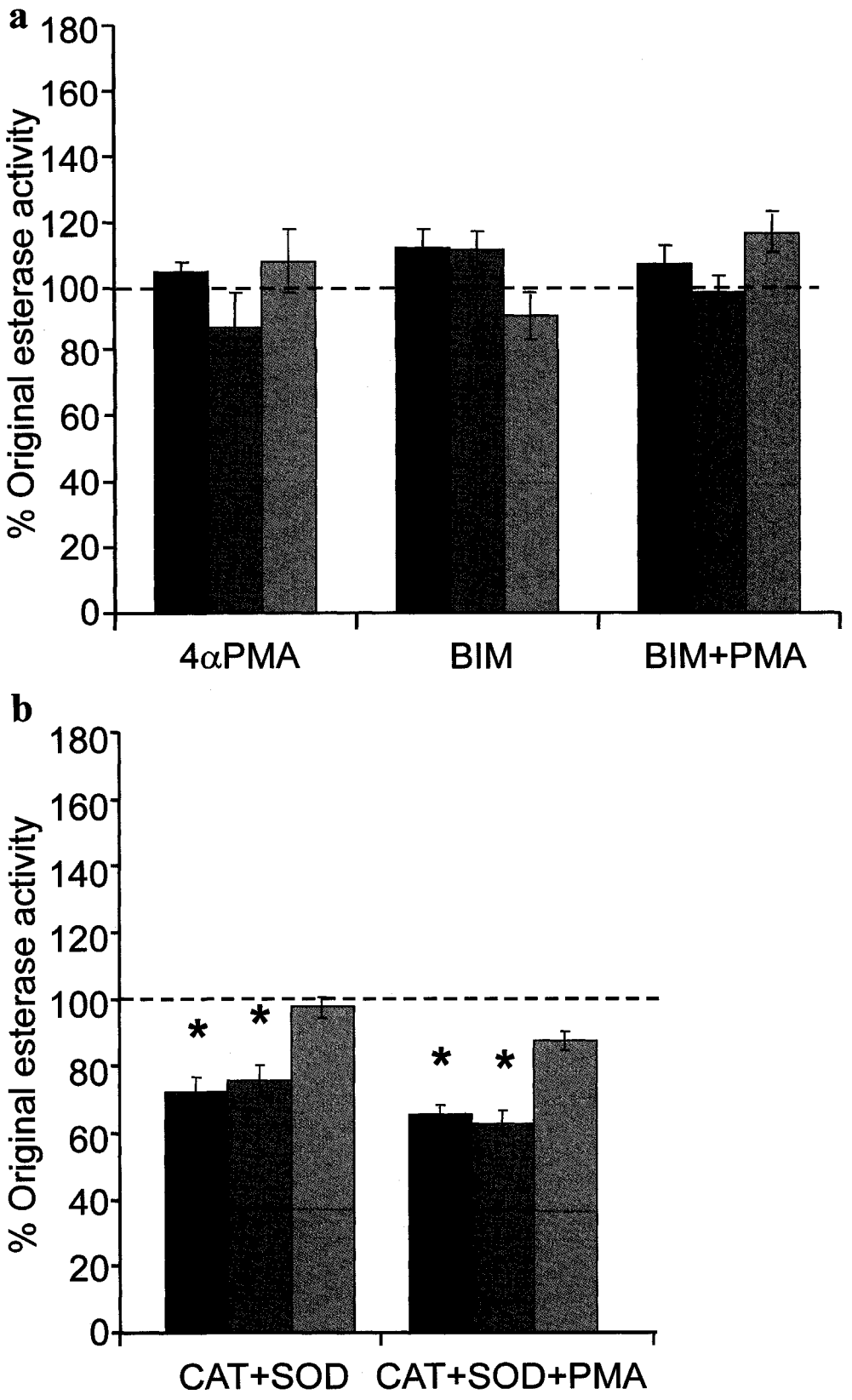
a
% Original esterase activity
180
160
140
120
100
80
60
40
20
0
4αPMA
BIM
BIM+PMA
b
% Original esterase activity
180
160
140
120
100
80
60
40
20
0
*
*
*
*
CAT+SOD
CAT+SOD+PMA

Effect of ROS scavengers on the esterase activity elicited by MDM re-seeded on PCNU surfaces- CAT+SOD treatment significantly affected the esterase activity in the adherent MDM with differences between the HDI PCNUs and MDI321. CAT+SOD as well as CAT+SOD with PMA had a significant inhibitory effect on the esterase activity in the MDM on the HDI surfaces. However, the MDM on MDI321 did not respond to the ROS scavengers showing no effect on the esterase activity when compared to cells in media alone (Figure 4.3b).

Effect of PKC activation or inhibition on the amount of MSE protein in MDM re-seeded on PCNU surfaces- Figure 4.4 shows that MDM that underwent treatment conditions that caused decreased radiolabel release (MDM with PMA on HDI PCNUs, Figure 4.1) and esterase activity (MDM with PMA on HDI PCNUs, Figure 4.1) also produced less MSE protein than MDM under control conditions (Figure 4.4a and 4.4b, $p<0.001$).

When 4αPMA was added to the MDM culture, the level of MSE protein was not reduced (Figure 4.4a and 4.4b). In addition, BIM alone had no effect on MSE protein level, nevertheless, when BIM and PMA were combined, the decrease in MSE protein for MDM on the HDI PCNU surfaces was reversed (Figure 4.4a and 4.4b, $p<0.001$), giving similar results to the influence of BIM on the PMA effect for both radiolabel release (Figure 4.2a) and esterase activity (Figure 4.3a). As was observed for the esterase activity in Figures 4.1 and 4.3, MSE protein level in MDM on MDI321 was unaffected by the treatment conditions (Figure 4.4). MSE immunoblotting analysis was performed

with the MDM lysates that were treated with CAT+SOD, however there was no significant difference in the MSE protein with this treatment for the MDM on all 3 PCNUs (data not shown).

Effect of ROS scavengers on the amount of intracellular and released HMGB1 protein in MDM re-seeded on PCNU surfaces- The secretion of HMGB1 was significantly higher from MDM adherent to HDI431 than MDM on HDI321 or MDI321 ($p=0.002$ and 0.05 respectively). PMA significantly decreased the secretion from MDM on HDI431 and HDI321, ($p=0.002$ and 0.03 respectively), but had no effect on the secretion of HMGB1 from the MDM on MDI321 (Figure 4.5a). The intracellular levels of HMGB1 demonstrated an opposite trend to the secreted levels in that the MDM on HDI431 had significantly less HMGB1 than cells on either HDI321 or MDI321 ($p= 0.002$ and 0.006 respectively, Figure 4.5b). The effects of PMA significantly increased intracellular HMGB1 levels on HDI431 ($p=0.012$) but had no effect on the HMGB1 levels in MDM on HDI321or MDI321 (Figures 4.5b).

When the MDM were treated with CAT+SOD, attenuation of intracellular HMGB1 occurred when MDM were on HDI431 ($p=0.015$) and MDI321 ($p=0.03$) but not HDI321. However, when PMA was combined with CAT+SOD, the HMGB1 levels in the MDM on HDI431 remained unchanged ($p=0.2$), but there was a decrease in HMGB1 in MDM on HDI321 ($p=0.02$). In addition, the effect of CAT+SOD on the level in MDM on MDI321 was reversed by the addition of PMA ($p=0.037$; Figure 4.6).

Figure 4.4: Effect of PKC activation or inhibition on the amount of MSE protein in MDM re-seeded on PCNU surfaces. Monocytes were differentiated to MDM for 14 days on TCPS prior to re-seeding onto ^{14}C-labeled: HDI431 (red bar), HDI321 (blue bar) or MDI321 (green bar) PCNU coated slips in the presence or absence of PMA, 4αPMA, BIM or BIM+PMA in complete medium. After 48 hours cell lysates were assayed for MSE protein by immunoblotting as described in Materials and Methods (a) and blots were then quantified using Quantity One Software® and expressed as a percent relative to the intensity of MSE for each treatment in cells in media only (b). The control was the same for BIM and BIM+PMA because these lysates were all from the same isolation/donor. n=3 and data are reported with standard errors of the mean. * There was a significant inhibition compared to cells in media only. ** There was a material surface difference where the indicated surface was significantly higher than the other surfaces.

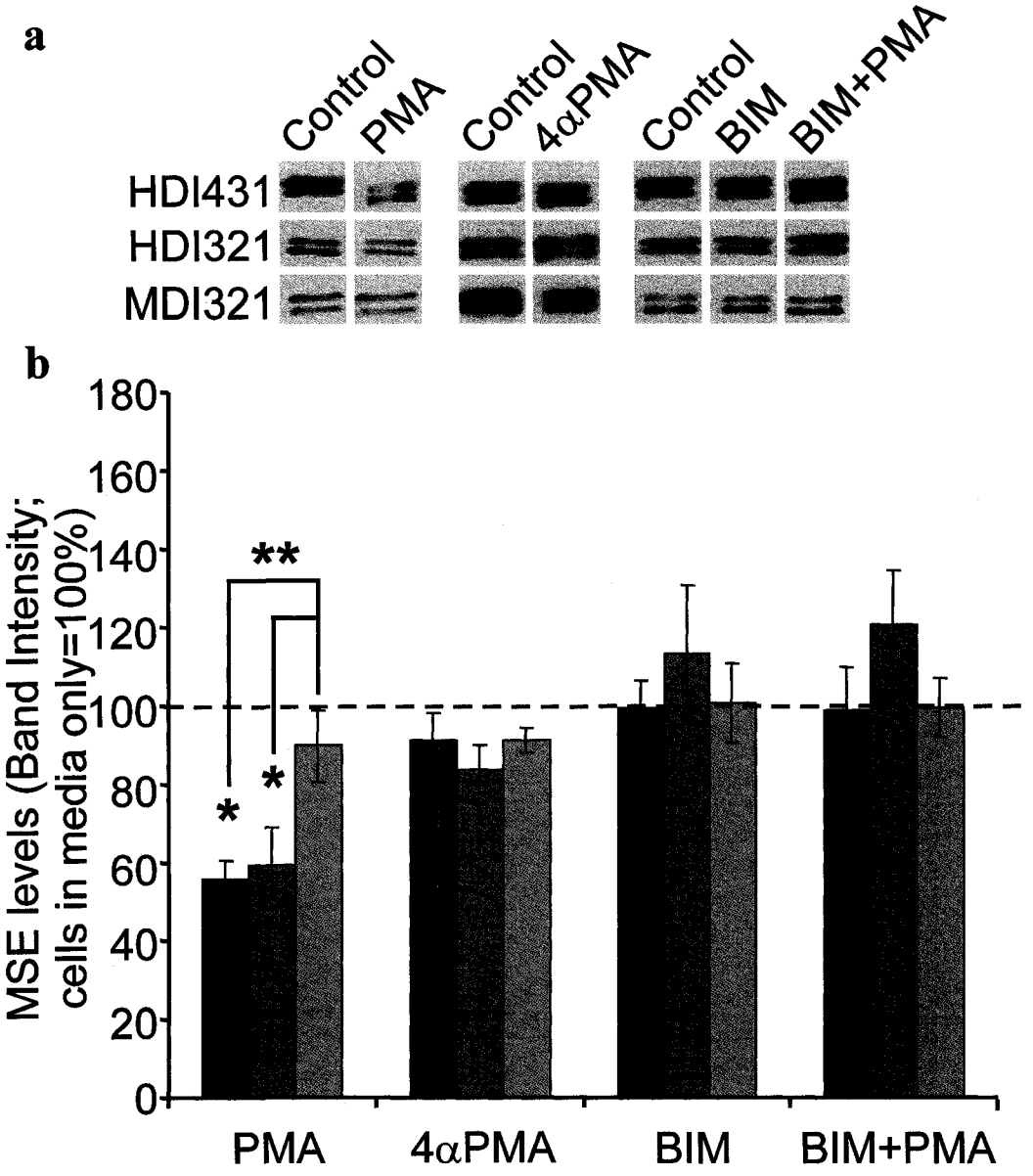
a
Control
PMA
Control
4αPMA
Control
BIM
BIM+PMA
HDI431
HDI321
MDI321
b
MSE levels (Band Intensity; cells in media only=100%)
180
160
140
120
100
80
60
40
20
0
**
*
*
PMA
4αPMA
BIM
BIM+PMA

Figure 4.5: Effect of PMA on HMGB1 protein from MDM re-seeded on PCNU surfaces. Monocytes were differentiated to MDM for 14 days on TCPS prior to re-seeding onto HDI431 (red/orange bar), HDI321 (blue/light blue bar), or MDI321 (green/light green bar) surfaces in the absence (red, blue, or green bar) or presence of PMA (orange, light blue, or light green bar). After 24 hours the media were replaced with FBS free media +/- PMA and incubated for an additional 24 hours. The FBS-free supernatants (a) and cell lysates (b) were analyzed for HMGB1 expression by immunoblotting as described in the Materials and Methods. Blots were quantified using Image J software and reported relative to levels measured from cells on HDI431 in FBS-free media without PMA (set to 100%). n=3, data are reported with standard errors of the mean. * There was a significant inhibition of secreted HMGB1 relative to levels measured from cells without PMA on HDI431. ** There was a significant decrease in HMGB1 levels relative to that on HDI321 without PMA. *** There was a significant increase in intracellular HMGB1 levels relative to levels measured in cells on HDI431 without PMA.

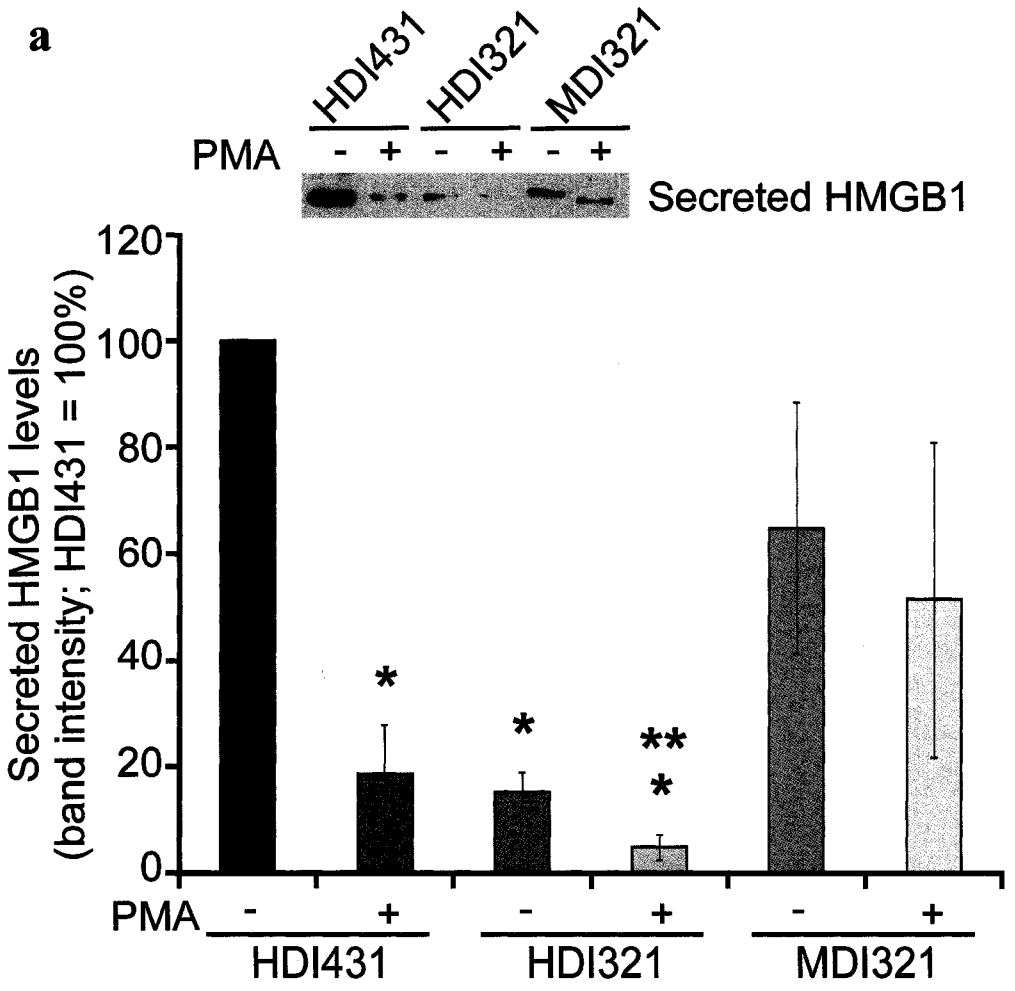
a
HDI431
HDI321
MDI321
PMA
- + - + - +
Secreted HMGB1
Secreted HMGB1 levels
(band intensity; HDI431 = 100%)
120
100
80
60
40
20
0
*
*
**
*
PMA
- + - + - +
HDI431
HDI321
MDI321

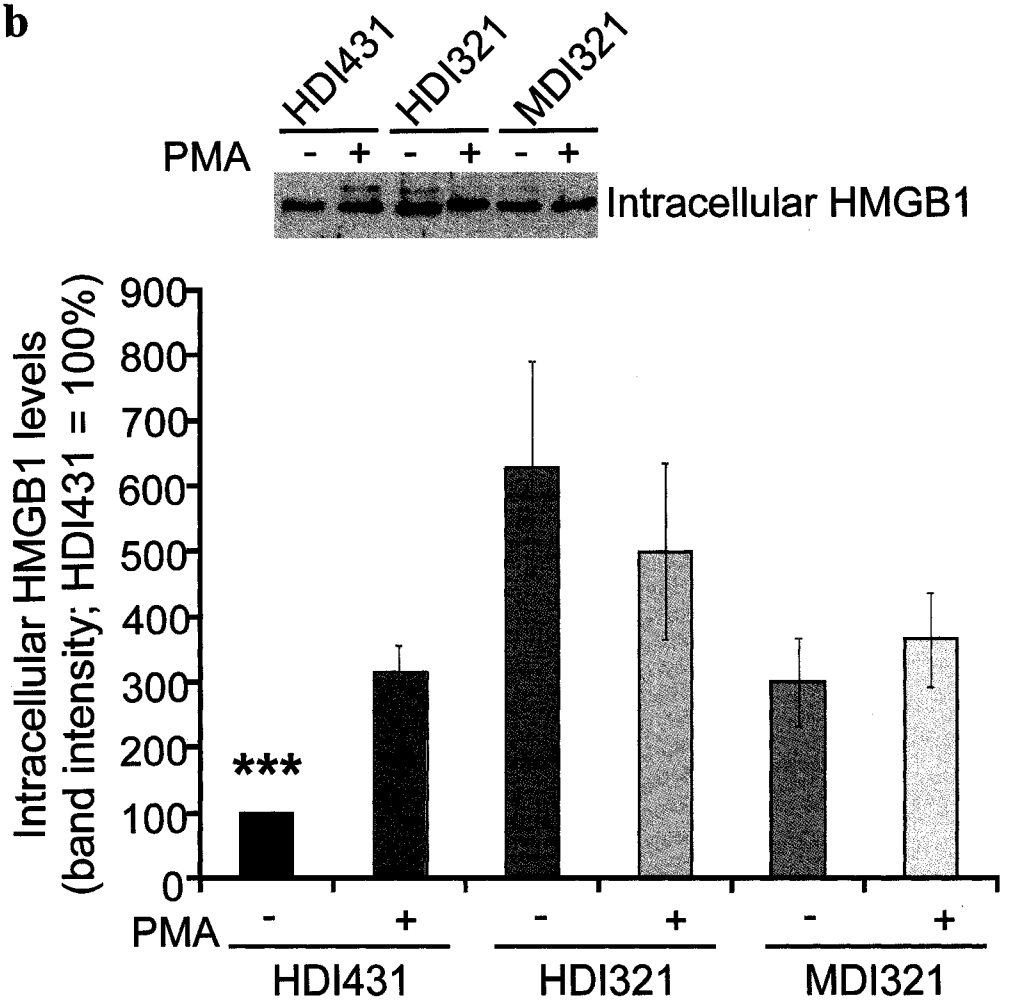
b
HDI431
HDI321
MDI321
PMA
- + - + - +
Intracellular HMGB1
Intracellular HMGB1 levels
(band intensity; HDI431 = 100%)
900
800
700
600
500
400
300
200
100
0
***
PMA
- + - + - +
HDI431
HDI321
MDI321

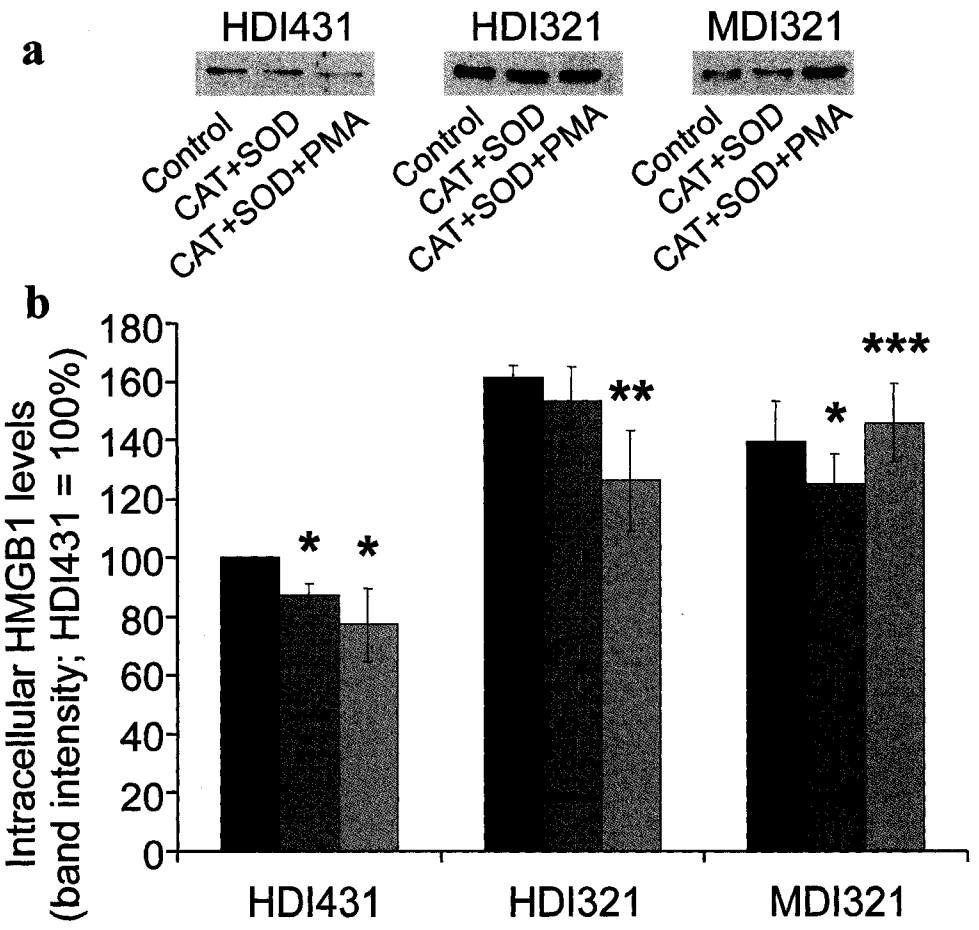

Figure 4.6: Effect of ROS scavengers on HMGB1 expression in MDM re-seeded on PCNU surfaces. Monocytes were differentiated to MDM for 14 days on TCPS prior to re-seeding onto HDI431, HDI321, or MDI321 surfaces in the absence or presence of PMA (red bar) , CAT+SOD (blue bar) or CAT+SOD+PMA (green bar) for 48 hours. Cell lysates were then analyzed for HMGB1 expression by immunoblotting as described in the Materials and Methods (a). Blots were quantified using Image J Software and reported relative to levels in cells on HDI431 in media without PMA (b). n=3 and data are reported with standard errors of the mean. * There was a significant decrease in HMGB1 levels relative to levels measured in cells in media alone. ** There was a significant decrease in HMGB1 levels with the addition of PMA relative to cells on HDI321 in media alone. *** There was a significant increase in HMGB1 levels with the addition of PMA relative to the effect of CAT+SOD in cells on MDI321.

Effect of phorbol esters on the morphology of MDM re-seeded on different PCNU surfaces- In order to assess the effect of PKC activation on MDM morphology, MDM were re-seeded on the three PCNU surfaces with or without PMA for 48 hours and then prepared for SEM. When examining the SEM analyses of MDM on HDI431 and HDI321 treated with PMA (Figures 4.7aii and 4.7bii), an increase in intercellular connections was apparent. Little change in MDM morphology was observed between MDM re-seeded on MDI321 in the presence (Figure 4.7ci) or absence of PMA (Figure 4.7cii), agreeing with the lack of an effect of PMA on MDM-when adherent on MDI321 with respect to any of the measured parameters (radiolabel release, esterase activity, MSE and HMGB1 protein) (Figures 4.1-4.5).

Effect of phorbol esters on the size of MDM re-seeded on different PCNU surfaces- When examining the MDM after staining the actin cytoskeleton with rhodamine phalloidin it was possible to demonstrate an effect of phorbol esters on MDM cell size. Regardless of the treatment (PMA, BIM, BIM + PMA), MDM on MDI321 were found to be significantly larger (43000 +/- 1000 pixels) than MDM on HDI431 (36000+/- 1000 pixels, $p=0.007$) or HDI321 (31000 +/- 1000 pixels, $p<0.0001$). However, PMA decreased the size of MDM on HDI431 by 20% ($p<0.001$) but had no effect on the size of MDM on the other surfaces.

Figure 4.7: Effect of phorbol esters on MDM morphology re-seeded on PCNU surfaces. Monocytes were differentiated to MDM for 14 days on TCPS prior to re-seeding onto HDI431 (a), HDI321 (b) or MDI321 (c) surfaces in the absence (ai-ci) or presence of PMA (aii-cii). After 48 hours, the MDM on the PCNU surfaces were fixed and analyzed by SEM as described in the Materials and Methods.

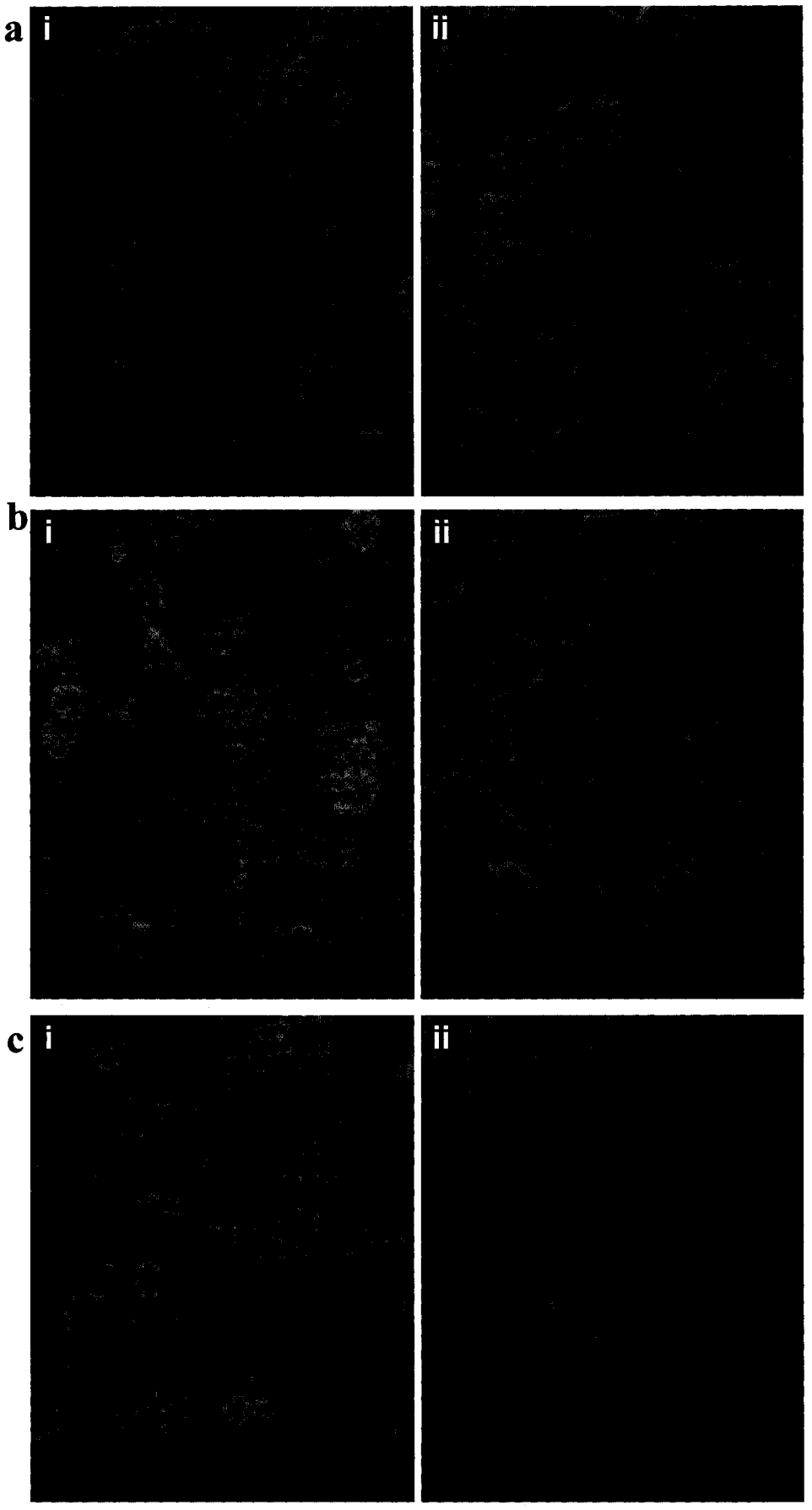
a
i
ii
b
i
ii
c
i
ii

DISCUSSION

The results of this study provide evidence that both activation and inhibition of PKC have an important role in the FBR of MDM, which is directed by the chemistry of the material surface to which they have adhered. In order to further define the role of PKC and ROS, PKC inhibitors, PKC active and inactive phorbol esters, as well as ROS scavengers were used to treat the MDM while cultured on the three PCNU surfaces.

Previously and in this study it was found that PMA inhibited the radiolabel release, esterase activity and MSE protein production in MDM re-seeded on HDI431 and HDI321 ((McBane et al. 2005) and Figure 4.1). Although the specific PKC isoform required for the PMA effect on MDM-biodegradation was not determined, it appeared that one or more of the conventional or novel PKC isoforms was involved in the effects observed with the HDI PCNUs (Ma et al. 2006, Newton 1995). Evidence that confirmed the involvement of PKC activation in the HDI PCNUs was found when the 4α isoform of PMA, which does not activate PKC (Hecker 1985), did not affect the MDM in the manner that PMA did (Figures 4.2 and 4.3). Many studies with other cell types (neutrophils, monocytes, A549 cells) demonstrated the involvement of PKC using 4α phorbol esters as negative controls (Downey et al. 1992, Gladwin et al. 1990, Kim et al. 2007, Lee et al. 2006). Kim *et al* showed that PMA switched A549 glucose depleted cells from necrosis to apoptosis whereas 4αPMA did not (Kim et al. 2007).

When MDM were adherent to MDI321, there were no PMA effects on esterase or radiolabel release observed. However, when the PKC inactive 4αPMA was added to the

MDM on this surface, there was a significant increase in radiolabel release indicating that PKC may not be the dominant biodegradation pathway tied to the action of MDM on MDI321. Interestingly, further work showed that this effect was not observed when another PKC inactive diterpene phorbol ester precursor (no ester bond) (4α–phorbol) was used at the same concentration with the MDM on MDI321 (data not shown). This suggests that there is something specific about the PMA structure with the 4α-hydroxyl that allowed for enhanced MDM-mediated degradation of MDI321 (Figure 4.2), but had no effect on esterase activity or MSE protein (Figures 4.3, 4.4).

Other studies have shown that phorbol esters can have effects other than those relating to PKC. For example, chimaerins, a family of Rac-GTPase-activating proteins, have non-PKC phorbol ester/diacylglycerol (DAG) receptors similar in homology to the phorbol ester/DAG binding domains on PKC (Caloca et al. 1997). Previously it has been shown that the 4α–phorbol ester derivative 4α–phorbol 12,13-didecanoate can induce TRPV4 channels to release calcium from endothelial cells better than PMA or 4β–phorbol 12,13-didecanoate (Watanabe et al. 2002), suggesting a PKC-independent phorbol ester-dependent pathway. Therefore, it is possible that the increased radiolabel release from MDI321 observed with 4αPMA induced the MDM-mediated degradation of MDI321 through activation of a PKC-independent pathway, and one that does not appear to correlate with increased esterase activity. There may be other possibilities for the lack of an effect of PMA on the MDM when adherent to MDI321. In an earlier study (McBane et al. 2005) it appeared that it could have been the MDI321 surface itself that activated

PKC in MDM maximizing the PKC activation in the control condition such that any further activity of PKC could not be stimulated by PMA.

One might consider that the lack of an increase in esterase activity (Figure 4.3) and MSE protein (Figure 4.4) to match the increase in radiolabel release (Figure 4.2) caused by 4αPMA with MDI321 may have been due to down-regulation of one of the PKC isoforms shown to be unresponsive after 48 hours of exposure to PMA. A recent study on the PKC-mediated accumulation of cholesterol in macrophages showed that after prolonged exposure to PMA some PKC isozymes initially activated by PMA were partially or completely down-regulated (Ma et al. 2006). There was a down-regulation seen in PKC-β and δ in macrophages between a 24-hour and 48-hour exposure to PMA (Joy et al. 2005, Ma et al. 2006). Another study with A549 cells showed that PMA switched glucose depleted cells from necrosis to apoptosis whereas after prolonged treatment (24h in this case) accelerated the glucose depleted cell death mode (Kim et al. 2007). The present study looked at cumulative radiolabel release from PCNUs elicited by MDM after 48 hours with or without PMA. Therefore, no information was obtained on whether or not this late PKC down-regulation affected biodegradation or esterase activity. If PKC were maximally activated by the MDI321 surface, then activation by PMA would have no effect. The lack of an effect of PMA on MDM-mediated MDI321 biodegradation could also be due to the fact that MDI321 was inherently much less degradable than the HDI PCNUs because of the relative chemical stability (McBane et al. 2005, McBane et al. 2007, Tang et al. 2003).

Aside from using structural analogues of PMA to establish whether or not PMA influences the MDM-mediated biodegradation of PCNUs via the activation of PKC, an inhibitor of PKC was also assessed. BIM, or GF 109203X is a selective inhibitor of PKC that competes with ATP for binding to the active site on PKC (Toullec et al. 1991, Wilkinson et al. 1993). Although BIM itself had no significant effect on radiolabel release (Figure 4.2), esterase activity (Figure 4.3), or MSE protein (Figure 4.4), it was able to reverse the effects due to PMA when these two reagents were added to the MDM together. Again, this effect was also found in alveolar macrophages where treatment with BIM inhibited a PMA induced respiratory burst (Forman et al. 1998) and in human MDM where BIM inhibited the PMA induced uptake or macropinocytosis of low-density lipoproteins (Kruth et al. 2002, Ma et al. 2006), but had no effect when added alone. Although BIM alone had no effect on cell size or morphology, adding both BIM+PMA to cells on all the surfaces stimulated cell spreading and significantly increased the cell size of MDM on all three surfaces. The hyper-growth of cells was unexpected since only a reversal of the PMA induced cell size reduction was anticipated. This suggests that there is a phorbol ester effect on MDM that is independent of PKC activation. The increase in size, viability and degradation of BIM+PMA treated cells on MDI321 (the only material that did not respond to PMA) suggest that there is possibly a non-PKC pathway activated by PMA that is physiologically favored when PKC is inhibited.

ROS scavengers CAT+SOD were added to the MDM to assess how oxidation may play a role in the MDM response to the material surface. Previously it was found that only cells on HDI431 showed a significant increase in ROS production when treated with PMA

(McBane et al. 2007). PMA treatment of cells on MDI321 produced no further increase in ROS production, once more confirming that the material surface itself had stimulated PKC maximally and so MDM could not further respond. However, MDM on HDI321 produced less ROS (McBane et al. 2007). In this study, CAT+SOD treatment stimulated radiolabel release elicited by MDM on MDI321 (Figure 4.2b), and inhibited radiolabel release from HDI321, but had no effect on MDM-mediated degradation of HDI431. In a previous study, pre-treatment of the PCNUs with H_2O_2 decreased subsequent MDM-mediated degradation of MDI321, (McBane et al. 2007) so removal of H_2O_2 by CAT+SOD in the current study may have been able to promote MDI321 degradation (Figure 4.2b). MDM-mediated degradation of HDI431 was not inhibited by pre-treatment with H_2O_2 (McBane et al. 2007) and in this study there was no effect by treatment of MDM with CAT+SOD (Figure 4.2b). The effect of H_2O_2 pre-treatment of the PCNUs on esterase activity in the MDM on the PCNUs matched the effect of CAT+SOD; MDM on both HDI PCNUs pre-treated with H_2O_2 had less esterase activity and this was true of treatment with CAT+SOD as well. There was no effect on the esterase activity in MDM on MDI321 (Figure 4.3b) treated with CAT+SOD or in MDM on MDI321 that had been pre-treated with H_2O_2 (McBane et al. 2007). Together these data show that ROS release has more of an effect on the MDM response to HDI PCNUs in terms of esterase-mediated degradation than the MDM response to MDI321.

Although the results for the HDI PCNUs appear paradoxical (i.e. PMA, which causes the release of ROS, had the same effect as CAT+SOD that removes ROS), in another study with A549 cells, both PMA and CAT had the same effect on these cells. The effect of

PMA treatment was to activate PKC since inhibitors of PKC and the PKC inactive 4αPMA eliminated the PMA effect and this PKC activation switched the glucose-depleted A549 cells from necrosis to apoptosis (Kim et al. 2007). Treatment with CAT also was able to switch the death mode of glucose-depleted cells from necrosis to apoptosis. The explanation for these effects provided by Kim et al was that PMA likely exerted its cell death mode switch activities through PKC activation of the ERKl/2 – dependent pathway causing increased MnSOD expression and inhibition of CuZnSOD degradation in A549 cells (Kim et al. 2007). With PKC activation by PMA, intracellular MnSOD was increased, whereas, in glucose-depleted cells, CuZnSOD was degraded (Kim et al. 2007). When comparing the results of the current study to the PKC effects on glucose-depleted A549 cells, some similarities appeared. If one considers material chemistry to elicit a stress-induced response, the effects of glucose-depletion may be analogous. MDMs must respond to the site of the foreign body (the PCNU surface), just as the A549 lung cancer cells must respond to being in a state of glucose-depletion.

In the specific situation of the MDM FBR to materials, there are two components that can be observed and may not necessarily be correlated. These are the effects of various treatments on the degradation of the materials and the effects of these same treatments on the typical properties of the innate immune response. A material that is more degradable may not necessarily elicit a greater FBR. Although the response may lead to degradation of the material, the chemistry of the material also will dictate the degree to which it is degraded. For example TCPS, a non-degradable surface, elicited more esterase activity and caused greater protein synthesis in U937 cells than when these cells were on PCNUs

that were being degraded (Matheson et al. 2007). Although HDI431 is the most degradable PCNU by MDM and esterases, it does not always elicit the greatest FBR in MDM. In a study where monocytes were differentiated on these three PCNUs, it was MDI321 that elicited the most esterase activity after 14 days when compared to TCPS, HDI431 and HDI321 (Labow et al. 2005a).

The nuclear protein HMGB1, which is almost ubiquitously expressed in eukaryotic cells, has recently emerged as being important in inflammation and the MDM-mediated FBR. Previously it was found that HMGB1 is secreted by activated MDM and acts as a potent pro-inflammatory mediator (Yang et al. 2005). When studying the effects of material surface chemistry on the role of PKC in MDM, HMGB1 secretion behaved in a similar manner to the other parameters measured. For example, PMA caused a decrease in degradation, esterase activity and MSE protein by MDM on HDI-based PCNUs with no effect on MDM when on MDI321. This was true of HMGB1 secretion as well (Figure 4.5a). Moreover, CAT+SOD significantly reduced esterase activity in the MDM on HDI-based PCNUs and this was true of intracellular HMGB1 levels measured in cell lysates from MDM on HDI431 and MDI321 but not HDI321 (Figure 4.6). The results with HMGB1 and material surface chemistry effects on MDM were similar to the effects of glucose depletion on the release of HMGB1 on A549 cells. Both CAT and PMA treatment reversed the effects of glucose depletion on HMGB1 release from A549 cells and significantly reduced HMGB1 release (Kim et al. 2007). HMGB1 results in this study suggest that HDI431 is the most pro-inflammatory of the PCNUs tested and that

this marker of inflammation, measured both in the cell and in the conditioned media, may be useful for assessing the extent of a FBR *in vitro*.

When examining the effect of PKC on cell size, it was found that the size of PMA treated MDM on HDI431 decreased, which may account for the decreased protein expression and ability to degrade the PCNU. It was interesting to note that MDM on MDI321 showed very little difference in morphology with or without PMA treatment. Since MDM on MDI321 always showed a spread out morphology, they could be insensitive to the effects of PMA, particularly if the material has already maximally activated PKC as was previously discussed (McBane et al. 2005).

In summary, this study provides further evidence that MDM respond specifically to the material surface, triggering or suppressing oxidative and/or hydrolytic pathways in order to respond to a foreign body. Previously models were proposed for the MDM-mediated degradation of HDI-based and MDI-based PCNUs that suggested roles for both oxidative and hydrolytic means of degradation (McBane et al. 2005). Figures 4.8 and 4.9 show modified models of the MDM-mediated degradation to HDI and MDI-based PCNUs (respectively) that includes the data from the present study. As Figure 4.8 suggests, the MDM-mediated degradation of HDI PCNUs is largely dependent on esterase activity. Treatments such as PMA that decrease esterase activity and MSE protein cause a decrease in MDM-mediated HDI PCNU degradation. The effect of PMA on esterase activity is dependent on PKC activation. PMA treatment also decreases HMGB1 secretion in MDM on HDI-PCNUs suggesting that induction of the pro-inflammatory

phenotype in these cells induced by the surface can be suppressed by PKC activation suggesting a possible target for regulation.

Scavenging ROS from MDM on HDI-based PCNUs with CAT+SOD had no effect on esterase or degradation except when PMA was added and then there was an inhibition of both these related parameters, suggesting that esterase activity may be more important than ROS in HDI PCNU degradation. Figure 4.9 suggests that there is another hydrolytic enzyme, (Enzyme X) produced in MDM on MDI-based PCNUs other than esterase that can be stimulated by phorbol esters when PKC is not activated or when ROS are eliminated by CAT+SOD. HMGB1 secretion is not stimulated in MDM on MDI321 as much as the HDI-based PCNUs suggesting a less pro-inflammatory phenotype. However, HMGB1 secretion cannot be inhibited by PKC activation in these cells suggesting PKC may already be activated by the surface. Scavenging ROS with CAT+SOD did not affect esterase but stimulated degradation. However, when CAT+SOD was added with PMA there was an inhibition of degradation without change in esterase activity. In summary, the mechanisms proposed in Figures 4.8 and 4.9 suggest that ROS and Enzyme X are more important in MDM-mediated degradation of MDI-based PCNUs than esterase, whereas esterase is the most important hydrolytic activity involved in the MDM-mediated degradation of HDI-based PCNUs.

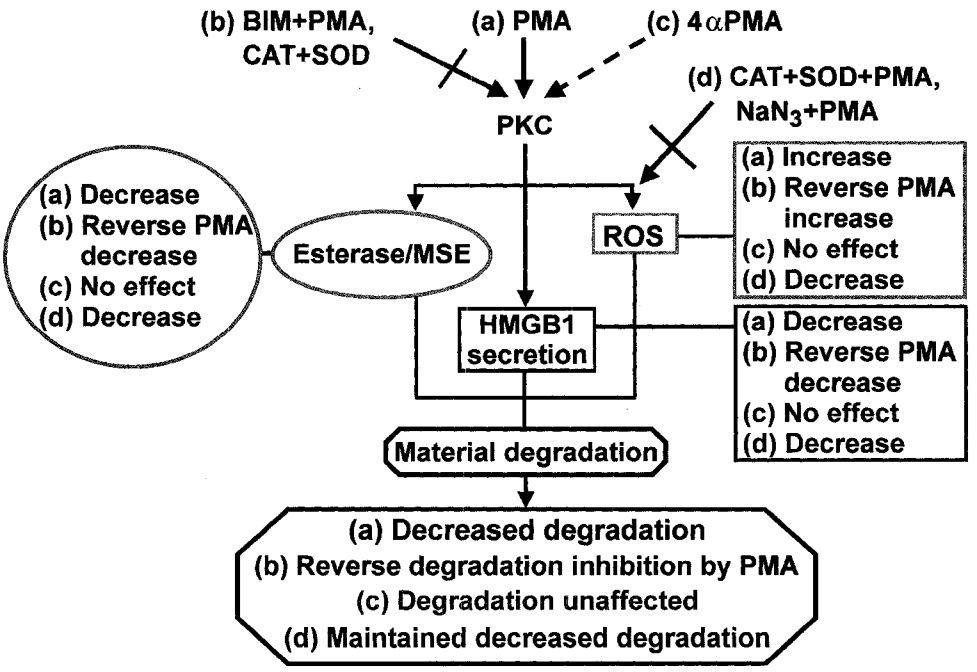

Figure 4.8: Modified model of MDM-mediated HDI-based PCNU degradation. The HDI PCNU surface stimulates ROS production, esterase activity, and MSE protein in MDM, the release of which causes material degradation. HMGB1 secretion from MDM is also stimulated by the HDI surface. **(a)** PMA causes the activation of PKC. PKC activation inhibits esterase activity, MSE protein, and the release of HMGB1 while activating ROS production in MDM. This leads to an inhibition of esterase activity and MSE protein and the intracellular accumulation of HMGB1. **(b)** Inhibiting PKC by adding BIM or H7 to PMA reverses the inhibition of esterase activity and MSE protein by PMA. Extra ROS production is suppressed and material degradation is no longer inhibited. **(c)** 4αPMA cannot induce the same effects as PMA (no effect on esterase activity, HMGB1 secretion, ROS or degradation), suggesting again that PMA works through PKC activation. **(d)** CAT+SOD+PMA or NaN_3+PMA inhibit ROS release by scavenging ROS or inhibiting peroxidases (respectively). The PMA inhibition of esterase activity is maintained under these conditions and there is still a decrease in degradation. CAT+SOD+PMA treatment decreased intracellular HMGB1, suggesting increased secretion.

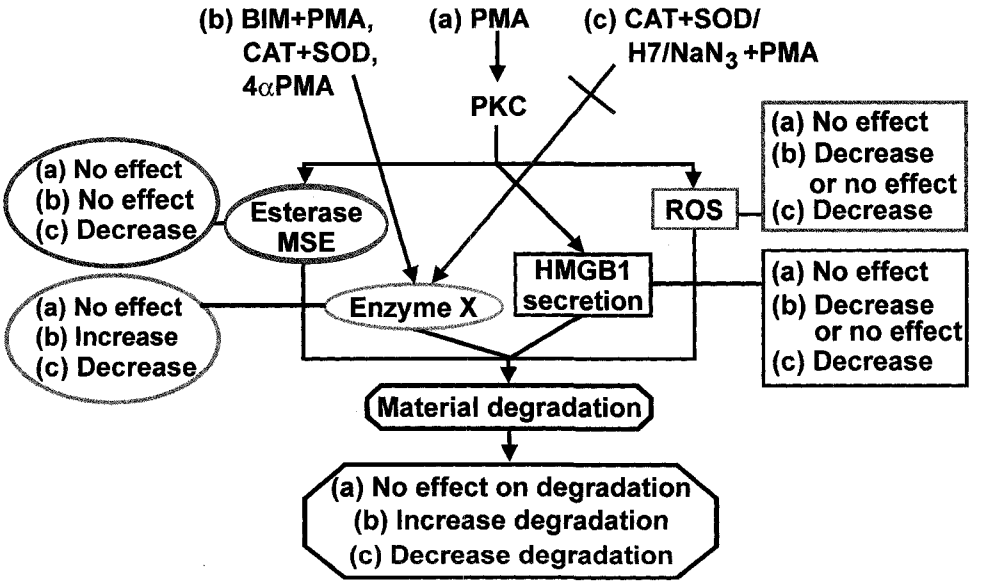

Figure 4.9: Modified model of MDM-mediated MDI-based PCNU degradation. MDM on MDI321 are stimulated to produce ROS but are less stimulated to produce esterase activity and MSE and secrete HMGB1 than MDM on HDI PCNUs. (a) PMA had no effect on the ROS, HMGB1 secretion, esterase activity or MSE produced by MDM on MDI321, suggesting that PKC is already stimulated maximally by the surface. (b) BIM+PMA, CAT+SOD, and 4αPMA all caused an increase in MDM-mediated degradation without an increase in esterase activity. This suggests that another hydrolytic enzyme (Enzyme X) is stimulated by these treatments. CAT+SOD alone decreased intracellular HMGB1. (c) CAT+SOD+PMA, H7+PMA, and NaN_3+PMA inhibit esterase activity and may also inhibit ROS and Enzyme X. These treatments cause an inhibition of the MDM-mediated degradation of MDI321. CAT+SOD+PMA increased intracellular HMGB1, suggesting secretion is inhibited.

The results of this study showed that the FBR of MDM is dictated by the material surface chemistry on which they are cultured first, before the MDM responds to exogenous agents. The MDM response when adherent to HDI PCNUs was different to the MDM on MDI321 for almost every treatment (PMA, BIM, 4αPMA, CAT+SOD) and every parameter measured (material degradation, esterase activity, MSE protein, and HMGB1 protein (secreted and intracellular)). Certainly more than one signaling pathway was triggered in the MDM by the different surfaces, one that is dependent on PKC activation that was affected by ROS production and one that was not (i.e. a pathway dependent on PKC inhibition). Biomaterial applications are diversifying and MDM are becoming an increasingly important element in the implementation of these material strategies. For instance MDM have been recently shown to be important players in the wound-healing response that can be used for spinal cord regeneration (Schwartz and Yoles 2006). Therefore, depending on the purpose of the implanted device, material chemistry will need to be tailored in order to stimulate the appropriate cell signaling pathway(s) in MDM.

ACKNOWLEDGEMENTS

The polymers were synthesized by Dr. Meilin Yang of the Faculty of Dentistry at the University of Toronto in Toronto, Ontario. The SEM analysis was performed by Robert Chernecky at the Faculty of Dentistry, University of Toronto. JE McBane was partially funded by a CIHR Strategic Training Fellowship for Cell Signaling in Mucosal Inflammation and Pain (STP-53877) and by an Ontario Graduate Scholarship in Science and Technology. LA Matheson was funded by an NSERC post-doctoral fellowship.

These studies were funded in part by a grant from the Canadian Institutes for Health Research (CIHR).

REFERENCES

Caloca, M.J., Fernandez, N., Lewin, N.E., Ching, D., Modali, R., Blumberg, P.M., and Kazanietz, M.G. 1997. Beta2-chimaerin is a high affinity receptor for the phorbol ester tumor promoters. J Biol Chem. **272**(42): 26488-96.

Cannon, G.J., and Swanson, J.A. 1992. The macrophage capacity for phagocytosis. J Cell Sci. **101 (Pt 4)**: 907-13.

Christenson, E.M., Dadsetan, M., Wiggins, M., Anderson, J.M., and Hiltner, A. 2004. Poly(carbonate urethane) and poly(ether urethane) biodegradation: in vivo studies. J Biomed Mater Res A. **69**(3): 407-16.

Ding, Q., Jin, T., Wang, Z., and Chen, Y. 2007. Catalase potentiates retinoic acid-induced THP-1 monocyte differentiation into macrophage through inhibition of peroxisome proliferator-activated receptor gamma. J Leukoc Biol. **81**(6): 1568-76.

Dinnes, D.L., Santerre, J.P., and Labow, R.S. 2005. Phospholipase A2 pathway association with macrophage-mediated polycarbonate-urethane biodegradation. Biomaterials. **26**(18): 3881-9.

Dinnes, D.L., Santerre, J.P., and Labow, R.S. 2008. Intracellular phospholipase A(2) expression and location in human macrophages: Influence of synthetic material surface chemistry. J Cell Physiol. **214**: 136-144.

Downey, G.P., Chan, C.K., Lea, P., Takai, A., and Grinstein, S. 1992. Phorbol ester-induced actin assembly in neutrophils: role of protein kinase C. J Cell Biol. **116**(3): 695-706.

Forman, H.J., Zhou, H., Gozal, E., and Torres, M. 1998. Modulation of the alveolar macrophage superoxide production by protein phosphorylation. Environ Health Perspect. **106 Suppl 5**: 1185-90.

Gladwin, A.M., Hassall, D.G., Martin, J.F., and Booth, R.F. 1990. MAC-1 mediates adherence of human monocytes to endothelium via a protein kinase C dependent mechanism. Biochim Biophys Acta. **1052**(1): 166-72.

Hecker, E. 1985. Cell membrane associated protein kinase C as receptor of diterpene ester co-carcinogens of the tumor promoter type and the phenotypic expression of tumors. Arzneimittelforschung. **35**(12A): 1890-903.

Jackson, S.H., Gallin, J.I., and Holland, S.M. 1995. The p47phox mouse knock-out model of chronic granulomatous disease. J Exp Med. **182**(3): 751-8.

Joy, S.V., Scates, A.C., Bearelly, S., Dar, M., Taulien, C.A., Goebel, J.A., and Cooney, M.J. 2005. Ruboxistaurin, a protein kinase C beta inhibitor, as an emerging treatment for diabetes microvascular complications. Ann Pharmacother. **39**(10): 1693-9.

Kalinina, N., Agrotis, A., Antropova, Y., DiVitto, G., Kanellakis, P., Kostolias, G., Ilyinskaya, O., Tararak, E., and Bobik, A. 2004. Increased expression of the DNA-binding cytokine HMGB1 in human atherosclerotic lesions: role of activated macrophages and cytokines. Arterioscler Thromb Vasc Biol. **24**(12): 2320-5.

Kim, C.H., Han, S.I., Lee, S.Y., Youk, H.S., Moon, J.Y., Duong, H.Q., Park, M.J., Joo, Y.M., Park, H.G., Kim, Y.J., Yoo, M.A., Lim, S.C., and Kang, H.S. 2007. Protein kinase C-ERK1/2 signal pathway switches glucose depletion-induced necrosis to apoptosis by regulating superoxide dismutases and suppressing reactive oxygen species production in A549 lung cancer cells. J Cell Physiol. **211**(2): 371-85.

Kruth, H.S., Huang, W., Ishii, I., and Zhang, W.Y. 2002. Macrophage foam cell formation with native low density lipoprotein. J Biol Chem. **277**(37): 34573-80.

Labow, R.S., Meek, E., Matheson, L.A., and Santerre, J.P. 2002. Human macrophage-mediated biodegradation of polyurethanes: assessment of candidate enzyme activities. Biomaterials. **23**(19): 3969-75.

Labow, R.S., Meek, E., and Santerre, J.P. 1998. Differential synthesis of cholesterol esterase by monocyte-derived macrophages cultured on poly(ether or ester)-based poly(urethane)s. J Biomed Mater Res. **39**(3): 469-77.

Labow, R.S., Meek, E., and Santerre, J.P. 2001a. Hydrolytic degradation of poly(carbonate)-urethanes by monocyte-derived macrophages. Biomaterials. **22**(22): 3025-33.

Labow, R.S., Meek, E., and Santerre, J.P. 2001b. Model systems to assess the destructive potential of human neutrophils and monocyte-derived macrophages during the acute and chronic phases of inflammation. J Biomed Mater Res. **54**(2): 189-97.

Labow, R.S., Meek, E., and Santerre, J.P. 2001c. Neutrophil-mediated biodegradation of medical implant materials. J Cell Physiol. **186**(1): 95-103.

Labow, R.S., Sa, D., Matheson, L.A., Dinnes, D.L., and Paul Santerre, J. 2005a. The human macrophage response during differentiation and biodegradation on polycarbonate-based polyurethanes: Dependence on hard segment chemistry. Biomaterials. **26**(35): 7357-66.

Labow, R.S., Sa, D., Matheson, L.A., and Santerre, J.P. 2005b. Polycarbonate-urethane hard segment chemistry influences esterase substrate specificity for human macrophage mediated biodegradation. J Biomater Sci Polym Ed. **16**: 1167-77.

Lee, J.Y., Visser, F., Lee, J.S., Lee, K.H., Soh, J.W., Ho, W.K., Lytton, J., and Lee, S.H. 2006. Protein kinase C-dependent enhancement of activity of rat brain NCKX2 heterologously expressed in HEK293 cells. J Biol Chem. **281**(51):39205-16.

Ma, H.T., Lin, W.W., Zhao, B., Wu, W.T., Huang, W., Li, Y., Jones, N.L., and Kruth, H.S. 2006. Protein kinase C beta and delta isoenzymes mediate cholesterol accumulation in PMA-activated macrophages. Biochem Biophys Res Commun. **349**(1): 214-20.

Marchant, R.E., Miller, K.M., and Anderson, J.M. 1984. In vivo biocompatibility studies. V. In vivo leukocyte interactions with Biomer. J Biomed Mater Res. **18**(9): 1169-90.

Matheson, L.A., Labow, R.S., and Santerre, J.P. 2002. Biodegradation of polycarbonate-based polyurethanes by the human monocytes-derived macrophage and U937 cell systems. J Biomed Mater Res. **61**(4): 505-13.

Matheson, L.A., McBane, J.E., Malowany, J.I., Santerre, J.P., and Labow, R.S. 2007. Is cell culture stressful? Effects of degradable and nondegradable culture surfaces on U937 cell function. Biotechniques. **42**(6): 744, 746-50.

Matheson, L.A., Santerre, J.P., and Labow, R.S. 2004. Changes in macrophage function and morphology due to biomedical polyurethane surfaces undergoing biodegradation. J Cell Physiol. **199**(1): 8-19.

McBane, J.E., Santerre, J.P., and Labow, R.S. 2005. The role of protein kinase C in the monocyte-derived macrophage mediated biodegradation of polycarbonate-based polyurethanes. J Biomed Mater Res. **74A**: 1-11.

McBane, J.E., Santerre, J.P., and Labow, R.S. 2007. The interaction between hydrolytic and oxidative pathways in macrophage-mediated polyurethane degradation. J Biomed Mater Res A. **82**(4): 984-94.

Newton, A.C. 1995. Protein kinase C: structure, function, and regulation. J Biol Chem. **270**(48): 28495-8.

Passalacqua, M., Zicca, A., Sparatore, B., Patrone, M., Melloni, E., and Pontremoli, S. 1997. Secretion and binding of HMG1 protein to the external surface of the membrane are required for murine erythroleukemia cell differentiation. FEBS Lett. **400**(3): 275-9.

Schubert, M.A., Wiggins, M.J., Anderson, J.M., and Hiltner, A. 1997. Role of oxygen in biodegradation of poly(etherurethane urea) elastomers. J Biomed Mater Res. **34**(4): 519-30.

Schwartz, M., and Yoles, E. 2006. Immune-based therapy for spinal cord repair: autologous macrophages and beyond. J Neurotrauma. **23**(3-4): 360-70.

Tang, Y.W., Labow, R.S., and Santerre, J.P. 2001a. Enzyme-induced biodegradation of polycarbonate polyurethanes: dependence on hard-segment concentration. J Biomed Mater Res. **56**(4): 516-28.

Tang, Y.W., Labow, R.S., and Santerre, J.P. 2001b. Enzyme-induced biodegradation of polycarbonate-polyurethanes: dependence on hard-segment chemistry. J Biomed Mater Res. **57**(4): 597-611.

Tang, Y.W., Labow, R.S., and Santerre, J.P. 2003. Enzyme induced biodegradation of polycarbonate-polyurethanes: dose dependence effect of cholesterol esterase. Biomaterials. **24**(12): 2003-11.

Thomas, E.L., and Fishman, M. 1986. Oxidation of chloride and thiocyanate by isolated leukocytes. J Biol Chem. **261**(21): 9694-702.

Toullec, D., Pianetti, P., Coste, H., Bellevergue, P., Grand-Perret, T., Ajakane, M., Baudet, V., Boissin, P., Boursier, E., Loriolle, F., and et al. 1991. The bisindolylmaleimide GF 109203X is a potent and selective inhibitor of protein kinase C. J Biol Chem. **266**(24): 15771-81.

Watanabe, H., Davis, J.B., Smart, D., Jerman, J.C., Smith, G.D., Hayes, P., Vriens, J., Cairns, W., Wissenbach, U., Prenen, J., Flockerzi, V., Droogmans, G., Benham, C.D., and Nilius, B. 2002. Activation of TRPV4 channels (hVRL-2/mTRP12) by phorbol derivatives. J Biol Chem. **277**(16): 13569-77.

Wilkinson, S.E., Parker, P.J., and Nixon, J.S. 1993. Isoenzyme specificity of bisindolylmaleimides, selective inhibitors of protein kinase C. Biochem J. **294 (Pt 2)**:335-7.

Yang, H., Wang, H., Czura, C.J., and Tracey, K.J. 2005. The cytokine activity of HMGB1. J Leukoc Biol. **78**(1): 1-8.

5.0 DISCUSSION

This thesis has contributed to the understanding of one of the cell signaling pathways (PKC) that may determine the mechanism of how material surface chemistry directs the MDM foreign body action. The perfect biocompatible material for every medical application does not exist. Each medical device or application requires the biomaterial to perform a specialized function and must perform this function in a different location. Every location in the body is subject to stress due to the foreign body response but the degree of stress and types of stresses differ. For instance, the implant site has been found to affect the foreign body response in terms of fibrous capsule formation and phagocytic cell attachment (1). Polyurethanes are a versatile group of polymers with a segmented chemistry (2) that can be adapted to a wide spectrum of therapeutic uses in the medical device industry. By surface modifications (3-7), altering chemical components (8) or the ratio of components (9), polyurethanes can be tailored for use in a stable implant or in a degradable tissue engineering application or drug delivery system.

MDMs are the often forgotten rulers of the foreign body response to biomaterials. It is known that they are responsible for material degradation; but the trigger and mechanism of release of their biological activities are not completely understood. Several research groups have tried to elucidate how the MDM responds to the material surface to cause material degradation. Some studies have suggested that CE and hydrolytic enzymes cause an insignificant amount of degradation in PCNUs when compared to oxidative degradation (10, 11). Other studies have shown by both direct and indirect means that CE and CXE or MSE can cause significant amounts of PCNU degradation and that

balance between oxidation and hydrolysis influences PCNU degradation in part by the nature (chemical content) of the hard segment phase (8, 12-17).

PMA effects on macrophage-mediated PCNU degradation

PMA is a phorbol ester that activates PKC and can inhibit the neutrophil-mediated degradation of HDI431 by significantly increasing the amount of HOCl produced (15). Since the neutrophil-mediated degradation of a polyurethane; is negligible compared to the MDM-mediated degradation of a polyurethane it was of interest to see how PMA would affect MDM on different PCNUs. In this thesis, PMA was used to activate PKC in MDM to investigate the effect of PKC activation on the MDM response to different PCNUs and the MDM-mediated degradation of these PCNUs.

As reported in manuscript #1, PMA treatment caused different effects on MDM responses based on the chemistry of the PCNU hard segment. MDM re-seeded on the PCNUs with HDI (HDI431, HDI321) showed an inhibition of PCNU degradation, esterase activity and MSE protein production with PMA treatment (Figures 2.1 and 2.2). However, MDM re-seeded on the aromatic PCNU MDI321 showed no effect of PMA on these parameters. It has been found that HDI PCNUs are more susceptible to CE and CXE-mediated degradation than MDI321 (8, 14) and that HDI431 is more degradable than HDI321 by CE (9). This is also true for MDM-mediated degradation, as it has been found that, in terms of biodegradation, HDI431 is the most degradable followed by HDI321 and MDI321 (18). In addition, it has been found that CE and MSE synthesis and esterase activity is greater in MDM on HDI431 than MDI321 (18, 19). Together thess

results suggest that the extra esterase triggered in MDM on the HDI PCNUs can be directly or indirectly stopped through a PKC-regulated pathway. This was the first study to suggest PKC as a possible target to control esterase activation in MDM on HDI PCNUs.

PKC activation required for PMA effects on HDI re-seeded MDM

The effect of PMA on MDM-mediated degradation of HDI PCNUs was striking; however, it was still not confirmation that activation of PKC caused the inhibition of degradation. To confirm that PKC was directly responsible for the effect of PMA on degradation, inhibitors of PKC (H7 and BIM), and a PKC inactive phorbol ester, 4αPMA, were used (Manuscripts#1 and 3). H7 could reverse the effect of PMA on MDM-mediated degradation of HDI431 but not HDI321 (Figure 2.4a). Since previously it was found that H7 was not a specific inhibitor of PKC, but could also inhibit protein kinase A and G (20), these experiments were repeated with the more specific PKC inhibitor BIM. As Figure 4.2a shows, BIM can reverse the effects of PMA on esterase activity and MDM-mediated degradation of HDI PCNUs re-seeded MDM. Furthermore, 4αPMA could not inhibit esterase activity or MDM-mediated degradation of MDM re-seeded on either HDI PCNU (Figure 4.2a), suggesting that the PMA effect is indeed dependent on PKC activation.

PKC has many *in vivo* substrates, one of which being NADPH oxidase, the initiating enzyme of the respiratory burst (21-23). In order to determine if activation of the respiratory burst was responsible for the down-regulation of esterase by PMA the

peroxidase inhibitor NaN_3 was used. Previously, it was also found that NaN_3 could reverse the effect of PMA on the neutrophil-mediated radiolabel release and HOCl release from neutrophils on HDI431 (15). As Figure 2.3 shows, NaN_3 could partially reverse the PMA inhibition of MDM degradation of the HDI PCNUs. To test this further, ROS scavengers CAT+SOD were used to remove H_2O_2 and superoxide anion before their oxidative effects on the materials could occur (24, 25). It was hypothesized that these would more specifically scavenge ROS from MDM than the myeloperoxidase inhibitor NaN_3. Interestingly, CAT+SOD alone had no effect on the MDM-mediated degradation of HDI431, but inhibited the degradation of HDI321 (Figure 4.2b). When PMA was added to CAT+SOD there was an inhibition of the MDM-mediated degradation of both HDI PCNUs, which was inhibited more than the esterase activity (Figure 4.2b). This suggests that although PMA can increase ROS release from MDM, ROS do not inhibit MDM-mediated degradation of the HDI PCNUs. However, PKC activation by PMA can inhibit esterase activity and MSE in MDM on HDI PCNUs, which can account for the inhibited degradation (Manuscripts 1&3, Figures 2.1, 2.2, 4.1, and 4.4). Therefore this model system showed that the MDM-mediated degradation of HDI-based PCNUs relies more on the hydrolytic esterase enzymes than ROS.

Non-PKC mediated effects of phorbol esters on MDM interactions with MDI321

MDM on MDI321 may not be sensitive to PKC activation, however they are sensitive to phorbol ester treatment and ROS scavenger treatment. When MDMs on MDI321 were treated with NaN_3 there was a significant inhibition of degradation and esterase activity, which continued when PMA was added to NaN_3 (Figure 2.3). H7 could also significantly

inhibit MDM-mediated degradation and esterase activity of MDM on MDI321 with or without PMA (Figure 2.4); however, the PKC inhibitor BIM did not inhibit MDM-mediated degradation and actually stimulated MDM-mediated degradation of MDM on MDI321 when treated with PMA (Figure 4.2). 4αPMA treatment also stimulated the MDM-mediated degradation of MDI321 (Figure 4.2). Interestingly, this stimulation by BIM+PMA and 4αPMA was not seen in esterase activity elicited by the MDI321 re-seeded MDM (Figure 4.3), suggesting that there was another mechanism of degradation stimulated by the phorbol ester, which was inhibited when PKC was activated. This suggests that there is an unidentified hydrolytic enzyme (Enzyme X) that is better than esterase for degrading MDI321 that can be stimulated by phorbol ester when PKC is not activated (Figure 4.9).

Effect of ROS pre-treatment of polyurethanes

In previous work (15), it was suggested that the inhibition of neutrophil-mediated PCNU degradation by PMA treatment was due to the increased release of the oxidative agent HOCl from neutrophils. It was proposed that HOCl release altered the surface, thereby making it less susceptible to cleavage by esterases. To test this theory, HDI and MDI based PCNUs were pre-treated with HOCl for a week prior to CE treatment. The results showed an inhibition of CE-mediated degradation for the HDI PCNU but not the MDI based PCNU (15). Since the final product of the respiratory burst in MDM is H_2O_2 and not HOCl, it was of interest to pre-treat PCNUs with H_2O_2 to study its effect on subsequent hydrolytic and MDM-mediated PCNU degradation. First, 20% H_2O_2 was tested on the three PCNUs to check for degradation. All three PCNUs were degraded by

this treatment; however, after 24 hours, MDI321 was degraded significantly less than the HDI PCNUs (Figure 3.1). By 72 hours, there was no longer a significant difference in degradation of the surfaces (Figure 3.1). 72-hour pre-treatment inhibited the CXE-mediated degradation of HDI431 and HDI321 but stimulated the degradation of MDI321 (Figure 2.5), similar to the above results for HOCl pre-treatment prior to CE (15). A 24-hour pre-treatment with 20% H_2O_2 inhibited the MDM-mediated degradation of HDI321 and MDI321 but not HDI431 (Figure 3.5). Interestingly, esterase activity of MDM was inhibited on H_2O_2 pre-treated HDI431 and HDI321 but not MDI321 (Figure 3.5). Therefore, it was possible that the 24-hour and 72-hour H_2O_2 treatments affected the HDI and MDI321 surfaces differently, causing varying subsequent hydrolytic degradation. For MDI321, a 24-hour H_2O_2 treatment caused minimal degradation (Figure 3.1) and protected the surface from subsequent degradation (Figure 3.5). However, after incubating MDI321 for 72 hours with H_2O_2 there was more material degradation (Figure 3.1) and subsequent hydrolytic degradation was stimulated (Figure 2.5). For HDI PCNUs, especially HDI431, the 24-hour treatment did not affect degradation as much as the 72-hour treatment, which cleaved most of the bonds susceptible to degradation, leaving fewer available for hydrolytic degradation (Figure 3.5). In Manuscript#2, Figures 3.2-3.4 and 3.6-3.8 highlight how the bonds that are cleaved on the HDI PCNUs (especially HDI431) are different than the bonds cleaved on MDI321 by H_2O_2 and H_2O_2 followed by seeding with MDM. Holes can be seen on the HDI431 surface treated with H_2O_2 (Figures 3.2 and 3.6) whereas there are cracks seen on the surface of H_2O_2 pre-treated MDI321 (Figures 3.4 and 3.8). Previously it was shown that MDM on HDI431 for 28 days could cause holes in the material surface without H_2O_2 pre-treatment (13).

Cracks (as seen on MDI321) are more indicative of the ESC seen in the foreign body response to an implanted biomaterial, rather than holes. The holes suggest a greater amount of MDM-mediated degradation of HDI431 compared to MDI321 which agrees with the MDM-mediated radiolabel release data (18).

Reactive oxygen species production in MDM on the three PCNUs

Previously, it was found that the quantification of ROS production in phagocytic cells requires the use of a PKC activator such as PMA (26-29). Part of the problem was finding an assay sensitive enough to detect ROS production. Fluorescent probes such as dihydroethidium (HET) (30, 31), 2'7'-dichlorofluorescin diacetate (26, 32), and dihydrorhodamine 123 (26) have been found to be more sensitive than colormetric assays for ROS detection. The oxidation of HET by superoxide anion to the red fluorescent ethidium was quantified by live cell microscopy in MDM on the three PCNUs with or without PMA. ROS production was triggered in MDM on all three surfaces, but the effect of PMA varied (Figure 3.9). The fact that HDI431 and HDI321 re-seeded MDMs were sensitive to PMA but not MDI321 re-seeded MDMs led to the hypothesis that the MDI321 surface itself could maximally trigger PKC and ROS without an exogenous agent such as PMA. This held true, since there was no significant difference in ROS production from MDM on MDI321 with or without PMA (Figure 3.9). PMA increased ROS in MDM on HDI431, but decreased ROS in MDM on HDI321 (Figure 3.9), confirming how sensitive the ROS production in MDM is to the material surface chemistry.

The effects of PMA on MDM morphology and activation

For degradable tissue engineering applications, the ideal polyurethane candidate would be sensitive to MDM-mediated degradation while inducing the MDM to differentiate towards a wound-healing phenotype instead of an inflammatory MDM. HDI431 is the most degradable PCNU studied in this thesis (18) and may be responsible for activating the MDM to an inflammatory phenotype. Previously, it was found that there was significantly more multi-nucleation and foreign body giant cell formation in MDM on HDI431 compared to the less degradable MDI321 (19). MDM on the HDI PCNUs, especially HDI431, take on a rounded, protruding morphology compared to the flatter, more spread out MDM on MDI321 (Figures 3.6-3.8) (19) suggesting MDM want to minimize contact with the HDI PCNUs. PMA caused an increase in the cellular protrusions connecting MDMs on HDI431 and HDI321, however the morphology of MDI on MDI321 was not significantly affected by PMA (Figure 4.7). It is unknown if this could lead to FBGC formation; however, previously it has been shown that PMA can stimulate phagosome-lysosome fusion in mouse macrophages (33) and blood monocyte fusion (34). Together, these suggest that, although PMA helps HDI-re-seeded MDM adopt a less inflammatory phenotype in terms of esterase activity and MSE, it also encourages cell fusion, transport and communication of cells.

Esterase staining is used to classify monocytes in a variety of pathological states (35, 36). In recent studies with PCNUs, esterase activity and MSE protein levels have been shown to be sensitive to material surfaces. PMA-differentiated U937 macrophage-like cells cultured on HDI PCNUs contained more esterase and MSE protein than MDI321 re-

seeded cells (18). This suggests that esterase activity may be a sign of MDM activation. The fact that PMA stimulated ROS in MDM on HDI431, but inhibited esterase activity, made it difficult to decide if this treatment stimulated MDM or not. However, recently it has been found that intracellular esterase activity was significantly higher in MDM on the non-degradable tissue culture polystyrene when compared to MDM on PCNUs (18), suggesting that MDM activation is not necessarily linked to degradation. Nevertheless, when comparing PCNUs, intracellular esterase activity was significantly higher in MDM on HDI431 than MDM on MDI321 (18), therefore suggesting that MDM on the more degradable HDI431 are in a more activated or inflammatory state than MDM on MDI321.

Other markers assessed in this thesis for MDM activation were the levels of intracellular and released AP and HMGB1. AP is a lysosomal protein that can be activated to be released by material surface chemistry (18, 37) and strain (38-40). Previously, it was found that there was no significant difference between AP released by PMA-differentiated U937 macrophage-like cells on the three PCNUs, however there was significantly more AP released from the PMA-differentiated U937 cells on non-degradable polydimethylsiloxane (18). Interestingly, 20% H_2O_2 pretreatment of the three PCNU surfaces caused a significant inhibition of total AP activity, however there was less inhibition for MDM on HDI431 (Figure 3.5). This followed the trend for the radiolabel release data that showed 20% H_2O_2 pretreatment inhibited MDM-mediated degradation of HDI321 and MDI321 more than HDI431 but not the trend for esterase activity, which showed pre-treated MDI321 as being the most activating (Figure 3.5).

This suggests different cellular localizations for AP and esterase as well as different means of activation.

The effects of biomaterials on the intracellular levels of HMGB1 and its secretion from MDM (see subsection 1.3.3.2) have not been extensively investigated. More HMGB1 was secreted from MDM on HDI431, which was significantly inhibited by treatment with PMA (Figure 4.5). However, MDM on MDI321 secreted the same amount of HMGB1 with or without PMA treatment (Figure 4.5), again suggesting a lack of sensitivity to PKC activation. In terms of HMGB1 and esterase activity, HDI431 is the most activating PCNU surface, which appears to be attenuated by PMA. MDM on MDI321 appear to be less activated and therefore do not respond to PMA treatment. Therefore HMGB1 levels and esterase activity may be better indicators of MDM activation by a PCNU surface than AP. Since AP is a lysosomal enzyme, it is activated by a different pathway than HMGB1 or esterase.

Relating oxidative and hydrolytic degradation of polyurethanes

Most studies have focused on oxidative degradation or hydrolytic degradation but few have studied the effects of one on the other. Manuscript#1 proposed that the MDM-mediated degradation of HDI (Figure 2.6) and MDI PCNUs (Figure 2.7) required the differential activation of hydrolytic and oxidative pathways of degradation. Figures 4.8 and 4.9 from Manuscript#3 propose new models for the MDM-mediated degradation of HDI (Figure 4.8) and MDI (Figure 4.9) based PCNUs using information in the literature and the results from the experiments described in this thesis (Manuscripts #1-3). Both

MDI and HDI PCNU surfaces stimulate ROS production, HMGB1 secretion, esterase activity and MSE protein in MDM, the release of which causes material degradation; however the amount produced and effect of these MDM products on the PCNU surface is dependent on material surface chemistry, especially hard segment chemistry. Manuscript#3, Figure 4.8 proposes that HDI PCNU degradation by MDM depends on esterase activity, especially MSE protein, and the reason that PMA inhibits MDM-mediated degradation is that PKC activation leads to an inhibition of esterase activity and MSE protein. The fact that HMGB1 secretion is inhibited by PKC activation of MDM on HDI431 suggests that the MDM change from an inflammatory MDM to a less activated state. Figure 4.9 (Manuscript#3) proposes that MDI-based PCNUs are less susceptible to esterase-mediated degradation but may be sensitive to another hydrolytic enzyme (Enzyme X). PKC activation by PMA had little effect on the MDM cultured on MDI321, suggesting that PKC is maximally activated in these cells by the surface itself. However, when PKC is inhibited there is another effect of phorbol esters to stimulate degradation esterase suggesting the stimulation of another hydrolytic pathway (Enzyme X).

Conclusions

i) The MDM-mediated degradation of HDI PCNUs is inhibited when PKC is activated by PMA due to an increase in ROS and an inhibition of total esterase activity and MSE protein. **Proposed future studies:** In order to determine the specific PKC isoform involved in this inhibition, western blots could be performed to check for PKC isoforms that are activated by PMA. Then these isoforms could be inhibited individually by chemical inhibitors or short-

interfering RNAs (siRNA) in MDM on these surfaces to determine the effects on PCNU degradation, esterase activity and MSE protein.

ii) The MDM-mediated degradation of MDI321 is activated by phorbol esters only when PKC is not activated and by scavenging ROS with CAT+SOD. That esterase is not stimulated, suggests another hydrolytic enzyme is activated by these treatments (Enzyme X). **Proposed future studies:** 2-dimensional gel electrophoresis followed by mass spectrometry could be performed on these lysate samples to identify potential candidate hydrolytic enzymes up-regulated by phorbol esters without PKC or CAT+SOD in MDM on MDI321. The candidate enzymes could then be individually inhibited in MDM on MDI321 to check for an inhibition of degradation by these MDM.

iii) ROS can be stimulated by select PCNU material surface chemistry (MDI-based) without PMA. **Proposed future studies:** Measure the effect of inhibiting PKC on the ROS produced by these cells and MDM on the HDI PCNUs. In addition, it would be interesting to create an automated version of this test with a standard curve so that a more quantitative value could be obtained.

iv) H_2O_2 pretreatment affects subsequent MDM-mediated degradation and MDM-elicited esterase activity differently depending on the material surface. **Proposed future studies:** Analyze the supernatants of MDM on pretreated

and untreated PCNU surfaces to determine the difference in degradation products using high-performance liquid chromatography and mass spectrometry as previously described (17).

v) HMGB1 secretion is differentially induced in MDM on PCNUs, with MDM on HDI431 showing the greatest amount of secretion and therefore activation. PMA can inhibit the secretion of HMGB1 from MDM on HDI431 but not MDM on MDI321. **Proposed future studies:** HMGB1 secretion by MDM on the three PCNU surfaces with or without PMA could be more quantitatively assessed by ELISA. Next it would be interesting to determine specifically which PKC isoform(s) inhibit this secretion by individually inhibiting PKC isoforms with siRNA.

Significance of this thesis

Significant findings from this thesis (Manuscripts #1-3) and previous work (19, 41) showed that material surface chemistry can direct the MDM's response. In addition this first response changes the way an MDM will respond to other stimuli, for instance exogenous agents such as PMA. These findings have made it possible to focus our research on tailoring PCNUs to a specific application. As our research continues, by utilizing the information gained thus far, it may be possible to generate a vessel for a peripheral artery vascular graft. The hard segment BD-diisocyanate component, which appears from this work to have such a sensitive influence on the MDM response (Manuscripts 1-3) will not be used. Instead, a novel vinyl PCNU with an LDI-based hard

segment (VPU) will be tailored so that the cells required (endothelial cells, vascular smooth muscle cells) will be directed by MDM to perform their desired functions. As previously shown, an LDI based polyurethane will be a polyurethane that is degradable similar to HDI PCNUs but has the physiologically acceptable degradation product of lysine (4, 42-44). Previous attempts to make an *in vitro* model of an artery using a Dacron mesh with layers of collagen (45) or a fibrin gel (46) as a scaffold for EC and VSMC recruitment and tissue formation have been unsuccessful. This may be due to the fact that the essential role of a wound healing MDM phenotype (47) in this process has yet to be investigated. These novel VPU scaffolds with variable polycarbonate cross-linking and bio-active peptides attached (3), will be tested for their ability to recruit ECs and VSMCs, promote vessel formation, and induce MDMs into a wound healing phenotype. Wound healing MDMs are needed to degrade the scaffold and promote functional markers in VSMCs and ECs. This will require stimulating the controlled release of esterases and ROS in the MDMs to slowly degrade the scaffold without stimulating the secretion of pro-inflammatory cytokines such as HMGB1. Each cell will be assayed separately and then a co-culture of MDMs, VSMCs and ECs on VPU scaffolds will be assessed as a basis for a peripheral artery vascular graft. The generation of a vascular graft is only one example of the necessity to test each material separately when used for a new application since each material will be exposed to a different local environment and stimuli so that the attached MDM may react differently. Further elucidation of the MDM response to a polyurethane biomaterial will aid in the development of new polyurethanes with material chemistries that are tailored to perform a specific function and induce the desired response from MDM *in vivo*.

5.1 REFERENCES

1. Bakker D, van Blitterswijk CA, Hesseling SC, Grote JJ. Effect of implantation site on phagocyte/polymer interaction and fibrous capsule formation. Biomaterials 1988;9(1):14-23.

2. Stokes K, McVenes R, Anderson JM. Polyurethane elastomer biostability. J Biomater Appl 1995;9(4):321-54.

3. Ernsting MJ, Bonin GC, Yang M, Labow RS, Santerre JP. Generation of cell adhesive substrates using peptide fluoralkyl surface modifiers. Biomaterials 2005;26(33):6536-46.

4. Ernsting MJ, Labow RS, Santerre JP. Surface modification of a polycarbonate-urethane using a vitamin-E-derivatized fluoroalkyl surface modifier. J Biomater Sci Polym Ed 2003;14(12):1411-26.

5. Tang YW, Santerre JP, Labow RS, Taylor DG. Use of surface-modifying macromolecules to enhance the biostability of segmented polyurethanes. J Biomed Mater Res 1997;35(3):371-81.

6. Wilson DJ, Rhodes NP, Williams RL. Surface modification of a segmented polyetherurethane using a low-powered gas plasma and its influence on the activation of the coagulation system. Biomaterials 2003;24(28):5069-81.

7. Zdrahala RJ, Zdrahala IJ. Biomedical applications of polyurethanes: a review of past promises, present realities, and a vibrant future. J Biomater Appl 1999;14(1):67-90.

8. Tang YW, Labow RS, Santerre JP. Enzyme-induced biodegradation of polycarbonate-polyurethanes: dependence on hard-segment chemistry. J Biomed Mater Res 2001;57(4):597-611.

9. Tang YW, Labow RS, Santerre JP. Enzyme-induced biodegradation of polycarbonate polyurethanes: dependence on hard-segment concentration. J Biomed Mater Res 2001;56(4):516-28.

10. Salacinski HJ, Tai NR, Carson RJ, Edwards A, Hamilton G, Seifalian AM. In vitro stability of a novel compliant poly(carbonate-urea)urethane to oxidative and hydrolytic stress. J Biomed Mater Res 2002;59(2):207-18.

11. Christenson EM, Patel S, Anderson JM, Hiltner A. Enzymatic degradation of poly(ether urethane) and poly(carbonate urethane) by cholesterol esterase. Biomaterials 2006;27(21):3920-6.

12. Labow RS, Meek E, Matheson LA, Santerre JP. Human macrophage-mediated biodegradation of polyurethanes: assessment of candidate enzyme activities. Biomaterials 2002;23(19):3969-75.

13. Labow RS, Meek E, Santerre JP. Hydrolytic degradation of poly(carbonate)-urethanes by monocyte-derived macrophages. Biomaterials 2001;22(22):3025-33.

14. Labow RS, Sa D, Matheson LA, Santerre JP. Polycarbonate-urethane hard segment type influences esterase substrate specificity for human macrophage mediated biodegradation. J Biomater Sci Polym Ed 2005;16(9):1167-1177.

15. Labow RS, Tang Y, McCloskey CB, Santerre JP. The effect of oxidation on the enzyme-catalyzed hydrolytic biodegradation of poly(urethane)s. J Biomater Sci Polym Ed 2002;13(6):651-65.

16. Tang YW, Labow RS, Santerre JP. Enzyme induced biodegradation of polycarbonate-polyurethanes: dose dependence effect of cholesterol esterase. Biomaterials 2003;24(12):2003-11.

17. Tang YW, Labow RS, Santerre JP. Isolation of methylene dianiline and aqueous-soluble biodegradation products from polycarbonate-polyurethanes. Biomaterials 2003;24(17):2805-19.

18. Matheson LA, McBane JE, Malowany JI, Santerre JP, Labow RS. Is cell culture stressful? Effects of degradable and nondegradable culture surfaces on U937 cell function. Biotechniques 2007;42(6):744, 746-50.

19. Matheson LA, Santerre JP, Labow RS. Changes in macrophage function and morphology due to biomedical polyurethane surfaces undergoing biodegradation. J Cell Physiol 2004;199(1):8-19.

20. Quick J, Ware JA, Driedger PE. The structure and biological activities of the widely used protein kinase inhibitor, H7, differ depending on the commercial source. Biochem Biophys Res Commun 1992;187(2):657-63.

21. Bey EA, Xu B, Bhattacharjee A, Oldfield CM, Zhao X, Li Q, et al. Protein kinase C delta is required for p47phox phosphorylation and translocation in activated human monocytes. J Immunol 2004;173(9):5730-8.

22. Johnson JL, Park JW, Benna JE, Faust LP, Inanami O, Babior BM. Activation of p47(PHOX), a cytosolic subunit of the leukocyte NADPH oxidase. Phosphorylation of ser-359 or ser-370 precedes phosphorylation at other sites and is required for activity. J Biol Chem 1998;273(52):35147-52.

23. Jackson SH, Gallin JI, Holland SM. The p47phox mouse knock-out model of chronic granulomatous disease. J Exp Med 1995;182(3):751-8.

24. Tanabe T, Otani H, Mishima K, Ogawa R, Inagaki C. Phorbol 12-myristate 13-acetate (PMA)-induced oxyradical production in rheumatoid synovial cells. Jpn J Pharmacol 1997;73(4):347-51.

25. Medan D, Wang L, Toledo D, Lu B, Stehlik C, Jiang BH, et al. Regulation of Fas (CD95)-induced apoptotic and necrotic cell death by reactive oxygen species in macrophages. J Cell Physiol 2005;203(1):78-84.

26. Vowells SJ, Sekhsaria S, Malech HL, Shalit M, Fleisher TA. Flow cytometric analysis of the granulocyte respiratory burst: a comparison study of fluorescent probes. J Immunol Methods 1995;178(1):89-97.

27. Wang JF, Komarov P, de Groot H. Luminol chemiluminescence in rat macrophages and granulocytes: the role of NO, O2-/H2O2, and HOCl. Arch Biochem Biophys 1993;304(1):189-96.

28. Shen YC, Chiou WF, Chou YC, Chen CF. Mechanisms in mediating the anti-inflammatory effects of baicalin and baicalein in human leukocytes. Eur J Pharmacol 2003;465(1-2):171-81.

29. Barbieri SS, Eligini S, Brambilla M, Tremoli E, Colli S. Reactive oxygen species mediate cyclooxygenase-2 induction during monocyte to macrophage differentiation: critical role of NADPH oxidase. Cardiovasc Res 2003;60(1):187-97.

30. Neuspiel M, Zunino R, Gangaraju S, Rippstein P, McBride H. Activated mitofusin 2 signals mitochondrial fusion, interferes with Bax activation, and reduces susceptibility to radical induced depolarization. J Biol Chem 2005;280(26):25060-70.

31. Budd SL, Castilho RF, Nicholls DG. Mitochondrial membrane potential and hydroethidine-monitored superoxide generation in cultured cerebellar granule cells. FEBS Lett 1997;415(1):21-4.

32. Amer J, Goldfarb A, Fibach E. Flow cytometric measurement of reactive oxygen species production by normal and thalassaemic red blood cells. Eur J Haematol 2003;70(2):84-90.

33. Kielian MC, Cohn ZA. Phorbol myristate acetate stimulates phagosome-lysosome fusion in mouse macrophages. J Exp Med 1981;154(1):101-11.

34. Hassan NF, Kamani N, Meszaros MM, Douglas SD. Induction of multinucleated giant cell formation from human blood-derived monocytes by phorbol myristate acetate in in vitro culture. J Immunol 1989;143(7):2179-84.

35. Griffin JD, Mayer RJ, Weinstein HJ, Rosenthal DS, Coral FS, Beveridge RP, et al. Surface marker analysis of acute myeloblastic leukemia: identification of differentiation-associated phenotypes. Blood 1983;62(3):557-63.

36. Uphoff CC, Hu ZB, Gignac SM, Ma W, Rainey FA, Kreutz M, et al. Characterization of the monocyte-specific esterase (MSE) gene. Leukemia 1994;8(9):1510-26.

37. Afaq F, Abidi P, Matin R, Rahman Q. Activation of alveolar macrophages and peripheral red blood cells in rats exposed to fibers/particles. Toxicol Lett 1998;99(3):175-82.

38. Matheson LA, Maksym GN, Santerre JP, Labow RS. The functional response of U937 macrophage-like cells is modulated by extracellular matrix proteins and mechanical strain. Biochem Cell Biol 2006;84(5):763-73.

39. Matheson LA, Maksym GN, Santerre JP, Labow RS. Cyclic biaxial strain affects U937 macrophage-like morphology and enzymatic activities. J Biomed Mater Res A 2006;76(1):52-62.

40. Matheson LA, Jack Fairbank N, Maksym GN, Paul Santerre J, Labow RS. Characterization of the Flexcell Uniflex cyclic strain culture system with U937 macrophage-like cells. Biomaterials 2006;27(2):226-33.

41. Labow RS, Sa D, Matheson LA, Dinnes DL, Santerre JP. The human macrophage response during differentiation and biodegradation on polycarbonate-based polyurethanes: dependence on hard segment chemistry. Biomaterials 2005;26(35):7357-66.

42. Bruin P, Smedinga J, Pennings AJ, Jonkman MF. Biodegradable lysine diisocyanate-based poly(glycolide-co-epsilon-caprolactone)-urethane network in artificial skin. Biomaterials 1990;11(4):291-5.

43. Abraham GA, Marcos-Fernandez A, Roman JS. Bioresorbable poly(ester-ether urethane)s from L-lysine diisocyanate and triblock copolymers with different hydrophilic character. J Biomed Mater Res A 2006;76(4):729-36.

44. Zhang JY, Beckman EJ, Hu J, Yang GG, Agarwal S, Hollinger JO. Synthesis, biodegradability, and biocompatibility of lysine diisocyanate-glucose polymers. Tissue Eng 2002;8(5):771-85.

45. Weinberg CB, Bell E. A blood vessel model constructed from collagen and cultured vascular cells. Science 1986;231(4736):397-400.

46. Dorweiler B, Torzewski M, Dahm M, Ochsenhirt V, Lehr HA, Lackner KJ, et al. A novel in vitro model for the study of plaque development in atherosclerosis. Thromb Haemost 2006;95(1):182-9.

47. Lazarov-Spiegler O, Solomon AS, Zeev-Brann AB, Hirschberg DL, Lavie V, Schwartz M. Transplantation of activated macrophages overcomes central nervous system regrowth failure. Faseb J 1996;10(11):1296-302.

presence of various inhibitors or activators of key cell pathways. Experiments were performed with human monocyte-derived macrophages or U937 cells that were differentiated into macrophage-like cells with phorbol myristate acetate prior to seeding on the polyurethane surface. This study found that inhibiting esterase or phospholipase A_2 could inhibit polyurethane degradation and that activating protein kinase C could also inhibit polyurethane degradation. Inhibition of degradation differed depending on the material surface chemistry and could be correlated to a decrease in esterase activity. **Publication#3** included the degradation data showing that the hexane diisocyanate polycarbonate-based polyurethanes were more susceptible to macrophage-mediated degradation than the methylene bisphenyl diisocyanate polycarbonate-based polyurethanes.

High School Diploma 1998

St. Mark High School (Manotick, ON, Canada)
Ontario Scholar
French Immersion French Language Certificate

PUBLICATIONS

(1) McBane, J.E., Santerre, J.P. and Labow, R.S. The Role of Protein Kinase C in the Monocyte-Derived Macrophage Mediated Biodegradation of Polycarbonate-Based Polyurethanes. (2005) *Journal of Biomedical Materials Research* 74A: 1-11.

(2) McBane, J.E., Santerre, J.P. and Labow, R.S. The interaction between hydrolytic and oxidative pathways in macrophage-mediated polyurethane degradation. (2007) *Journal of Biomedical Materials Research* 82(4): 984-994.

(3) Matheson, L.A., **McBane, J.E.,** Malowany, J.I., Santerre, J.P., and Labow, R.S. Is cell culture stressful? Effects of degradable and nondegradable culture surfaces on U937 cell function. (2007) *Biotechniques* 42: 744-750.

(4) McBane, J.E., Santerre, J.P. and Labow, R.S. The effects of phorbol ester activation, inhibition, and reactive oxygen species scavengers on the macrophage-mediated foreign body reaction to polyurethanes. *Biochemistry and Cell Biology* (submitted December 5th, 2007).

PRESENTATIONS

Peer-reviewed presentations:

(1) **McBane, J.E.,** Santerre, J.P. and Labow, R.S. The Role of Macrophages in the Biodegradation of Polyurethane Cardiovascular Devices: Assessment of Material Surface Chemistry on Biodegradation. Poster presentation - CFBS conference (June 2003) Ottawa Congress Centre, Ottawa, ON, Canada.

(2) **McBane, J.E.,** Santerre, J.P. and Labow, R.S. A Role for Protein Kinase C in the Macrophage Biodegradation of Polyurethanes. Poster presentation - 10th Annual Ottawa Life Sciences Council Conference, BioNorth 2003 (November 2003) Ottawa Congress Centre, Ottawa, ON, Canada.

(3) Labow, R.S., **McBane, J.E.,** Waghray, G. and Santerre, J.P. The Response of Human Neutrophils and Monocyte-Derived Macrophages to Material Chemistry: Role of Protein Kinase C. 2nd Author, not attending, Oral Presentation - 7th World Biomaterials Conference (May 2004) Sydney, Australia.

(4) **McBane, J.E.,** Santerre, J.P. and Labow, R.S. Protein Kinase C and the Respiratory Burst in the Macrophage-Mediated Biodegradation of Polyurethanes. Poster presentation - 11th Annual Ottawa Life Sciences Council Conference, BioNorth 2004 (November 2004) Ottawa Congress Centre, Ottawa, ON, Canada.

(5) **McBane, J.E.,** Santerre, J.P. and Labow, R.S. Does Protein Kinase C Affect Monocyte-Derived Macrophage Mediated Biodegradation of Polycarbonate-Based Polyurethanes? Poster presentation - 30th Annual Meeting and Exposition for the Society for Biomaterials (April 2005) Memphis Cook Convention Center, Memphis, TN, USA.

(6) **McBane, J.E.,** Santerre, J.P. and Labow, R.S. Protein Kinase C and the Biodegradation of Polyurethanes by Macrophages. Oral presentation - 24th Annual Meeting of the Canadian Biomaterials Society, (May 2005) University of Waterloo, Waterloo, ON, Canada.

(7) **McBane, J.E.,** Santerre, J.P. and Labow, R.S. Polycarbonate-based Polyurethanes Stimulate Reactive Oxygen Species Production in Macrophages. Poster presentation- 31st Annual Meeting and Exposition for the Society for Biomaterials, (April 2006) David Lawrence Convention Center, Pittsburgh, PA, USA.

(8) **McBane, J.E.,** Santerre, J.P. and Labow, R.S. The Macrophage-Mediated Biodegradation of Hydrogen Peroxide Pretreated Polycarbonate-Based Polyurethanes. Oral presentation - 25th Annual Meeting of the Canadian Biomaterials Society, (May 2006) University of Calgary, Calgary, AB, Canada.

(9) **McBane, J.E.,** Santerre, J.P. and Labow, R.S. The Effect of Oxidation on the Degradation of Model Polyurethanes for Cardiovascular Medical Devices. Oral presentation - World Society of Cardio-Thoracic Surgeons 16th World Congress, (August 2006) Ottawa Congress Centre, Ottawa, ON, Canada.

(10) **McBane, J.E.,** Santerre, J.P. and Labow, R.S. The Interaction Between Hydrolytic and Oxidative Pathways in Macrophage-Mediated Polyurethane Degradation. Poster presentation - 32nd Annual Meeting and Exposition for the Society for Biomaterials, (April 2007) Chicago, IL, USA.

(11) **McBane, J.E.,** Santerre, J.P. and Labow, R.S. The macrophage-mediated biodegradation of polyurethanes: Oxidants, antioxidants and hydrolysis. Oral presentation - 26th Annual Meeting of the Canadian Biomaterials Society, (May 2007) University of Western Ontario, London, ON, Canada.

(12) **McBane, J.E.,** Matheson, L.A., McDonald, S.M., Santerre, J.P. and Labow, R.S. Effect of Phorbol Myristate Acetate on the Differentiation of Monocytes on Polycarbonate-based Polyurethanes. 8th World Biomaterials Congress: Crossing frontiers in biomaterials and regenerative medicine. Amsterdam, The Netherlands, May 28-June 1, 2008. Submitted for oral presentation.

(13) **McBane, J.E.,** Sharifpoor, S., Santerre, J.P. and Labow, R.S. Differentiation of Monocytes on Vinyl-Lysine Polyurethanes: Effect of Collagen on Cell Attachment and Hydrolytic Activities. 8th World Biomaterials Congress: Crossing frontiers in biomaterials and regenerative medicine. Amsterdam, The Netherlands, May 28-June 1, 2008. Submitted for oral presentation.

(14) Sharifpoor, S., **McBane, J.E.,** Santerre, J.P. and Labow, R.S. Interaction of Monocyte-Derived Macrophages with Biodegradable Vinyl-Polyurethane Porous Scaffolds. 8th World Biomaterials Congress: Crossing frontiers in biomaterials and regenerative medicine. Amsterdam, The Netherlands, May 28-June 1, 2008. Submitted for oral presentation.

(15) Sharifpoor, S., **McBane, J.E.,** Santerre, J.P. and Labow, R.S. Synthesis and Characterization of Biodegradable Vinyl-Polyurethanes: Assessment of Monocyte Attachment and Morphology. 8th World Biomaterials Congress: Crossing frontiers in biomaterials and regenerative medicine. Amsterdam, The Netherlands, May 28-June 1, 2008. Submitted for oral presentation.

(16) Matheson, L.A., **McBane, J.E.**, Sharifpoor, S., Rosenberg, A.M., Santerre, J.P. and Labow, R.S. Regulating the balance between inflammation and repair: modulation of cytokine release by differentiating monocytes via vinyl-polyurethane films. 8th World Biomaterials Congress: Crossing frontiers in biomaterials and regenerative medicine. Amsterdam, The Netherlands, May 28-June 1, 2008. Submitted for oral presentation.

Non-refereed presentations:

(1) **McBane, J.E.,** Santerre, J.P. and Labow, R.S. A role for protein kinase C in the biodegradation of polyurethanes. Poster presentation – University of Ottawa Graduate Department of Biochemistry Poster Day (April 2004) University of Ottawa, Ottawa, ON, Canada.

(2) **McBane, J.E.,** Santerre, J.P. and Labow, R.S. A Role for Protein Kinase C in Polycarbonate-based Polyurethane Biodegradation. Oral presentation - University of Ottawa Heart Institute Research Day, (April 2004) University of Ottawa Heart Institute, Ottawa, ON, Canada.

(3) **McBane, J.E.,** Santerre, J.P. and Labow, R.S. Protein kinase C, reactive oxygen species, and the macrophage-mediated biodegradation of polyurethanes. Oral presentation - University of Ottawa Graduate Department Seminar Series (February 2005) University of Ottawa Heart Institute, Ottawa, ON, Canada.

(4) **McBane, J.E.,** Santerre, J.P. and Labow, R.S. Polycarbonate-based Polyurethanes Stimulate Reactive Oxygen Species Production in Macrophages. Poster presentation – University of Ottawa Graduate Department of Biochemistry Poster Day (May 2006) University of Ottawa, Ottawa, ON, Canada.

(5) **McBane, J.E.,** Santerre, J.P. and Labow, R.S. Materials used in cardiovascular devices are affected by macrophage-mediated oxidation. Oral presentation - University of Ottawa Heart Institute Research Day, (May 2006) University of Ottawa Heart Institute, Ottawa, ON, Canada.

(6) **McBane, J.E.,** Santerre, J.P. and Labow, R.S. Scavenging a role for PKC in polyurethane biodegradation. Oral Presentation - Graduate Student Seminar Day, (February 2007) University of Ottawa, Ottawa, ON, Canada.

(7) **McBane, J.E.,** Santerre, J.P. and Labow, R.S. Monitoring the macrophage diet: Do phorbol esters make polyurethane products more tasty? Oral presentation - University of Ottawa Heart Institute Research Day, (April 2007) University of Ottawa Heart Institute, Ottawa, ON, Canada.

(8) **McBane, J.E.,** Santerre, J.P. and Labow, R.S. Macrophage responses to polyurethanes: Oxidation versus hydrolysis – The fork on the road to degradation. Oral presentation - PhD Research Seminar, (October 2007) University of Ottawa, Ottawa, ON, Canada.

ACADEMIC AWARDS

University of Ottawa OGSST September 2005-August 2007
-Ontario Graduate Scholarship in Science and Technology Scholarship
-$15000 per year.

CIHR Strategic training fellowship July 2005-Present
-Cell Signalling in Mucosal Inflammation & Pain, CIHR Strategic Training Program
-Joined group of Cell Signals as a CIHR Strategic Training Fellow and received $23,500 over three years.

University of Ottawa PhD Tuition Waiver May 2005-Present
-Admission scholarship for entrance into the PhD in Biochemistry program

Heart & Stroke Foundation-OGSST Scholarship September 2004-August 2005
-Ontario Graduate Scholarship in Science and Technology Scholarship
-$15000 per year

Reuben Fisher Scholarship 2003
-MSH Foundation (Montreal, QC) sponsored scholarship for graduate students in respiratory medicine
-$10,000 per year

EMPLOYMENT

University of Ottawa January 2007-April 2007
Teaching Assistant
-BCH2333 and BCH3346 (2nd and 3rd year undergraduate Biochemistry Laboratory course)
-supervision of laboratory sessions and grading of lab reports

University of Ottawa April 2004
Teaching Assistant Ottawa, ON, Canada
-BCH4125Cellular regulation and control
-4th year undergraduate Marked final exam

University of Ottawa Heart Institute May 2002-August 2003
Summer Student/ Co-op placement/Honours research project Ottawa, ON, Canada

Environment Canada September 2001-December 2001
Student Assistant (third co-op placement) Hull, QC, Canada
-Summarized scientific articles on endocrine disrupting substances and added the information to a ChemOffice database on endocrine disrupting substances that will one day be available for public consultation

-Received scientific articles and updated the library by adding the references to their local network Reference Manager database
-Researched Ovanes Mekenyan and wrote a report on his chemical modeling computer databases

Iogen Corporation January 2001-August 2001
Student Assistant (first and second co-op placement) Ottawa, ON, Canada
-Learned proper format for a written report
-Presented findings of part of one project to a client
-Applied previously learned and new laboratory skills (titration, dilutions, acid hydrolysis, etc.)

DISTINCTIONS/CREDENTIALS

Canadian Biomaterials Society Oral Presentation Award May 2007
Honorable mention at the 26th Annual Meeting in London, ON, Canada.

Canadian Biomaterials Society 25th Annual Meeting, Travel Award May 2006
$300 toward travel to Calgary, AB for the meeting. Sponsored by Fisher Scientific, Angiotech, BOSE/Enduratech, Mandel, and AB Ingenuity

University of Ottawa Heart Institute Research Day Award May 2006
Honorable mention for oral presentation in basic science category ($50)

Society for Biomaterials Research Award November 2004
2005 Student Award for Outstanding Research in the Masters or Health Science Degree Category. Received at the April 2005 SFB 30th Annual Meeting, Memphis, TN, April 27, 2005.

LABORATORY TECHNIQUES

1D Gel Electrophoresis
Bacterial Culture
Cell Culture
-cell lines
-primary cells
Laser Scanning Confocal Microscopy
Radioisotope Techniques
Cell Fractionation
Distillation/Fractionation
2D Gel Electrophoresis
ELISA
Enzyme Assays
Immunoprecipitation
Immunofluorescence
Live Cell Video Microscopy
Western Blotting
Polyurethane Synthesis